REGULATION AND FUNCTION OF ACID SPHINGOMYELINASE (ASM)/CERAMIDE PATHWAY IN IRRADIATION-INDUCED CELL DEATH

Inaugural-Dissertation
zur
Erlangung des Doktorgrades
Dr. rer. nat.

der Fakultät für
Biologie
an der

Universität Duisburg-Essen
vorgelegt von
Deepa Sharma
aus (Kapilvastu, Nepal)
(Juli 2015)

Die der vorliegenden Arbeit zugrundeliegenden Experimente wurden am Institut für Molekularbiologie (Tumorforschung) der Universität Duisburg-Essen durchgeführt.

1. Gutachter: Prof. Dr. Erich Gulbins

2. Gutachter: Prof. Dr. Shirley Knauer
3. Gutachter: Prof. Dr. Verena Jendrossek

Vorsitzender des Prüfungsausschusses: Prof. Dr. Verena Jendrossek

Tag der mündlichen Prüfung: 16.09.2015

TABLE OF CONTENTS

ABBREVIATIONS

ABBREVIATIONS

AC	acid ceramidase
ALS	amyotrophic lateral sclerosis
Akt/PKB	protein kinase B
AML	acute myeloid leukemia
AP-1	activator protein-1
APS	ammonium persulfate
ASM	acid sphingomyelinase
ATM	ataxia telangiectasia mutated
ATP	adenosine triphosphate
BAECs	bovine aortic endothelial cells
BAD	Bcl-2-antagonist of cell death
BAX	Bcl2-associated X protein
Bcl-2	B-cell lymphoma 2
BFGF	basic fibroblast growth factor
BH3	Bcl-2 homology region 3
BSA	bovine serum albumin
^{14}C	Carbon-14
µCi	microcurie
C1P	ceramide-1-phosphate
C1PP	C1P phosphatase
CAECs	coronary arterial endothelial cells
CaLB	calcium-dependent lipid binding
CAPP	ceramide-activated protein phosphatases
CD	cluster of differentiation

CDases	ceramidases
cDNA	complementary DNA
C. elegans	*Caenorhabditis elegans*
CEACAM	Carcinoembryonic antigen-related cell adhesion molecules
CEP-1	C. elegans p53-like protein 1
CERK	ceramide kinase
CerS	ceramide synthase
CK	ceramide kinase
Cm	centimeters
CNS	central nervous system
CO_2	carbon dioxide
$cPLA_2$	calcium-dependent phospholipase A_2
CRAC	calcium release activated calcium channel
Cu^{2+}	copper ion
CYBB	cytochrome b beta
DAG	diacylglycerol
ddH_2O	double distilled water
DDR	DNA damage response
DES	di-hydro-ceramide desaturase
dhCer	di-hydro-ceramide
DHE	dihydroethidium
DMEM	dulbecco's modified eagle medium
DMSO	dimethyl sulfoxide
DNA	deoxyribonucleic acid
dNTPs	deoxynucleotide triphosphates

DTT	dithiothreitol
EDTA	ethylenediaminetetraacetic acid
ECL	enhanced chemiluminescence
ER	endoplasmic reticulum
ERK1/ERK2	extracellular regulated kinases1/2
ETC	electron transport chain
FACS	fluorescence activated cell sorting
FAPP2	four-phosphate adaptor protein 2
FasL	Fas ligand
FCS	fetal calf serum
FITC	fluorescein isothiocyanate
FQR	flavoprotein-ubiquinone oxidoreductase
GalC	galactosylceramide
GalCS	galactosylceramide synthase
GC	glucosylceramide
GCase	glucosyl CDase
GCS	glucosylceramide synthase
GI	gastrointestinal
GPDH	glycerol-3-phosphate dehydrogenase
GPI	glycosylphosphatidylinositol
GPLs	glycerophospholipids
GSLs	glycosphingolipids
grp75	glucose-regulated protein 75
GTP	guanosine triphosphate
Gy	gray
H_2DCF-DA	2',7'-dichlorodihydrofluorescein diacetate

h	hour
hASMase	human acid sphingomyelinase
HRP	horseradish peroxidase
IP	immunoprecipitation
IR	ionizing radiation
JNK	c-Jun N-terminal kinase
kDa	kilodaltons
KDS	3-ketodihydrosphinganine
KSR	kinase suppressor of RAS
kV	kilovolt
LAG1p	longevity assurance gene 1 protein
LAMP-1	lysosomal-associated membrane protein 1
LC-MS/MS	liquid chromatography–mass spectrometry/mass spectrometry
LD	lethal dose
L-SMase	lysosomal sphingomyelinase
mg	milligrams
ml	milliliters
mm	millimeters
min	minute
μM	micromolar
MCRM	mitochondrial ceramide-rich macrodomains
MAPK	mitogen-activated protein kinases
MAPKAPK2	mitogen-activated protein kinase-activated protein kinase 2
MES	2-(*N*-morpholino)ethanesulfonic acid

Mg^{2+}	magnesium ion
mTOR	mechanistic target of rapamycin
N. gonorrhoeae	*Neisseria gonorrhoeae*
NaCl	sodium chloride
NADH	nicotinamide adenine dinucleotide
NADPH	nicotineamide adenine dinucleotide phosphate
NOX	NADPH oxidase
NF-kappaB	nuclear factor kappa-light-chain-enhancer of activated B cells
NP-40	nonidet P-40
NPD	Niemann-Pick disease
OGDH	2 oxoglutarate dehydrogenase
Opa proteins	opacity proteins
OXPHOS	oxidative phosphorylation
^{32}P	Phosphorus-32
γ-H2AX	phosphorylation of histone H2AX at Ser-139
P. aeruginosa	*Pseudomonas aeruginosa*
PBS	phosphate buffered saline
PI3K-Akt	phosphatidylinositol 3-kinase –Akt
PC	phosphatidylcholine
PCR	polymerase chain reaction
PCNA	proliferating cell nuclear antigen
PDH	pyruvate dehydrogenase
PDMP	DL-threo-1-phenyl-2-decanoylamino-3-morpholino-1-propanol
P. falciparum	*Plasmodium falciparum*
PFA	paraformaldehyde

PI	propidium iodide
PKC	protein kinase C
PPMP	DL-threo-1-phenyl-2-palmitoylamino-3-morpholino-1-propanol
Rac-1/2	Ras-related C3 botulinum toxin substrate 1/2
RIPA	radioimmunoprecipitation assay
RNAse	ribonuclease
ROS	reactive oxygen species
RT	room temperature
S.D.	standard deviation
SDS-PAGE	sodium dodecyl sulfate polyacrylamide gel electrophoresis
sec	second
SiRNA	small interfering RNA
SK	sphingosine kinases
SM	sphingomyelin
SMases	sphingomylinases
SMPD1	sphingomyelin phosphodiesterase 1
SMS	SM synthase
Sph	sphingosine
S1P	sphingosine-1-phosphate
S-SMase	secretory sphingomyelinase
SNARE	soluble *N*-ethylmaleimide-sensitive-factor activating protein receptor
SPT	serine palmitoyltransferase
SPPase	Sph phosphate phosphatase
TBE	Tris/Borate/EDTA

TBST	tris-buffered saline and tween 20
TCS	true confocal scanner
TEMED	tetramethylethylenediamine
TIMM23	translocase of the inner mitochondrial membrane 23
TLB	tissue lysis buffer
TLC	thin-layer chromatography
TNF	tumor necrosis factor
TRAIL	TNF-related apoptosis-inducing ligand
TRIS	(tris(hydroxymethyl)aminomethane
V	voltage
UV	ultraviolet
VDAC	voltage-dependent anion channel
Zn^{2+}	zinc ion

1 INTRODUCTION

1.1 RADIATION

1.1.1 OVERVIEW OF RADIATION-FORMS

Radiation is defined as a process of energy emission in the form of particles or waves. It can be categorized into two forms: ionizing radiation (IR) and non-ionizing radiation. IR holds high energy and has the capability to remove tightly bound electrons from atoms. It comprises subatomic particles, ions or atoms and also electromagnetic waves positioned on the short wavelength end of the electromagnetic spectrum. Alpha and beta particles as well as neutrons are typical particles, whereas gamma rays and X-rays are ionizing electromagnetic waves. Non-ionizing radiation is inadequate to remove tightly bound electrons from atoms, and it is mainly used for common purpose, for instance as infrared, microwaves, or radio waves (Ng 2003).

The use of high-energy IR to treat cancer is known as radiation therapy. For more than 100 years, IR has been used as the standard clinical treatment to cure different cancers in humans. Today, radiation therapy remains to be one of the most common respective treatments: around half of all cancer patients worldwide receive radiation therapy either alone or in combination with surgery or chemotherapy (Baskar et al 2012). Radiation therapy is delivered to patients in two different ways: internally or externally. Internal radiation therapy refers to a radioactive source like radioactive seeds being applied to the body. External radiation therapy is applied through a machine that delivers high-energy X-rays to the cancer (Kaliberov and Buchsbaum 2012).

Radiation therapy can harm cancer cells or can kill those cells using waves or high-energy particles. Radiation exerts two types of effects upon exposure to cells, namely a direct and an indirect effect. When radiation directly interacts with deoxyribonucleic acid (DNA), the bonds between the atoms can break or some other important components of cell playing a vital role in cell survival can be damage. This kind of effect might lead to a failure of cell reproducibility and can also cause damage in chromosomes to replicate properly (Morgan and Sowa 2005) (see Figure 1). On the other hand, indirect radiation effects are caused when radiation interacts with water molecules. The water molecule inside the cells are ionized and free radicals are produced which are highly reactive molecules. These free radicals can break the bonds between cell components including DNA and thus cause cell destruction (Lewanski and Gullick 2001) (see Figure 1).

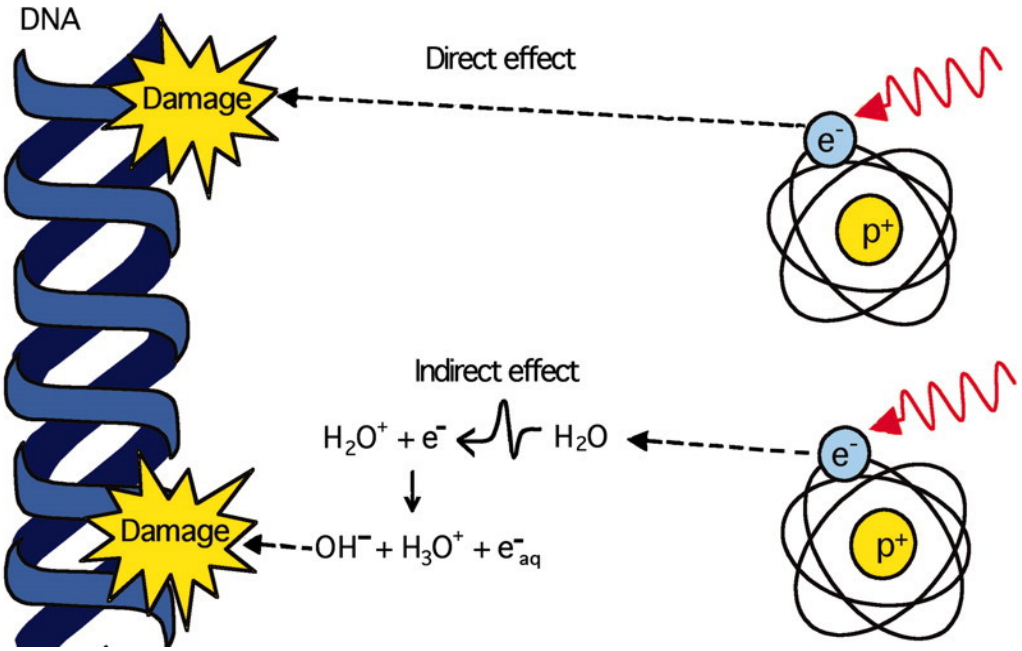

Figure 1: Direct and indirect effects of radiation. Different cellular cell components or atoms of DNA molecules can be affected directly by radiation (direct effect; upper part), whereas radiation may also activate water molecules (indirect effect; lower part). The latter effect results in breaking the bonds between the water molecules and the production of free radicals. Adapted from (Morgan and Sowa 2005).

Even though radiation therapy is considered to be one of the important treatments for curing cancer, it also remains a curse by harming normal cells with some side effects. Nevertheless, radiation therapy holds a huge potential promise for further cancer treatments (Thariat et al 2013).

1.1.2 TYPES OF RADIATION-INDUCED APOPTOTIC CELL DEATH

Exposure to IR results in a variety of malfunctions like damage of DNA resulting in DNA double strand breaks. This damage of DNA is found to be dose-dependent (Chang et al 1999, Haines et al 2002). Both high and low IR doses are able to cause adverse effects depending on the sensitivity of the cells. Radiation is known to target cells by depositing the energy directly on them but it was shown that even the cells that have never been directly exposed to irradiation are impaired because of the radiation dose applied to neighboring cells. This kind of effect is termed as the "*bystander effect*" (Prise et al 2003, Suzuki and Yamashita 2014, Ward 2002) and is able to induce apoptosis (programmed cell death) (Belyakov et al 2002) in unaffected cells or can also cause transformation processes in proteins associated with apoptosis (Vines et al 2009).

IR mediates cell death in two different ways, early (1.1.2.1) and late cell death (1.1.2.2). These two types of cell death are distinguished by two factors: firstly by the amount of time taken by cells to undergo apoptosis, and secondly by the characteristic biochemical changes observed in the cells (Shinomiya 2001). Furthermore, depending on the cell type, the mechanism of IR-induced cell death can vary (Joiner and van der Kogel 2009). It has been reported that under modulated changes in the IR doses, the same cells can exhibit both types of cell death. For example: compared to an IR dose of 20 Gy, where early cell death (within 4 to 6 h) could be observed with a vigorous apoptosis on the other hand radiation dose up to 5 Gy induced a late cell death (after 24 h or later) with moderate apoptosis in a U937 human monoblastoid cell line (Shinomiya et al 2000). Similar results were obtained in human leukemia cell lines (MOLT-4; HL-60) demonstrating that these particular cell lines were able to undergo both types of cell death upon IR, depending on different radiation doses (Mareková et al 2003, Shinohara and Nakano 1993).

1.1.2.1 Early cell death: pre-mitotic apoptosis

Early or pre-mitotic cell death is caused when cell death occurs before the mitosis. It is known to occur in certain or rather specific cell types (Kondo 2013, Shinomiya et al 2000). It is also known as interphase death. The affected cells undergo shrinkage, condensation, pyknosis and disruption of DNA (Shinomiya 2001, Yamada and Ohyama 1988). Early cell death occurs by irradiation-caused damage at cellular levels leading to an activation of various pathways for example the p53-pathway activated after IR-induced DNA double strand breaks ultimately resulting in cell death. Cells are, vice versa, no longer able to undergo early cell death when they bear a defect in the respective p53 gene (Joiner and van der Kogel 2009).

1.1.2.2 Late cell death: post-mitotic apoptosis

When cells pursuit mitosis and cell death occurs after a long period of time upon irradiation it is termed as late cell death or post-mitotic. This type of cell death is also named reproductive cell death, as the cells stop dividing. Affected cells lose their potential to form colonies, the hallmark of late cell death (Forrester et al 1999, Shinomiya 2001). Within some minutes after irradiation DNA damage response (DDR) is activated leading to activation of p53 and thus resulting in stimulation of various pro-apoptotic proteins (Sakaguchi et al 1998). On the other hand cell-cycle checkpoints and DNA repair systems are also activated by the DDR (Zhou and Elledge 2000). Even though provocation of pro-survival pathway is initiated by DDR, the

cells still prolong in the phase of apoptosis because of the initial deterioration affect in cells upon irradiation (Joiner and van der Kogel 2009).

1.1.3 RADIORESISTANCE AND CANCER CELLS

Radioresistant tumor cells are the results of certain factors (Peters et al 1982); however, the major reason still needs to be characterized. Even though a lot of efforts are undertaken to overcome a possible resistance of tumor cells towards radiation therapy however failure to this process has often been recorded. Most cancer cells can overcome the fractionated doses of irradiation and become radioresistant (Li et al 2014), but there are some cancer cell types showing inherited radioresistant capacities (Weichselbaum et al 1985).

A number of factors possibly promote cancer cells to become radioresistant. Some genes have been identified to modulate the radiation response of some cancer cells, being regulated up and down shown particularly in radioresistant pancreatic cancer cell lines. Genes that were found to be up-regulated were associated with amphiregulin, mitogen-activated protein kinase-activated protein kinase 2 (MAPKAPK2), regucalcin, and angiopoietin 2 and the down-regulated genes were related with caspase 8, retinoid esterification (lecithin retinol acyltransferase), and calcium-activated chloride channel 1 (Ogawa et al 2006). Further studies on the functional pathways of these up- and down-regulated genes might provide a beneficial strategy to better understand and react to radioresistance of cancer cells.

Among all radioresistant tumors, certain types of glioblastoma (glioblastoma multiforme) remain a special challenge. Glioblastomas which arise from astrocytes belong to the malignant glioma forms (Facchino et al 2011). Even though the treatment of glioblastomas with radiotherapy was found to be potent, it still remains ultimately lethal (Zhou et al 2013) because of the tumor reoccurrence in most cases (Nagashima et al 1989).

Gliomas are known to overcome radiation treatment by various mechanisms one of which is their capacity for repairing DNA (Bao et al 2006). Particularly, it has been shown that, in comparison to normal human astrocytes, glioma cells exhibit higher expression of γH2AX and Rad51 (DNA repair proteins) upon irradiation, which are the most important proteins in the process of regulating DNA repair (Short et al 2007). Another player in radioresistance of glioma stem cells are the Notch proteins, the critical factors for providing resistance to gliomas upon irradiation. The down-regulation of Notch-1 and 2 resulted in loss of radioresistancy by sensitizing the cells towards irradiation (Wang et al 2010). Another factor that might strongly cause radioresistance of gliomas is hypoxia. It is known that tumor cells have significantly less oxygen content compared to normal cells, and the hypoxic conditions has a great impact on the expansion of tumors (Amberger-Murphy 2009). A further

intermediate reported to promote the radioresistance of glioblastoma is the phosphatidylinositol-4,5-bisphosphate 3-kinase-Akt (PI3K-Akt). The activation of PI3K-Akt induces an increase in radioresistance of glioblastoma cells, whereas the use of PI3K-Akt inhibitors or their inhibition at the genetic level carries the potential to abolish this effect (Li et al 2009).

1.2 REACTIVE OXYGEN SPECIES (ROS)

Reactive oxygen species (ROS), also known as oxygen radicals, are molecules derived from oxygen which are chemically active (Rada and Leto 2008). They are known to originate endogenously in the human body and play an important role in the pathophysiology of various diseases (Alfadda and Sallam 2012, Devasagayam et al 2004). Several categories of ROS are known to be generated in particular alkoxyl (RO·), hydrogen peroxide (H_2O_2), hydroxyl radicals (·OH), nitrogen dioxide ($\cdot NO_2$), nitric oxide (·NO) peroxynitrite ($ONOO^-$) and superoxide anions ($O_2^{\cdot -}$) (Finkel and Holbrook 2000). Cellular molecules like DNA (Luo et al 2013), lipids (El-Aal 2012) and proteins (Stadtman 1990, Stadtman and Levine 2000) can be harmed by the production of ROS. A damage of these macromolecules through oxidative stress leads to changes involved in a variety of human diseases including acute myeloid leukemia (AML) (Ghoti et al 2007, Novotna et al 2009, Zhou et al 2010), atherosclerosis (Ding et al 2013), bone related disorders (Ha et al 2004, Kanzaki et al 2013, Lean et al 2005, Lee et al 2005b, Srinivasan et al 2010), diabetes (Babizhayev et al 2014), fibrotic disease (Sampson et al 2012), neurological disorders (Okado-Matsumoto and Fridovich 2002, Palacino et al 2004, Shimoda-Matsubayashi et al 1996) and obesity (Calzadilla et al 2011, Furukawa et al 2004) etc. Recently it has been reported that ROS can act as an important target during cancer progression, showing ROS co-ordinates with other regulators like p53 in mediating cell death (Ribas et al 2015). ROS is also known to be an intermediate of various signaling pathways: protein kinase B /mechanistic target of rapamycin (Akt/mTOR) pathway (Cai and Andres 2014, Cao et al 2009, Fiorini et al 2015), extracellular-signal-regulated kinases (ERK) and activator protein-1 (AP-1) signaling (Czaja et al 2003), c-Jun N-terminal kinases (JNK/c-Jun) signaling pathway (Amir et al 2012, Singh et al 2009), mitogen-activated protein kinases (MAPK) activation (Olavarria et al 2015) and nuclear factor kappa-light-chain-enhancer of activated B cells (NF-kappaB) (Natarajan et al 2002, Storz and Toker 2003, Volanti et al 2002).

Various sources of ROS production have been reported: cyclooxygenase (Beak et al 2004), lipoxygenase (Mascayano et al 2014), mitochondrial electron transport enzymes (Lambert and

Brand 2009), nicotinamide adenine dinucleotide phosphate-oxidase (NADPH oxidase) (Paravicini and Touyz 2008), nitric oxide synthase (Vasquez-Vivar and Kalyanaraman 2000) and xanthine oxidase (Pritsos 2000). Both mitochondrial and NADPH oxidase ROS are the most studied means of ROS production.

1.2.1 MITOCHONDRIAL ROS PRODUCTION

Mitochondria are considered to be the most important sources of ROS production. Superoxide anions ($O_2^{\cdot -}$) are the best studied and understood ROS produced by mitochondria in mammals. The production of mitochondrial ROS is regulated by the oxidative phosphorylation (OXPHOS) process in the inner mitochondrial membrane through the electron transport chain (ETC). OXPHOS involves the formation of adenosine triphosphate (ATP) by using oxygen in the ETC. The latter contains various complexes namely: complex I (Nicotinamide adenine dinucleotide (NADH) dehydrogenase), complex II (succinate dehydrogenase), complex III (ubiquinol-cytochrome c reductase), complex IV (cytochrome c oxidase) and complex V (Adenosine triphosphate (ATP) synthase). In the ETC, a diffusion of electrons from complex I and III leads to a reduction of oxygen producing superoxide (Li et al 2013a, Murphy 2009) (see Figure 1.2.1).

Mitochondrial ROS is involved in a variety of diseases including amyotrophic lateral sclerosis (ALS) (Okado-Matsumoto and Fridovich 2002), atherosclerosis (Ding et al 2013), heart failure (Schwarzer et al 2014), ischaemia-reperfusion injury (Liang et al 2013) and Parkinson's disease (Palacino et al 2004, Shimoda-Matsubayashi et al 1996). Also, its involvement during the ageing process (Ames et al 1995, Terman et al 2010) and in tumor angiogenesis has been reported (Zhou and Ryeom 2014).

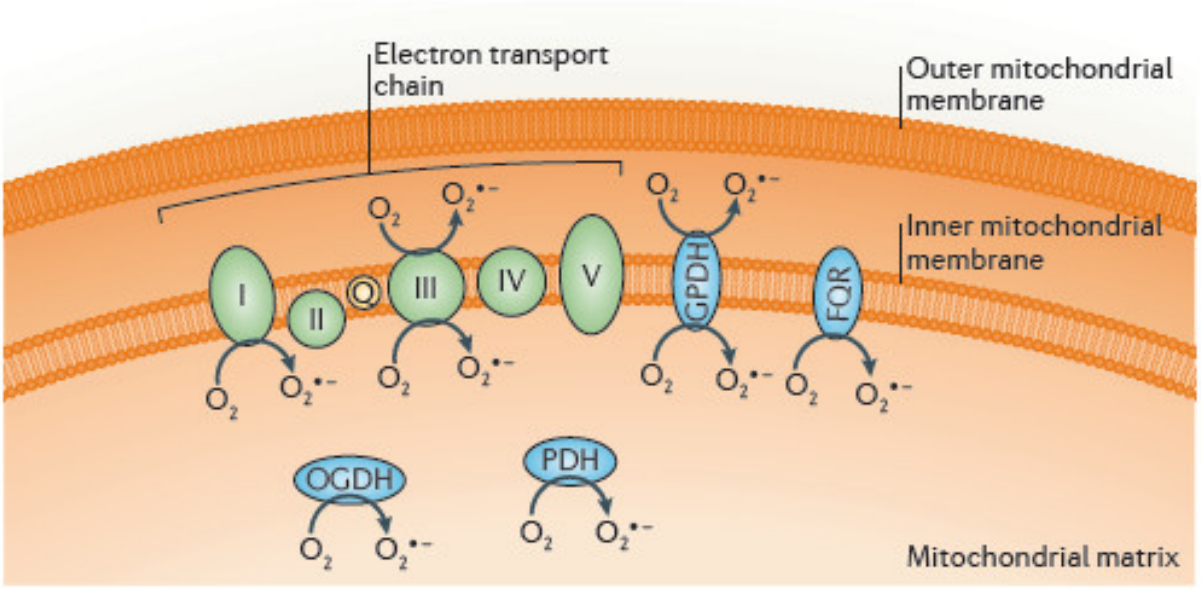

Figure 1.2.1: Superoxide is generated within the mitochondrial matrix and inner mitochondrial membrane. The complexes I and III of the ETC are the major sources of its production. However, 2-oxoglutarate dehydrogenase (OGDH), pyruvate dehydrogenase (PDH), glycerol 3-phosphate dehydrogenase (GPDH) and also the electron transfer flavoprotein-ubiquinone oxidoreductase (FQR) are additional sources for generating superoxide in mitochondria (Holmstrom and Finkel 2014).

1.2.2 NADPH OXIDASE SYSTEM AS A SOURCE OF ROS PRODUCTION

In addition to mitochondria, other sources for ROS production in a variety of cell lines has been identified, one of them include NADPH oxidase (NOX) (Weyemi and Dupuy 2012). NOX is known to be a strong regulator of ROS generation in phagocytic cells in mammals (Orient et al 2007). It is a membrane-bound enzyme and drives the release of superoxide from oxygen and NADPH. It is the complex assembled by components containing: the membrane subunits (gp91phox and p22phox) and the cytosolic subunits (p40phox, p47phox, p67phox, and two guanine nucleotide-binding proteins: guanosine triphosphate (GTP) Rac-1 and Rac-2) (Assari 2006). Upon various stress stimuli, phosphorylation of the cytosolic component p47phox takes place and results in a complete translocation of cytosolic proteins to the cell membrane. This process leads to activation and assembly of both the membrane and the cytosolic subunit forming a complete NOX complex (Figure 1.2.2). Rac-1 and Rac-2 play a pivotal role during cytosolic translocation and complex formation (Babior 1999, Dang et al 1999).

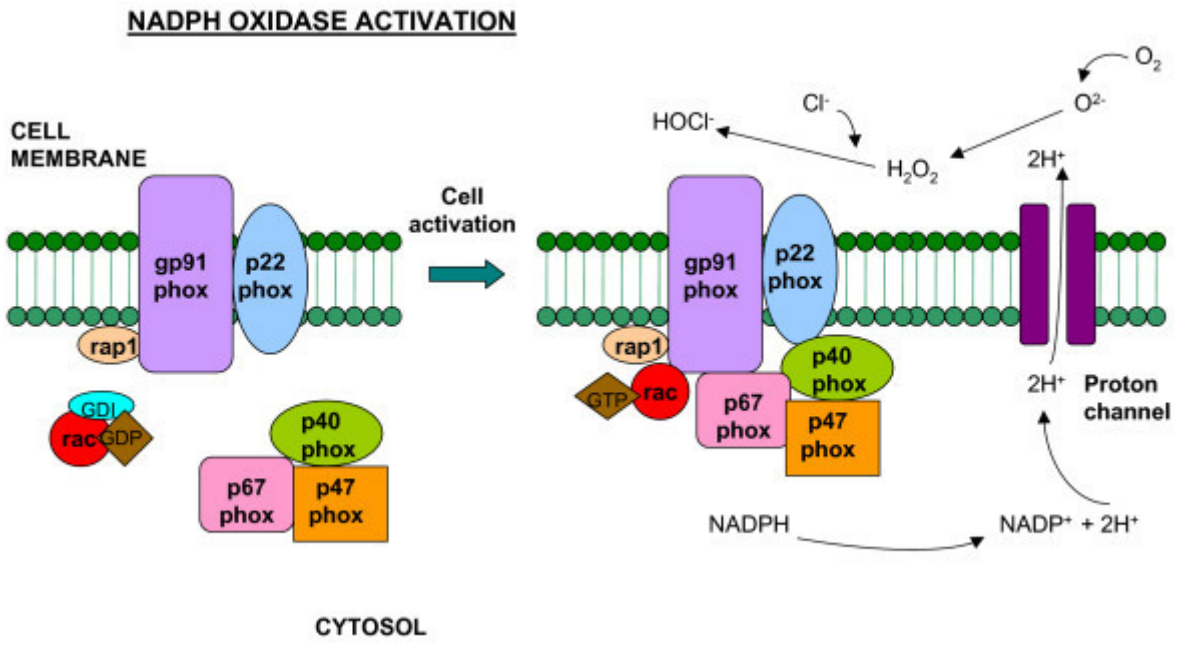

Figure 1.2.2: NOX comprises membrane subunits and cytosolic subunits. The membrane subunits consist of p22phox and gp91phox, and the cytosolic subunits consists of p40phox, p47phox, p67phox, and GTP binding proteins. Upon cell activation, the cytosolic subunits translocate to the cell membrane forming a complete NADPH oxidase complex, further resulting in ROS generation (Assari 2006).

NOX seems to play a vital role in various diseases including Alzheimer's disease (Shimohama et al 2000, Zekry et al 2003), atherosclerosis (Sorescu et al 2002), diabetes (Kowluru and Kowluru 2014, Padgett et al 2015), kidney disease (Thallas-Bonke et al 2014) and Parkinson disease (Zhang et al 2014) etc.

1.3 CERAMIDE AND CERAMIDE-ENRICHED MEMBRANE PLATFORMS

1.3.1 MEMBRANE RAFTS AND PLATFORMS

On the basis of thermodynamics, both structure and organization of lipids and proteins in cell plasma membranes were described through a model termed as *fluid mosaic model* (Singer and Nicolson 1972). Within the plasma membrane, lipid interaction appears weaker and short-termed when compared to protein-protein interactions (Harder and Simons 1997). High concentration of proteins in cell membranes can, however, affect the lipid-lipid organization (Garcia-Saez and Schwille 2010). The plasma membrane constitutes of several different lipids, namely glycerophospholipids, sphingolipids and cholesterol.

Several studies have suggested existence of a distinct membrane domains existing in a liquid-ordered phase. These domains are composed of sphingolipid and cholesterol. Sphingomyelin

which is the prevalent cellular sphingolipid in the membrane is composed of a hydrophobic ceramide moiety and a hydrophilic phosphorylcholine head group. Sphingolipids are known to associate with each other via hydrophilic interactions and cholesterol via hydrophobic van der Waal interactions or hydrogen bonds (Brown and London 1998, Harder and Simons 1997, Simons and Ikonen 1997). Cholesterol is known to fill the voids between sphingolipids and stabilizes these domains (Simons and Ikonen 1997, Xu et al 2001). These interaction between lipids results in lateral separation of sphingolipids and cholesterol which results in the formation of sphingolipid and cholesterol-enriched membrane domains (Brown and London 1998, Simons and Ikonen 1997) which are termed as membrane rafts. Because of the strong interaction between cholesterol with sphingolipids and the tight packing of acyl chains sphingolipids, phase separations within the membrane occurs resulting in a liquid-ordered phase (Brown and London 2000). On the other hand phospholipids with unsaturated acyl chains interact very weakly with cholesterol which results in liquid-disordered phase (Brown and London 2000, Brown 2006).

Two types of proteins within the lipid rafts have been identified to date: firstly those which contain caveolins with their further subtypes caveolin-1, 2, and 3 (Ostrom and Insel 2006) and secondly those containing flotillins with their further subtypes flotillin-1 and 2 (Volonte et al 1999). Caveolins and flotillins are plasma membrane proteins found in mammals (Parolini et al 1996, Salzer and Prohaska 2001). They are involved in a variety of cell functions like cell signaling, cell trafficking and cell signal transduction process (Alonso and Millan 2001, Simons and Toomre 2000). They are also known to play a role in various diseases including cancer (Cohen et al 2004). More specifically, the role of caveolin-1 has been reported clearly with its participation in promoting metastasis and tumor growth progression by suppression of apoptosis (Ho et al 2002, Ito et al 2002, Kato et al 2002, Shatz and Liscovitch 2008, Suzuoki et al 2002, Thompson et al 2010, Yang et al 1998).

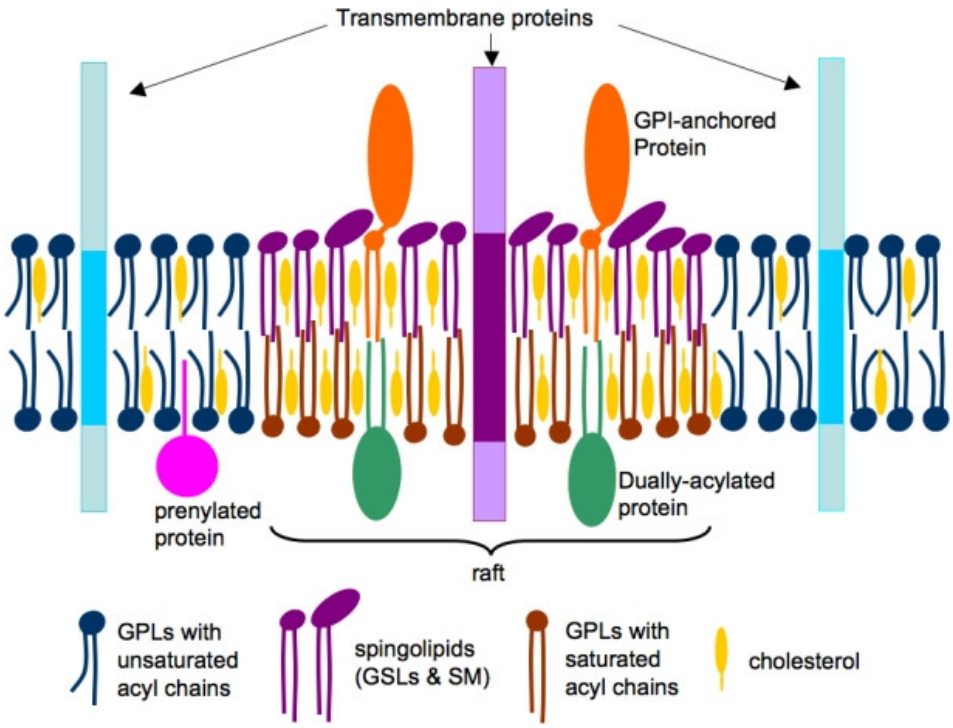

Figure 1.3.1 Structure of lipid rafts. Lipid rafts are composed of phospholipids with unsaturated fatty acyl chains (in dark blue) and saturated fatty acyl chains (in brown) plus cholesterol (in yellow). The distribution of phospholipids and cholesterol in the cell plasma membrane can be observed in the intracellular as well as in the extracellular compartment. However, sphingolipids (in purple) exist mainly in the external part. Various proteins are concentrated in a lipid raft: transmembrane proteins (light blue), glycosylphosphatidylinositol-anchored proteins (orange), dually acylated proteins (in green) and prenylated protein (in pink) (Waheed and Freed 2009). (GPI glycosylphosphatidylinositol; GPLs glycerophospholipids; GSLs glycosphingolipids; SM sphingomyelin)

Ceramide, a bio-active sphingolipid, plays a specific and important role in regulating the lipid rafts (Cremesti et al 2002). Ceramide-rich "domains" are known to be in a highly ordered state in comparison to cholesterol-containing rafts. Furthermore, ceramide shows the tendency to dislocate cholesterol from rafts which can cause a distinct property change in raft composition (Megha and London 2004, Yu et al 2005).

1.3.2 CERAMIDE STRUCTURE AND GENERATION

Ceramide is composed of a sphingosine joined with an amide bond to fatty acyl chains (Figure 1.3.2 a). Ceramide has been previously believed to be an entirely structural element found in the cell plasma membrane, but by now, its involvement in a variety of signaling pathways has been made clear (Chalfant et al 2002, Gulbins et al 1995, Hsieh et al 2014, Huwiler et al 1996, Kashiwagi et al 2002a, Yabu et al 2015, Zhang et al 1997).

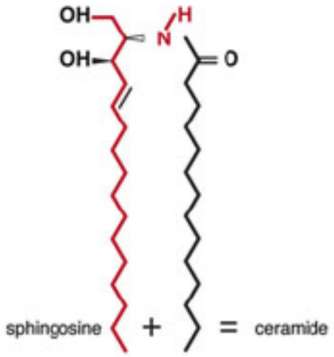

Figure 1.3.2 (a): **Structure of ceramide.** Ceramide consists of a long chain base which is linked to a fatty acid via an amide bond. Adapted from (Mencarelli and Martinez-Martinez 2013).

Two pathways are known to be involved in the generation of sphingolipids/ceramide (Figure 1.3.2 b).

1. The *sphingomyelin hydrolysis pathway* proceeds with the hydrolysis of sphingomyelin by activation of the enzyme sphingomylinases (SMases) resulting in the formation of ceramide and phosphorylcholine. Three different types of sphingomylinases (SMases) have been identified on the basis of their pH-optimum: acidic SMases, neutral SMases, and alkaline SMases. They are known to be localized in different compartments within the cells (Fensome et al 2000, Hofmann et al 2000, Rajagopalan et al 2015, Spence et al 1983, Stoffel 1999, Tomiuk et al 2000, Wu et al 2010, Wu et al 2005).
2. The *de novo pathway* involves merging of serine and palmitate-CoA giving rise to 3-ketosphinganine which contains 18 carbon. The reaction is catalyzed by the enzyme serine palmitoyltransferase (SPT). Further, 3-ketosphinganine is reduced by the enzyme 3-ketosphinganine reductase (KDS) producing sphinganine. The next reaction continues with the production of di-hydro-ceramide (dhCer) by the enzyme ceramide synthase (CerS) (Mathias et al 1998, Michel et al 1997). CerS consists of a family of six enzymes with each of them showing a preference towards the acyl CoA chain length (Pewzner-Jung et al 2006, Saddoughi et al 2008). Based on its resemblance with the yeast longevity assurance gene 1 protein (LAG1p), CerS has been named as Lass (Longevity Assurance) genes (Riebeling et al 2003, Venkataraman et al 2002). Thus, CerS is an important enzyme for ceramide generation. Finally, in the presence of the enzyme dihydro-ceramide (dhCer) desaturase (DES), dhCer which lacks 4, 5-*trans*-double bond is desaturated producing ceramide with 4, 5-*trans*-double bond. This pathway takes place within the endoplasmic reticulum (ER). The generated ceramide is then carried to the Golgi

apparatus by help of ceramide transporter proteins (Kawano et al 2006) or by vesicular or non-vesicular processing (Funato and Riezman 2001) (Figure 1.3.2 b).

Once ceramide is formed, it can be utilized by ceramidases (CDases) to produce sphingosine (Sph), which is phosphorylated to sphingosine-1-phosphate (S1P) by sphingosine kinases (SK) (Kohama et al 1998, Liu et al 2000). S1P can also be dephosphorylated by the action of enzyme SPPase (Sph phosphate phosphatase) to generate Sph (Mandala 2001, Mao and Obeid 2008). Ceramide can be phosphorylated by ceramide kinase (CK) which is then recycled by a ceramide-1-phosphate (C1P) phosphatase (C1PP) (Shinghal et al 1993) and further glycosylated to glucosylceramide (GC) and galactosylceramide (GalC) by the action of glucosylceramide synthase (GCS) or galactosylceramide synthase (GalCS) respectively. GC once formed can be translocated to leaflets from the late Golgi compartment with the involvement of four-phosphate adaptor proteins (FAPP2) (D'Angelo et al 2007). GC can be further processed and metabolized into complex glycosphingolipids which is essential for cell development and differentiation (Pescio et al 2012, Yamashita et al 1999). Ceramide glycosylated to GalC can be sulfated to form sulfatide.

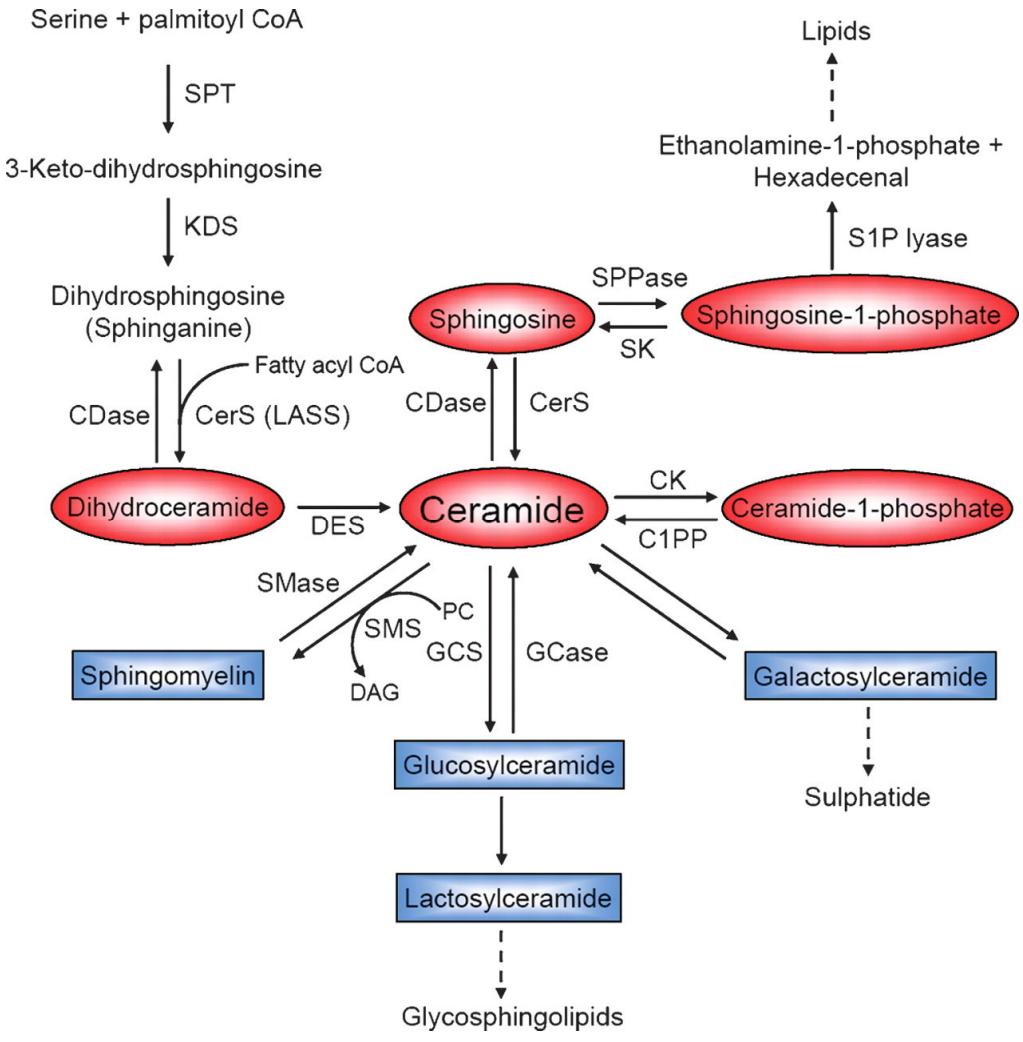

Figure 1.3.2 (b): **Sphingolipid/Ceramide metabolism.** The *sphingomyelin hydrolysis* pathway generates ceramide via actions of acid or neutral SMase. Both enzymes break down sphingomyelin giving rise to ceramide and phosphorylcholine. The *de novo* pathway is regulated by the enzyme serine palmitoyltransferase involving various other enzymes (Bartke and Hannun 2009). (SPT serine palmitoyltransferase; KDS 3-keto-dihydrosphingosine reductase; DES dihydroceramide desaturase; SPPase Sph phosphate phosphatase; CK Ceramide kinase; C1PP C1P phosphatase; SMS SM synthase; PC phosphatidylcholine; DAG diacylglycerol; GCS glucosylceramide synthase; GCase glucosyl CDase)

Among various sphingolipids, ceramide is known to be involved in different cell functions. It is certainly considered to be an important component for inducing apoptosis; it also participates in cancer cell death, differentiation and senescence (Karahatay et al 2007, Koybasi et al 2004, Ogretmen and Hannun 2004, Senkal et al 2007).

Ceramide is known to be involved in cell signaling pathways by interacting with varieties of targets. It activates the kinase **s**uppressor of RAS (KSR) (Zhang et al 1997). In intestinal epithelial cells, KSR is involved in the activation of extracellular-signal-regulated kinases (ERKs) ERK1/ERK2 mediated by ceramide (Yan and Polk 2001). If B-cell lymphoma 2 (Bcl-2)-antagonist of cell death (BAD), a pro-apoptotic member of the Bcl-2 family are absent, KSR stimulates pro-inflammatory response (Basu et al 1998, Kolesnick and Kronke 1998). Ceramide also interacts with c-Raf kinase and has been shown to increase its activity by selectively binding to it, resulting in a provocation of mitogen-activated protein kinases (MAPK) signaling process (Huwiler et al 1996). Along with kinases, ceramide also interacts with various other proteins like protein phosphatases called ceramide-activated protein phosphatases (CAPP) (Chalfant et al 1999, Dobrowsky et al 1993, Law and Rossie 1995, Wolff et al 1994) , protein kinase C (PKC) isoforms: (PKC)-alpha and –delta (Huwiler et al 1998), PKC-eta (Kashiwagi et al 2002b), PKC-zeta (Müller et al 1995) and cathepsin D (Heinrich et al 1999). An interaction of ceramide with its targets can be direct or indirect; however, the mechanisms underlying these interactions are not yet well known. Some of the direct interactions of ceramide to its targets have been clearly described: Ceramide for instance directly interacts with calcium-dependent phospholipase A_2 ($cPLA_2$) via the calcium-dependent phospholipid binding (CaLB) domain resulting in a pro-inflammatory response (Huwiler et al 2001). On the other hand, involvement of ceramide by indirect interactions has also been reported, involvement of ceramide in regulating ion channels: n-K^+ channel ($K_v1.3$) (Gulbins et al 1997, Szabó et al 1996) and calcium release-activated calcium channels (CRAC) (Lepple-Wienhues et al 1999).

1.3.3 ACID SPHINGOMYELINASE (ASM)

Acid sphingomyelinase (human: ASM, murine: Asm) (ASM EC 3.1.4.12) is one of the enzymes categorized as sphingomyelinases (SMases) identified to catalyze the hydrolysis of sphingomyelin to ceramide and phosphorylcholine. Depending on the optimum pH, SMases are divided into acid SMases, neutral SMases and alkaline SMases (Cheng et al 2002, Duan et al 2003, Quintern et al 1987, Stoffel 1999, Tomiuk et al 2000, Yamanaka and Suzuki 1982, Zou et al 1989). There exists three forms of neutral SMases: neutral SMase 1 (Tomiuk et al 2000), neutral SMase 2 (Kim et al 2010) and neutral SMase 3 (Krut et al 2006). It has been shown that neutral SMases depend on magnesium (Mg^{2+}) for their activity, whereas acid SMases do not require Mg^{2+} for activation (Liu and Hannun 1997). Though the alkaline SMase depicts the least studied enzyme out of the three, but its role in generating ceramide with anti-proliferating and anti-inflammatory functions has also been recognized (Hertervig et al 2003, Wu et al 2005, Wu et al 2006).

Among these SMases, ASM is the best characterized enzymes. This enzyme received a lot of attention when studies revealed its role in a genetically inherited disorder known as the Niemann-Pick disease (NPD) types A and B (Brady et al 1966, Horinouchi et al 1995, Schneider and Kennedy 1967). In both types, the sphingomyelin phosphodiesterase 1 (SMPD1) gene encoding ASM is mutated. NPD A appears during infancy with a fast accelerating atrophy of the nervous system leading to early childhood death, whereas NPD B, known as non-neurological type, does not involve the nervous system but has rather aggressive impacts on various organs leading to retarded growth, lung infections, hepatosplenomegaly etc. (Schuchman and Miranda 1997). NPD A remains to be a fatal disorder with rapid neurodegenerative progress resulting in death by 2-3 years whereas NPD B, a benign form is seen to occur with later outbreak and prolong survival. Clinically, these two forms of NPD are differentiated by the amount of lysosomal ASM activity (Graber et al 1994).

Two types of ASM are characterized based on their localization: lysosomal sphingomyelinase (L-SMase) (Fowler 1969, Jenkins et al 2011) and secretory sphingomyelinase (S-SMase) (Schissel et al 1996). The name L-SMase hints at its being located in lysosomes, whereas the S-SMase is secreted into the serum (Schissel et al 1998). The two ASM forms differ in the trafficking process controlled by the same protein precursor. There exists distinct glycosylation pattern between L-SMase and S-SMase: S-SMase is transported to plasma membrane via Golgi secretory pathway in contrast to L-SMase which depends on lysosomal trafficking (Schissel et al 1998). L-SMase is known to be independent of Zinc (Zn^{2+}) for its

activation in contrast to S-SMase (Schissel et al 1996, Schissel et al 1998). The role of L-SMase in mediating apoptosis is also been reported. Its involvement in activating Bcl-2-associated X protein (BAX) by stimulating apoptotic cascade signaling (Jin et al 2008a, Kashkar et al 2005), mitochondrial dysfunction (Zeidan et al 2008b), and activation of caspases with the involvement of cathepsin D (Heinrich et al 2004) has been well described. Compared to L-SMase, the role and function of S-SMase in stimulating ceramide production and inducing cells death is unclear to date, but an increase in the level and activity of S-SMase in serum has been found in multiple diseases, for instance in chronic heart failure (Doehner et al 2007), hemophagocytic lymphohistiocytosis (Takahashi et al 2002), severe sepsis (Claus et al 2005), type 2 diabetes (Górska et al 2003) and in context to spatially fractionated radiation treatment (Sathishkumar et al 2005).

1.3.4 ASM ENZYMOLOGY

Identified as a lysosomal enzyme (Fowler 1969), ASM was first purified and characterized from human sources like placenta, brain, urine etc. (Lansmann et al 1996, Quintern et al 1987, Sakuragawa 1982, Yamanaka and Suzuki 1982). The gene encoding ASM, designated as SMPD1, was isolated and further cloned and characterized (Quintern et al 1989, Schuchman et al 1992).

ASM protein possessing 629 amino acid exists in a monomeric form with a molecular weight of ~ 72 kDa, de-glycosylation reduces the protein to a molecular weight of ~ 60 kDa (Hurwitz et al 1994, Lansmann et al 1996). Further findings revealed that ASM complementary DNA (cDNA)-transfected COS-1 cells show the existence of two different forms: a 70 kDa ASM which is sited in lysosomal compartment, proteolytic cleavage results in the second ASM form with of 57 kDa, which is secreted. In contrast to the mature 70 kDa form, the latter 57 kDa ASM does not possess an oligomannosyl-phosphate residue (Ferlinz et al 1994). Using site-directed mutagenesis, the N-glycosylation sites of ASM was identified, showing that five out of these six sites were occupied. Eviction of two C-terminal N-glycosylation sites resulted in disturbed enzyme formation and activity whereas no observational changes were seen when the remaining four N-terminal glycosylation sites were removed (Ferlinz et al 1997).

ASM possesses 17 cysteine residues out of which only 16 cysteines are used for forming 8 intramolecular disulfide bonds; the C-terminal cysteine (Cys629) remains free (Lansmann et al 2003) and is involved in activating ASM; modification and deletion of C-terminal cysteine (Cys629) resulted in an increase activity of ASM. Cys629 was reported to be involved in the activation mechanism of the ASM and dimerization of enzyme via an oxidation reaction (Qiu

et al 2003). Thus it might be taken into consideration that C-terminal cysteine (Cys629) is an important factor involved in the regulation and activation of ASM.

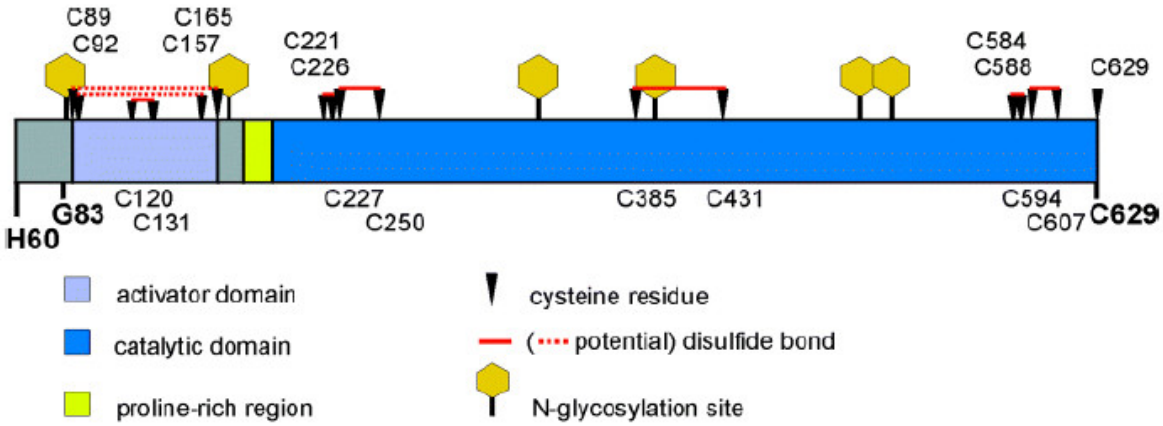

Figure 1.3.4: ASM disulfide bond and domain structure arrangement. The disulfide bond pattern is shown as the activator domains containing three bonds (C120-131, C89-C165, C92-C157) and the catalytic domain containing five bonds (C221-C226, C227-C250, C385-431, C584-C588, C594-C607) (Lansmann et al 2003).

1.3.5 ASM/CERAMIDE AND CERAMIDE-ENRICHED MEMBRANE PLATFORMS

Formation of ceramide and ceramide-enriched membrane platforms with the involvement of activated ASM has been shown to occur upon various stimuli including bacterial and viruses infection, death receptors, radiation, ultraviolet (UV)-light etc. (for complete details about stimuli and reference see Table 1). Activation of ASM is also known to be related to its translocation from lysosome to plasma membrane (Grassmé et al 2001a, Perrotta et al 2010). Hydrolysis of sphingomyelin in the presence of ASM or S-SMase results in the generation of ceramide (see section 1.3.3). These molecules have the tendency to rapidly fuse and form small ceramide-enriched membrane microdomains. The small microdomains again fuse resulting in the formation of ceramide-enriched membrane macrodomains (*ceramide-enriched membrane platforms*) (Grassmé et al 2001a, Grassmé et al 2001b, Megha and London 2004).

In general ceramide-enriched membrane platforms can intrigue various receptor molecules such as cluster of differentiation (CD)95 (Grassmé et al 2001a, Grassmé et al 2001b), CD40 (Grassmé et al 2002a) , FcγRII (Abdel Shakor et al 2004) and CD20 (Bezombes et al 2004) and thus results in clustering and re-organization of these molecules, creating a high receptor density in the surface of cells. Thus by possessing the ability to stabilize and organize receptors molecules, the ceramide-enriched membrane platforms play an important role in transmitting intracellular cell death signals.

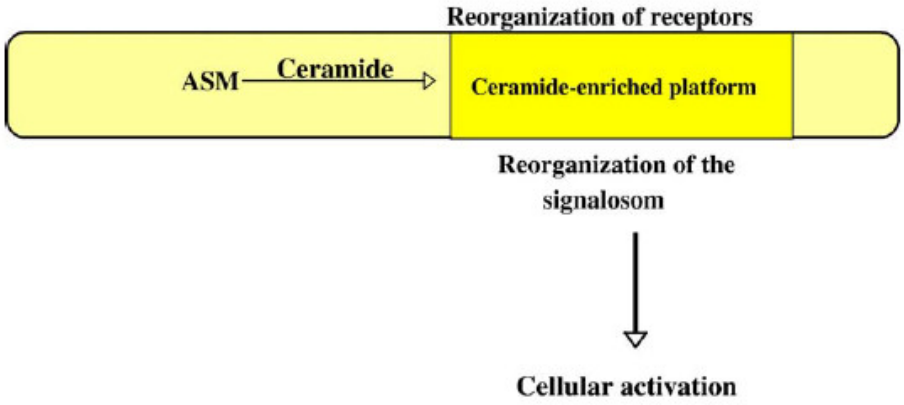

Figure 1.3.5: Formation of ceramide-enriched membrane platforms. The activation of ASM enzymes results in lipid raft alteration from the formation of small ceramide-enriched microdomains to ceramide-enriched macrodomains, i.e. membrane platforms. Ceramide-enriched membrane platforms are able to trap various receptors and hence transfer cell death signals inside the cells (Bollinger et al 2005).

Accordingly, role of ASM/ceramide and ceramide-enriched membrane platforms in infectious biology has also been marked in several studies. Ceramide-enriched membrane platforms was shown to be a central requirement for bacteria to infect the host cells, as found for *Neisseria gonorrhoeae* (*N. gonorrhoeae)*, and *Pseudomonas aeruginosa (P. aeruginosa)* (Grassmé et al 1997, Grassmé et al 2003b) or Rhinovirus and the Sindbis virus (Grassmé et al 2005, Jan et al 2000). In human epithelial cells, an infection with the bacterium *N. gonorrhoeae* resulted in activation of ASM, production of ceramide and the generation of ceramide-enriched membrane platforms. A genetical or pharmacological inhibition of ASM however interrupted this event preventing the *N. gonorrhoeae* infection in human epithelial cells (Grassmé et al 1997). In human neutrophils it was shown that ceramide-enriched membrane platforms reorganize the Carcinoembryonic antigen-related cell adhesion molecules (CEACAM) receptors and the intracellular signaling molecules resulting in an internalization of Opa_{52} protein of *N. gonorrhoeae* bacteria (Hauck et al 2000). Studies from Grassmé and coworkers demonstrated that CD95 receptors clustered in ceramide-enriched membrane platforms might be involved in the apoptosis induction by *P. aeruginosa* (Grassmé et al 2000). An infection of human epithelial cells with Rhinoviruses induces an uptake of viruses with further activation of ASM and formation of ceramide-enriched membrane platforms (Grassmé et al 2005). The role of ceramide-enriched membrane platforms in inducing the apoptotic cascade with an entry of Sindbis virus in neuroblastoma cells was also reported (Jan et al 2000). Similarly it was shown that *Plasmodium falciparum (P. falciparum)* expresses its own sphingomyelinase for generation of ceramide which is essential for erythrocyte infection with *P. falciparum* (Hanada et al 2002).

Similarly role of ASM/ceramide and ceramide-enriched membrane platforms has also been shown in context to chemotherapeutic drugs, radiation, UV-light and other stresses like ROS resulting in induction of apoptosis (for complete reference see Table 1). Upon irradiation various cells are able to activate ASM with generation of ceramide leading to apoptosis (Garcia-Barros et al 2003, Lee et al 2011, Morita et al 2000, Paris et al 2001, Peña et al 2000, Santana et al 1996). Requirement of ASM to induce apoptosis upon irradiation has been confirmed in cells as well as in mice model whereas deficiency of this enzyme has shown hindrance to this event (Santana et al 1996). Endothelial cells are the best-described example for radiation-induced apoptosis with the involvement of ASM (Garcia-Barros et al 2003, Paris et al 2001, Peña et al 2000). Upon irradiation, dose-dependent apoptosis was observed in central nervous system (CNS) of C57Bl/6 or C3H/HN mice and 20 % apoptosis was observed in endothelial cells whilst Asm knockout mice showed resistant up to 40 Gy (Peña et al 2000). Further studies showed that whole body irradiation of C57Bl/6 mice resulted in death of mice within 10-13 days with gastrointestinal (GI) syndrome. At 4 h after irradiation, apoptosis in the crypt/villus of micro vessels was noticed, severe apoptosis of endothelial cells at a dose rate 15 Gy was seen which corresponded with GI syndrome. Basic fibroblast growth factor (BFGF) administered intravenously abolished endothelial apoptosis and radiation-induced damage of crypt or failure of organs and GI death. Furthermore upon 15 Gy, protection of endothelial apoptosis and GI death in Asm-deficient mice was observed (Paris et al 2001). Similarly, involvement of BFGF as a savior from radiation-induced cell death in endothelial cells has also been significant in both *in vivo* and *in vitro* studies (Fuks et al 1994, Fuks et al 1995). Intravenous BFGF was able to protect radiation pneumonitis in C3H/HeJ mice with increment lethal dose (LD) $_{50/180}$ from 20.75 Gy to 23.0 Gy (Fuks et al 1995).

Apart from endothelial cells, oocytes of fertile female mice responded to radiation-induced Asm- dependent cell death. Apoptosis in oocytes was observed in Asm positive mice while Asm deficient mice rescued this phenomenon. When treated with sphingosine 1-phosphate (antagonist of ceramide), oocytes were protected against radiation as well as doxorubicin induced apoptotic cell death (Morita et al 2000). Along with radiation, UV-light is also involved in mediating ASM induced cell death (Charruyer et al 2005, Kashkar et al 2005, Rotolo et al 2005, Zhang et al 2001). Apoptosis induction was confirmed in ASM wild type B lymphocytes with results in activation of ASM, generation of ceramide leading to activation of signaling cascade of JNK whereas no such JNK activation was observed in ASM deficient B lymphocytes cells upon UV-light (Zhang et al 2001).

PATHOGENS (BACTERIA AND VIRUSES)	RECEPTORS	CHEMOTHERAPEUTIC DRUGS /RADIATION AND OTHER STRESSES	OTHER FACTORS
Listeria monocytogenes (Utermöhlen et al 2003)	**CD5** (Simarro et al 1999)	**Cisplatin** (Lacour et al 2004, Zeidan et al 2008a)	**Platelet activating factor** (Predescu et al 2013, Samapati et al 2012)
Measles virus (Avota et al 2011, Gassert et al 2009)	**CD14** (Pfeiffer et al 2001)	**Cu^{2+}-treatment** (Lang et al 2007)	**Tumor necrosis factor (TNF)** (Garcia-Ruiz et al 2003, Schütze et al 1992, Schütze et al 1994)
Mycobacterium avium (Utermöhlen et al 2008)	**CD20** (Bezombes et al 2004)	**Doxorubicin** (Dumitru et al 2007)	**Visfatin** (Boini et al 2010)
Neisseria gonorrhoeae (Grassmé et al 1997, Hauck et al 2000)	**CD28** (Boucher et al 1995)	**Heat damage** (Chung et al 2003)	
Pseudomonas aeruginosa (Grassmé et al 2003b, Zhang et al 2008)	**CD32 (FCγRII)** (Abdel Shakor et al 2004, Korzeniowski et al 2007)	**Ischemia-reperfusion injury** (Yu et al 2000)	
Rhinoviruses (Dreschers et al 2007, Grassmé et al 2005, Miller et al 2012)	**CD38** (Jia et al 2008)	**Oxidative stress** (Li et al 2012, Zhang et al 2007)	
Salmonella typhimurium (McCollister et al 2007)	**CD40** (Grassmé et al 2002b)	**Oxygen radicals** (Scheel-Toellner et al 2004)	
Sindbis virus (Jan et al 2000)	**CD95** (Cifone et al 1994, Cremesti et al 2001, Grassmé et al 2001a, Grassmé et al 2001b, Gulbins et al 1995, Perrotta et al 2010)	**UV-light** (Charruyer et al 2005, Kashkar et al 2005, Rotolo et al 2005, Zhang et al 2001)	
Staphylococcus aureus (Esen et al 2001)	**CD95- death-inducing signaling complex**	**γ-irradiation** (Lee et al 2011, Paris et al 2001,	

	(DISC) (Grassmé et al 2003a)	Santana et al 1996)	
	CD253 TNF-related apoptosis-inducing ligand (TRAIL) (Dumitru and Gulbins 2006, Dumitru et al 2007, Li et al 2013b)		
	interleukin (IL)-1 receptor (Mathias et al 1993)		
	TNF-receptor (Ardestani et al 2013, Edelmann et al 2011)		

Table 1: Overview of various factors stimulating activation/translocation of ASM and formation of ceramide and ceramide-enriched membrane platforms.

1.4 RADIATION AND ASM/CERAMIDE-INDUCED CELL DEATH

1.4.1 INVOLVEMENT OF ASM AND CERAMIDE IN IRRADIATION-INDUCED CELL DEATH

In treating various cancers like intraorbital tumors (Hein et al 2005), nasopharyngeal cancer (Hunt et al 2001, Wolden et al 2001), non-small-cell lung cancer (Grills et al 2003), pediatric tumors (Lee et al 2005a) or prostate cancer (Zelefsky et al 2001) radiation plays an important role and remains to date an important therapeutic option. In radiation therapy, high energy radiation is used to kill cancer cells by activating various cell death pathways (Zelefsky et al 2001).

DNA is identified as the primary target for triggering radiation-induced cell death (Radford 1986, Ward 1988). The lesions induce by IR results in formation of DNA single or double strand breaks. The damage in DNA is lethal and leads to activation of signal transduction pathways initiating various cellular responses one of which includes apoptosis (Crompton 1998). An alternative to this model with the involvement to sphingomyelin pathway in mediating radiation-induced apoptosis was provided. It was demonstrated that in bovine aortic endothelial cells (BAECs) radiation targets cell membrane resulting in activation of sphingomyelinase leading to hydrolysis of sphingomyelin to produce ceramide. The ceramide thus produced can activate apoptotic pathways (Haimovitz-Friedman et al 1994).

Participation of ASM/ceramide in mediating radiation induced cell death process both *in vivo* and *in vitro* conditions has been remarked many times in studies (Garcia-Barros et al 2003, Lee et al 2011, Morita et al 2000, Paris et al 2001, Peña et al 2000, Santana et al 1996). The role of ASM/ceramide was elucidated in lymphoblasts lacking ASM which were found to be insensitive towards IR. When irradiated with 20 Gy, lymphoblasts from NPD did not respond to IR-induced apoptotic cell death compared to normal lymphoblasts. This observation was reversed when ASM-cDNA was transferred using retroviral plasmids, which resulted in an increase of the ASM activity level, ceramide production and finally in apoptotic cell death. In addition, mice irradiated at a dose of 10 Gy responded by a vast increase in ceramide generation leading to apoptosis in lung, thymus and spleen tissues (Santana et al 1996).

Endothelial cells are the best studied targets upon irradiation in mediating apoptosis with the involvement of ASM (Garcia-Barros et al 2003, Paris et al 2001, Peña et al 2000). A dose dependent apoptosis was observed in CNS of C57Bl/6 or C3H/HN mice upon irradiation wherein 20 % apoptosis of endothelial cells were already noticed within 12 h. In contrary resistant up to 40 Gy upon irradiation of CNS as well as endothelial cells was observed in Asm knockout mice (Peña et al 2000). Similarly irradiating whole body of C57Bl/6 mice resulted in death of mice within 10-13 days with gastrointestinal (GI) syndrome. Apoptosis in the crypt/villus of micro vessels and severe apoptosis of endothelial cells upon 15 Gy after 4 h was noticed. Administration of BFGF intravenously abrogated endothelial apoptosis and radiation-induced damage of crypt or failure of organs and GI death. In addition, protection of endothelial apoptosis and GI death in Asm-deficient mice was detected upon 15 Gy (Paris et al 2001). Furthermore role of BFGF as a protector from radiation-induced endothelial cell death has been observed in both *in vivo* and *in vitro* studies (Fuks et al 1994, Fuks et al 1995).

Further studies showed ASM mediated apoptosis upon irradiation in ovary of fertile female mice. During embryogenesis Asm−/− mice are defective in the normal apoptotic deletion of fetal oocytes resulting in neonatal ovarian hyperplasia. *Ex vivo* studies confirmed that oocytes from Asm−/− mice, or wild-type oocytes treated with S1P (ceramide metabolite) prevented daunorubicin-induced apoptosis. It has to be mentioned that during this pathway BAX function downstream of ceramide and a dose of 0.1 Gy resulted in 90 % loss of oocytes and infertility in wild-type female mice, however this phenomenon was abolished *in vivo* upon S1P administration (Morita et al 2000).

IR-induced apoptosis by stimulating the *sphingomyelin* pathway had been identified much earlier (Haimovitz-Friedman et al 1994) than the involvement of *de novo* pathway. Transient ceramide produce within a few minutes after irradiation is known to be DNA–independent.

Whereas, ceramide generated several hours after irradiation depends on DNA regulating the Ataxia telangiectasia mutated (ATM) signaling pathway (Vit and Rosselli 2003). Similarly, involvement of the *de novo* pathway in generating ceramide leading to apoptotic cell death in prostate cancer cell line DU145 was also reported. DU145 cells are resistant to IR-induced cell death but these cells showed synergistically high levels of ceramide production ultimately leading to clonogenic cell death (Scarlatti et al 2007) when treated with IR in combination with resveratrol (3,5,4′-*trans*-trihydroxystilbene), one of the natural grapes products having chemotherapeutic characteristics (Gusman et al 2001, Jang et al 1997). The findings for IR-induced apoptotic cell death through ceramide were not only limited to cell lines or mice but were also confirmed in the nematode *Caenorhabditis elegans (C. elegans)*. It was shown that DNA damage induced by radiation activates *C. elegans* p53-like protein 1 (CEP-1) (the homologue of p53) which is required for increasing the expression of the Bcl-2 homology region 3 (BH3)-only proteins EGL-1 and CED-13. This in turn activated apoptotic signaling in mitochondria showing that ceramide and CEP-1 might function in parallel further increasing ceramide accumulation in mitochondria upon irradiation leading to induction of apoptosis in germ cells (Deng et al 2008).

Ceramide inducing apoptotic cell death has been one of the most important areas of biological research, its role in inhibiting various cell survival pathways with the involvement of phosphatidylinositol 3-kinase (PI3K), Akt, and BAD by promoting apoptosis has also been reported (Zundel and Giaccia 1998). However the fact that ceramide once degraded by either of the enzymes ceramidase or glycosyltransferase/glucosylceramide synthase (GCS) leads to formation of sphingosine, S1P and glycosylceramide which promote cell survival pathways. Acid ceramidase (AC), an enzyme catalyzing the conversion of ceramide to sphingosine and fatty acid (Ferlinz et al 2001, Li et al 1998, Romiti et al 2000) is known to be a regulator of the *de novo* ceramide generation pathway. The role of AC-mediated ceramide consumption conferred resistant to radio-and chemotherapy in prostate cancer cells was shown upon various studies (Cheng et al 2013, Mahdy et al 2009, Saad et al 2007). In particular radiation resulted in an up-regulation of AC finally leading to resistance of prostate cancer cells; the addition of AC inhibitors reversed this condition, making the cells as well as xenograft model radiosensitive to IR (Cheng et al 2013, Mahdy et al 2009). Similarly, glioblastoma cells possess higher levels of ceramide glucosyltransferase/GCS, an enzyme responsible for the conversion of ceramide to glucosylceramide which protects the cells from undergoing programmed cell death (Dumitru et al 2009, Giussani et al 2012). As reported by Dumitru and coworkers upon gemcitabine treatment glioma cells were able to rapidly

consumed ceramide promoting cell survival however treatment of those cells with gemcitabine and GCS inhibitor DL-threo-1-phenyl-2-palmitoylamino-3-morpholino-1-propanol (PPMP) were able to restore the cellular ceramide level leading to cell death. It has to be noted that using AC inhibitor showed no effect on the colony forming ability of those cells upon gemcitabine treatment (Dumitru et al 2009). On the other hand using the GCS inhibitor PPMP alone reduced the clonogenic cell death in human glioma cell lines, but it did not show any synergistic effect in combination with IR (Gramatzki et al 2013). In Jurkat cells, the use of DL-threo-1-phenyl-2-decanoylamino-3-morpholino-1-propanol (PDMP), another inhibitor for GCS enzyme resulted in IR-induced apoptotic cell death (Rodriguez-Lafrasse et al 2002).

1.4.2 ROS PRODUCTION AND IONIZING RADIATION (IR)

Various factors and/or stimuli like bacteria (Zhang et al 2008), chemotherapeutic drugs (Perez et al 2015), IR (Leach et al 2001), UV-light (Charruyer et al 2005) etc. are known to be involved in accelerating mitochondrial or NADPH oxidase (NOX) ROS production. IR targets both the mitochondrial (Leach et al 2001, Saenko Iu et al 2011, Yamamori et al 2012) and the NOX pathway (Collins-Underwood et al 2008, Liu et al 2008, Tateishi et al 2008) for generating ROS. To enlighten these interactions further, an involvement of mitochondrial ROS during IR-induced apoptosis has also been reported (Leach et al 2001). Similarly mitochondrial dependent apoptosis with production of massive ROS upon low dose of radiation has been shown in mouse testicular cells (Fang et al 2013). In various myeloma cells, two distinct level of ROS release were observed upon irradiation, differing in their temporal occurrence and being correlated with caspases activation and cytochrome c release finally leading to apoptosis (Chen et al 2003).

In addition to mitochondria, NOX remains to be the main contributor for ROS production upon irradiation (Collins-Underwood et al 2008). Different NOX components have their own role as IR-induced ROS generators: NOX proteins are seemingly involved in ROS production leading to apoptosis induction, particularly NOX1 appears to be the inducer of ROS generation: its mRNA levels were found upregulated after 10 Gy of irradiation (Tateishi et al 2008). In HeLa cells, NOX is one of the most important sources to contribute IR-induced ROS production finally leading to cell death. It was shown that upon IR, dose-dependent up-regulation of the membrane subunit gp91phox takes place and translocation of the cytoplasmic subunit of NOX: p47phox and its association with the other membrane subunits p22phox and gp91phox was also observed (Liu et al 2008). Furthermore, in prostate cancer

cells, radiation in combination with parthenolide (PN, a sesquiterpene lactone) resulted in ROS generation via NOX activation with the effect of cells being radiosensitive (Sun et al 2010).

1.4.3 PLASMA MEMBRANE TARGETED UPON IRRADIATION

Hydrolysis of the sphingolipid sphingomyelin (SM) catalyzed by ASM results in generation of ceramide at the outer layer of the plasma membrane. Various stress stimuli like bacterial infection (Grassmé et al 2003b, Zhang et al 2008), death receptors (Cifone et al 1994, Cremesti et al 2001, Perrotta et al 2010), oxidative stress (Li et al 2012, Zhang et al 2007), UV-light (Charruyer et al 2005, Kashkar et al 2005, Rotolo et al 2005, Zhang et al 2001) including irradiation (Paris et al 2001, Santana et al 1996, Sathishkumar et al 2005) are known to be involved in ASM activation resulting in the production of ceramide. Some studies have reported that translocation of ASM to the outer leaflet of the cell membrane is an initial step for activation of ASM (Grassmé et al 2001a, Perrotta et al 2010). Grassmé and coworkers first demonstrated that stimulation of CD95 resulted in translocation of ASM to outer surface of the plasma membrane resulting in clustering of CD95 in sphingolipid-rich membrane rafts finally resulting in apoptosis in lymphocytes whereas ASM-deficient lymphocytes rescued these events preventing apoptosis (Grassmé et al 2001a). Similar study was carried out using human glioma cells U373 where CD95 stimulation resulted in ASM activation through its translocation from intracellular compartments to the plasma membrane with the involvement of target- (soluble *N*-ethylmaleimide-sensitive-factor activating protein receptor) (t-SNARE) protein syntaxin 4. Down regulation of syntaxin 4 resulted in prevention of ASM translocation and its activation when stimulated with CD95 resulting in inhibition of caspase 3 and 9 activation finally rescuing apoptosis. These events leaded to activation of survival pathway (Perrotta et al 2010). In accordance, UV-light induced activation and translocation of ASM (Zn^{2+}-independent) to the plasma membrane in the human myeloblastic cell line U937 was also observed, the process was found to be ROS-dependent (Charruyer et al 2005). The role of ROS in monitoring UV-light-signaling had also been known before (Xing et al 2008). This phenomenon was validated using scavengers of ROS which overcome both ASM activation and its translocation to plasma membrane. ASM activation and translocation to plasma membrane resulted in ceramide generation which leaded to activation of the JNK pathway in human myeloblastic U937 cells (Charruyer et al 2005). Once ASM translocation and activation leads to formation of ceramide and ceramide-enriched platforms on plasma

membrane, the latter are able to cluster death receptors resulting in the induction of cell death (for details see section 1.3.5).

When it comes to radiation, ROS are the main important factors in mediating IR-induced cell death by participating in the signaling cascade (Mikkelsen and Wardman 2003). One of the first event that takes place when cells are exposed to IR is the generation of ROS (see section 1.1.1), and various enzymes are involved in IR-induced ROS generation, one of which is the NOX family (Collins-Underwood et al 2008, Liu et al 2008, Tateishi et al 2008). The ASM/ceramide pathway is known to be involved in IR-induced activation of NOX through formation of redox lipid rafts. The role of lipid rafts in redox signaling has been highlighted much in recent years. In coronary endothelial cells, upon Fas ligand (FasL) stimulation one of the NADPH oxidase (NOX) subunits, gp91phox, clustered in lipid rafts which further resulted in the translocation of other cytosolic subunits of NOX: p47 phox and Rac proteins to lipid rafts with an increase in full activity of NOX enzymes (Zhang et al 2006). Further studies showed involvement of both Asm and ceramide in lipid raft redox signaling. FasL stimulation resulted in increased ASM activity, production of ceramide, and LR clustering in coronary arterial endothelial cells (CAECs) however silencing Asm reversed this process. Silencing ASM using SiRNA resulted in inhibition of ceramide production and lipid raft clustering, finally leading to an inhibition of the NOX enzyme by blocking gp91phox aggregation and translocation of p47phox to the LR clusters (Zhang et al 2007). Though the complete mechanism of how ROS are mediating ASM activation has still not been elucidated, its particular role in activating ASM in airway epithelial cells has been cleared (Castillo et al 2007).

In addition IR is reported to change the organization of cytoskeleton (Friedman et al 1986, Gabrys et al 2007, Rousseau et al 2011). In shaping the cell structure, the cytoskeleton plays an important role. A linkage between both cell plasma membrane and actin cytoskeleton is formed by the interaction of lipid and protein molecules. Various proteins like glycophorin-protein 4.1, profilin are involved in transmitting the signal from the cell plasma membrane to the actin cytoskeleton (Anderson and Marchesi 1985, Lassing and Lindberg 1985). One of the best-studied proteins in maintaining the actin cytoskeleton structure is the Rho family (Rho, Rac and Cdc42) (Bishop and Hall 2000, Hall 1998, Helliwell et al 1998). Though the activation of these Rho proteins upon various factors one of which is IR has been repeatedly reported (Gabrys et al 2007, Zhai et al 2006), the accurate mechanism of IR activating Rho proteins is still unrevealed. However, as ceramide is known to activate Rho A (Gupta et al 2001) and Rac-1 (Brenner et al 1997), it can be assumed that IR indirectly stimulates the

activation of these Rho proteins with the involvement of ceramide formation after irradiation. Activated GTPase, Rac-1, is further known to interact with the lipid rafts membrane domain (del Pozo et al 2004).

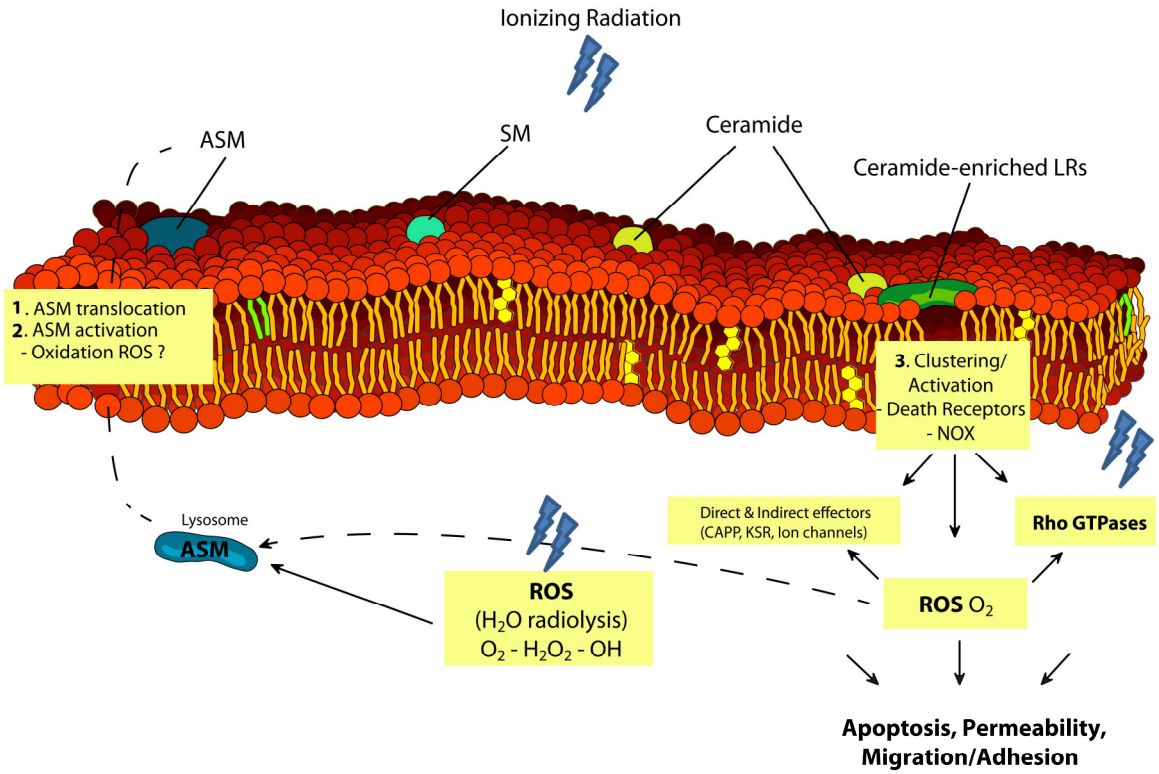

Figure 1.4: Model showing how IR targets the plasma membrane and results in ASM activation and its translocation. IR-induced ROS production might be a regulator of ASM translocation from the lysosome to the plasma membrane. Once activated ASM leads to the formation of ceramide and ceramide-enriched membrane platforms which further mediate signal transduction inside the cells. Ceramide formed within the plasma membrane might regulate various other signaling molecules.

1.5 AIMS OF THE STUDY

Several studies has shown that tumor cells have the ability to prevent the accumulation of ceramide by decreasing the total cellular concentration of ceramide and escape from cell death process (Cheng et al 2013, Dumitru et al 2009, Giussani et al 2012, Mahdy et al 2009, Saad et al 2007). In particular, ceramide glycosyltransferase/glycosylceramide synthase (GCS) mediated ceramide consumption is one of the drawbacks for treating glioblastoma in response to chemotherapy and radiation. The inhibition of GCS sensitizes the glioblastoma cells upon different chemotherapeutic drugs like gemcitabine (Dumitru et al 2009), temozolomide and Paclitaxel (Giussani et al 2012).

The present study will investigate whether irradiation of human glioblastoma cells results in the activation of ASM, formation of ceramide-enriched membrane platforms and clustering of NADPH oxidase in the plasma membrane.

Furthermore we will address the mechanism of ASM activation by testing if irradiating the cells induces free radical oxygen production which might mediate activation of the ASM.

The last part of the study will focus on identification of the interacting partners for ASM, ceramide and lipid rafts which might suggest if some the identified proteins are involved in conferring radioresistance in glioblastoma cells upon irradiation.

2 MATERIALS

2.1 LIST OF CHEMICALS

Acetic acid (CH_3COOH)	Merck KGaA, Darmstadt, Germany
Acetone (C_3H_6O)	Merck KGaA, Darmstadt, Germany
Acrylamide (C_3H_5NO)	Carl Roth GmbH & Co. KG, Karlsruhe, Germany
Adenosine Tri-Phosphate (ATP)	Sigma-Aldrich Chemie GmbH, Steinheim, Germany
Agarose	Gibco, Invitrogen,Karlsruhe, Germany
Ammonium persulfate (APS)	Carl-Roth GmbH & Co, Karlsruhe, Germany
Apocynin	Sigma-Aldrich Chemie GmbH, Steinheim, Germany
Bovine serum albumin (BSA)	Sigma-Aldrich Chemie GmbH, Steinheim, Germany
Bradford reagent	Bio-Rad, USA
Bromophenol blue	Sigma-Aldrich Chemie GmbH, Steinheim, Germany
Cardiolipin	Sigma-Aldrich Chemie GmbH, Steinheim, Germany
Chloroform ($CHCl_3$)	Applichem GmbH, Darmstadt, Germany
Crystal violet ($C_{25}H_{30}ClN_3$)	Sigma-Aldrich Chemie GmbH, Steinheim, Germany
1,4-diazabicyclo[2.2.2]octane ($C_6H_{12}N_2$) (DABCO)	Sigma-Aldrich Chemie GmbH, Steinheim, Germany
Deoxycholic acid ($C_{24}H_{40}O_4$)	Sigma-Aldrich Chemie GmbH, Steinheim, Germany
Deoxyribonucleotides (dNTP´s)	Bio-Budget Technologies GmbH, Krefeld, Germany and PEQLAB Biotechnology GmbH, Erlangen, Germany
Diethylenetriaminepentaacetic acid (DETAPAC)	Sigma-Aldrich Chemie GmbH, Steinheim, Germany
Dithiothreitol (DTT)	Carl-Roth GmbH & Co, Karlsruhe, Germany
Dulbecco's modified eagle's medium (DMEM)	Gibco Life Technologies,USA
Dimethyl sulfoxide (DMSO)	Sigma-Aldrich Chemie GmbH,

	Steinheim, Germany
2',7' – dichlorodihydrofluorescein diacetate (H_2DCFDA)	Life Technologies, USA
Enhanced chemiluminescence (ECL)	Thermo Scientific, USA
Ethanol (CH_3CH_2OH)	Sigma-Aldrich Chemie GmbH, Steinheim, Germany
Ethidium bromide	Serva Electrophoresis GmbH, Heidelberg, Germany
Ethylenediaminetetraacetic acid (EDTA)	Sigma-Aldrich Chemie GmbH, Steinheim, Germany
Fetal calf serum (FCS)	Gibco, Invitrogen, Karlsruhe, Germany
Glucose ($C_6H_{12}O_6$)	Sigma-Aldrich Chemie GmbH, Steinheim, Germany
Glycerol ($C_3H_8O_3$)	Sigma-Aldrich Chemie GmbH, Steinheim, Germany
Glycine ($C_2H_5NO_2$)	Applichem, GmbH, Darmstadt, Germany
HEPES	Carl Roth GmbH & Co. KG, Karlsruhe, Germany
Hydrochloric acid (HCl)	J.T. Baker, USA
Imidazole ($C_3H_4N_2$)	Sigma-Aldrich Chemie GmbH, Steinheim, Germany
Magnesium sulphate ($MgSO_4$)	Sigma-Aldrich Chemie GmbH, Steinheim, Germany
2-(*N*-morpholino) ethanesulfonic acid (MES)	Sigma-Aldrich Chemie GmbH, Steinheim, Germany
2-Mercaptoethanol	Sigma-Aldrich Chemie GmbH, Steinheim, Germany
Methanol (CH_3OH)	J.T. Baker, USA
Monopotassium phosphate (KH_2PO_4)	Merck KGaA, Darmstadt, Germany
Mowiol	Kuraray Specialities Europe GmbH, Frankfurt, Germany
N-octylglucopyranoside	Sigma-Aldrich Chemie GmbH, Steinheim, Germany
Nonfat dry milk powder	Applichem, GmbH, Darmstadt, Germany
Nonidet P-40 (NP-40)	Sigma-Aldrich Chemie GmbH, Steinheim, Germany
Paraformaldehyde (PFA)	Sigma-Aldrich Chemie GmbH, Steinheim, Germany
Penicillin/Streptomycin	Gibco, Invitrogen,Karlsruhe, Germany
Poly-L-lysine ($(C_6H_{12}N_2O)_n$)	Sigma-Aldrich Chemie GmbH, Steinheim, Germany

Potassium chloride (KCl)	Carl-Roth GmbH & Co, Karlsruhe, Germany
Protease inhibitor	Carl-Roth GmbH & Co, Karlsruhe, Germany
Scintillation cocktail	Beckman Coulter, Fullerton, CA, USA
Sodium acetate (CH_3COONa)	Sigma-Aldrich Chemie GmbH, Steinheim, Germany
Sodium chloride (NaCl)	Sigma-Aldrich Chemie GmbH, Steinheim, Germany
Sodium deoxycholate ($C_{24}H_{39}NaO_4$)	Sigma-Aldrich Chemie GmbH, Steinheim, Germany
Sodium dodecyl sulphate ($CH_3(CH_2)_{11}OSO_3Na$) (SDS)	Carl-Roth GmbH & Co, Karlsruhe, Germany
Sodium hydroxide (NaOH)	Sigma-Aldrich Chemie GmbH, Steinheim, Germany
Sodium phosphate (Na_3PO_4)	Merck, Darmstadt, Germany
Sucrose ($C_{12}H_{22}O_{11}$)	Carl-Roth GmbH & Co, Karlsruhe, Germany
Sodium carbonate (Na_2CO_3)	Sigma-Aldrich Chemie GmbH, Steinheim, Germany
Taq Polymerase	Invitrogen, Karlsruhe, Germany
Tetramethylethylendiamine ($C_6H_{16}N_2$) (TEMED)	Applichem, GmbH, Darmstadt, Germany
Tiron ($C_6H_4Na_2O_8S_2$)	Sigma-Aldrich Chemie GmbH, Steinheim, Germany
Tricine ($C_6H_{13}NO_5$)	Sigma-Aldrich Chemie GmbH, Steinheim, Germany
Tris(hydroxymethyl)aminomethane ($NH_2C(CH_2OH)_3$) (Tris)	Carl-Roth GmbH & Co, Karlsruhe, Germany
Triton X-100	Sigma-Aldrich Chemie GmbH, steinheim, Germany
Trypsin	Biochrom Berlin, Germany
Tween-20 ($C_{58}H_{114}O_{26}$)	Sigma-Aldrich Chemie GmbH, Steinheim, Germany

2.2 LIST OF ANTIBODIES, TRANSFECTION REAGENTS, PROTEIN BEADS AND LIPID BEADS

2.2.1 PRIMARY ANTIBODIES

Antigen	**Host**	**Dilution**	**Supplier**
Acid sphingomyelinase,	Rabbit	1:50	Areta International s.r.l. Gerenzano, Italy

ASM (for microscopic staining)			
Acid sphingomyelinase, ASM (for immunoprecipitation and western blotting)	Mouse	1:1000	Abcam, Cambridge, UK
Calnexin	Mouse	1:1000	BD Biosciences, USA
Ceramide	Mouse	1:50	Enzo life sciences, Germany
COX-IV	Goat	1:1000	Santa Cruz Biotechnology, USA
Flotillin-1	Rabbit	1:1000	Santa Cruz Biotechnology, USA
gp91phox (for microscopic staining)	Rabbit	1:50	Abcam, Cambridge, UK
gp91phox (for western blotting)	Rabbit	1:1000	Proteintech, Chicago, USA
LAMP-1	Rabbit	1:1000	Santa Cruz Biotechnology, USA
TIMM23 (for microscopic staining)	Rabbit	1:50	Proteintech, Chicago, USA
TIMM23 (for western blotting)	Rabbit	1:1000	Proteintech, Chicago, USA

2.2.2 SECONDARY ANTIBODIES

Antigen	**Host**	**Conjugation**	**Dilution**	**Supplier**
Beta-actin	Mouse	HRP	1:2000	Cell signaling, USA
Mouse IgM	Donkey	Cy3	1:250	Jackson ImmunoResearch Laboratories, USA
Rabbit IgG	Donkey	Cy5	1:250	Jackson ImmunoResearch Laboratories, USA
Rabbit IgG	Donkey	FITC	1:250	Jackson ImmunoResearch Laboratories, USA
Rabbit IgG	Rabbit	HRP	1:2000	Cell signaling, USA
Mouse IgM	Mouse	HRP	1:2000	Cell signaling, USA

2.2.3 TRANSFECTION REAGENTS

Transfection materials	Supplier
gp91phox/cytochrome b beta (CYBB) siRNA (ID 3915) (AM16708)	Ambion, Inc., Austin, TX, USA
Negative control siRNA (AM 4611)	Ambion, Inc., Austin, TX, USA
Ribonuclease (RNAse) free H_2O	Ambion, Inc., Austin, TX, USA
Transfection kit (containing EC buffer + enhancer + effectene transfection reagent) (Cat.no. 301425)	Qiagen, GmbH, Hilden, Germany

2.2.4 PROTEIN BEADS AND LIPID BEADS

Beads	Supplier
Ceramide beads (P-BCer)	Echelon Biosciences, USA
Control beads (P-B000)	Echelon Biosciences, USA
Protein A/G PLUS-Agarose beads sc-2003	Santa Cruz Biotechnology, USA

2.3 LIST OF CELL CULTURE MATERIALS

2.3.1 OVERVIEW OF CELL CULTURE MATERIALS

Round bottom petri dishes 35 mm	BD Falcon, USA
Tissue culture flasks 25cm²	TPP, Trasadingen, Switzerland
Tissue culture flasks 75cm²	TPP, Trasadingen, Switzerland
Tissue culture petri dishes (100, 60, 30 mm)	TPP, Trasadingen, Switzerland
Tissue culture 6 well plates	TPP, Trasadingen, Switzerland

2.3.2 PREPARATION OF CELL CULTURE MEDIA AND BUFFERS

Culture medium for A172 and LN308	500 ml DMEM 10 % FCS 1 % Antibiotics (10,000 units of penicillin and 10,000 µg of streptomycin)
Freezing medium	95 ml DMEM 5 ml FCS 5 ml DMSO
Trypsin	0.25 % Trypsin 5 mM Glucose 1.3 mM EDTA in PBS

2.4 CELL LINES

A172	Established human glioblastoma cell line (Prof. Michael Weller, Department of Neurology, University Hospital Zurich, Switzerland)
LN308	Established human glioblastoma cell line (Prof. Michael Weller, Department of Neurology, University Hospital Zurich, Switzerland)

Mycoplasma contamination was monthly tested in all cell lines by PCR.

2.5 PCR PRIMERS

Myco P1 5' –GTG CCA GCA GCC GCG GTA ATA C- 3'	Hölle & Hüttner AG, Germany
Myco P4 5' –TAC CTT GTT ACG ACT TCA CCC CA- 3'	Hölle & Hüttner AG, Germany

2.6 RADIOACTIVE SUBSTRATES

[^{32}P]γ-ATP	Hartmann Analytic, Braunschweig, Germany
[^{14}C]sphingomyelin	PerkinElmer, Boston, MA, USA

2.7 OTHER MATERIALS

Cell culture:	
Conical centrifuge tubes (15 and 50 ml)	BD Falcon, USA
Cryo 1C Freezing container	Nalgene, USA
FACS polystyrene round-bottom tubes	Becton, Dickinson and Company, Le Point de Claix, France
Neubauer chamber 0.1 mm	Marienfeld, Germany
Immunoblotting	
Cell scraper	TPP, Trasadingen, Switzerland
Cuvettes 10 x 4 x 45 mm	Sarstedt, Nümbrecht, Germany
Hybond blotting membranes	Amersham Biosciences, Buckinghamshire, UK
Whatman filter paper	Whatman, Maidstone, UK
X-Ray films	FUJIFILM Medical Systems, Stamford, USA

Immunostaining:	
Cover slips 12 mm diameter	Carl-Roth GmbH & Co, Karlsruhe, Germany
Microscopic slides	Engelbrecht Medizin und labortechnik GmbH, Germany
Parafilm	Peckiney, Chicago, IL, USA
Mass spectrometry:	
Dounce (glass-glass) homogenizer	Wheaton Science Products, Millville, USA
Ultracentrifuge tubes	Beckman Coulter, Germany
Others:	
Dihydroethidium (DHE)	Life Technologies, USA
H_2DCFDA	Life Technologies, USA
Hoechst 33342	Life Technologies, USA
MitoSOX red	Life Technologies, USA
Mitochondria isolation kit for cultured cells (89874)	Thermo Scientific, Life Technologies GmbH, Germany
NADPH assay kit (Cat.no. CY0100)	Sigma-Aldrich, Germany
Propidium iodide (PI)	Sigma-Aldrich, Germany
Silica G60 TLC plates	Merck, Darmstadt, Germany

2.8 LABORATORY EQUIPMENT

BD FACSCalibur flow cytometer	BD Biosciences, San Jose, CA, USA
Cell culture incubator	ThermoFisher Scientific,Waltham, MA, USA
Fluorescence microplate reader	BMG Labtech, Offenburg, Germany
Leica TCS SP5 laser scanning confocal microscope	Leica Microsystems GmbH, Mannheim, Germany
Portable datalogging spectrophotometer	Bachofer, Reutlingen, Germany
Phosphorimager	FUJIFILM Medical Systems, Stamford, USA
Real-Time PCR system	ABI PRISM® 7300 Real-Time PCR System, Applied Biosystems, Foster City, CA, USA
SpeedVac (Vacuum Concentrator)	Bachofer, Reutlingen, Germany
Sonorex bath sonicator	Bandelin electronic, Berlin, Germany
TriCarb liquid scintillation analyzer	Perkin Elmer, USA

Thermomixer	Eppendorf, Germany
TLA-55 rotor	Beckman Coulter, Germany
Rotary agitator	Neolab Migge Laborbedarf-Vertriebs GmbH, Germany
Ultracentrifuge	Beckman Coulter, Germany

2.9 LISTS OF COMPLETE GELS, BUFFERS AND SOLUTIONS

2.9.1 BUFFERS AND SOLUTIONS FOR WESTERN BLOTTING

APS	10 % APS In ddH_2O
Blocking buffer	5 % of non-fat dry milk powder in TBST (see below)
Primary antibodies dilution buffer	5 % of BSA in TBST (see below)
Running gel (10%)	3.75 ml Solution A (see below) 5.0 ml Solution B (see below) 6.11 ml H_2O 75 µl 20 % SDS 30 µl TEMED 30 µl 10 % APS in H_2O
SDS lysis buffer	25 mM HEPES pH 7.4 0.1 % SDS 0.5 % Deoxycholic acid 1 % Triton X-100 10 mM EDTA 10 mM Sodium pyrophosphate 10 mM Sodium fluoride 125 mM NaCl
SDS sample buffer (5x)	62.5 mM Tris pH 6.8 10 % Glycerol 2 % SDS 0.04 % Bromphenol blue 5 % 2-Mercaptoethanol
Solution A	40 % Acrylamide (39.2 g Acrylamide /100 ml; 0.8 g Bis-Acrylamide /100 ml)
Solution B	3M Tris pH 8.8
Solution C	3M Tris pH 6.8
Stacking gel	0.63 ml Solution A 0.21 ml Solution C 4.1 ml H_2O 0.025 ml 20 % SDS 0.02 ml TEMED 0.02 ml 10 % APS in H_2O
Transfer buffer	25 mM Tris

	192 mM Glycine 20 % Methanol
10 x Tris-buffered saline and 0.1% Tween-20 (TBST) (washing buffer)	200 mM Tris pH 7.4 1500 mM NaCl 1 % Tween-20
Secondary antibodies dilution buffer	5 % of non-fat dry milk powder in TBST

2.9.2 BUFFERS AND SOLUTIONS FOR VARIOUS EXPERIMENTS

ASM lysis buffer	250 mM Sodium acetate pH 5.0 1.3 mM EDTA 0.1 % NP-40
DAG-assay buffered saline solution	135 mM NaCl 1.5 mM $CaCl_2$ 0.5 mM $MgCl_2$ 5.6 mM Glucose 10 mM HEPES pH 7.2
DAG-assay detergent solution	7.5% N-octylglucopyranoside 5 mM Cardiolipin 1mM DETAPAC
DAG-kinase diluents	1 mM DETAPAC pH 6.6 0.01 M imidazole/HCl
DAG-kinase reaction buffer	100 mM imidazole/HCl pH 6.6 100 mM NaCl 25 mM $MgCl_2$ 2 mM EDTA 2.8 mM DTT 5 µM ATP 10 µCi [^{32}P]-γ ATP
10x HEPES-saline	200 mM HEPES 1.32 M NaCl 10 mM $CaCl_2$ 7 mM $MgCl_2$ 8 mM MgSO4 54 mM KCl
(NADPH activity assay) Enzyme dilution buffer	300 mM Potassium phosphate buffer, pH 7.8, containing 0.1 mM EDTA and 0.5 mg/ml bovine serum albumin
(NADPH activity assay) Working solution	9 mg Cytochrome c 20 ml Assay buffer (300 mM potassium phosphate buffer, pH 7.8, containing 0.1 mM EDTA)
NADPH stock solution (40 mg/ml)	25 mg NADPH 0.625 ml of H_2O
PBS	137 mM NaCl 2.7 mM KCl 7 mM $CaCl_2$ 0.8 mM $MgSO_4$ 1.4 mM KH_2PO_4 6.5 mM Na_2HPO_4

	Adjust pH to 7.6
PCR buffer (10x)	200 mM Tris-HCl pH 8.3 500 mM KCl 14 mM $MgCl_2$ 0.1% Gelatin
10 x Tris/Borate/EDTA (TBE) buffer	890 mM Tris Base 890 mM Boric Acid 20 mM EDTA
Tissue Lysis Buffer (TLB)	10 % 10 x PCR buffer 0.5 mM $MgCl_2$ 0.045 % Tween-20 0.045 % NP-40 300 µg/ml Proteinase K

2.9.3 BUFFERS AND SOLUTIONS FOR IMMUNOSTAINING (FLUORESCENCE MICROSCOPY)

Antibodies dilution buffer	1 % BSA in PBS
Mowiol	6 g Glycerol 2.4 g Mowiol 6 ml H_2O 12 ml 0.2 M Tris pH 8.5 0.1 % DABCO
PBS + 1 % BSA (blocking buffer)	1 % BSA in PBS
PBS + 0.2 % BSA (washing buffer)	0.2 % BSA in PBS
1 % PFA (fixing solution)	1 % PFA in PBS

2.9.4 BUFFERS AND SOLUTIONS FOR MASS SPECTROMETRY

(ceramide pull-down assay) Wash/binding buffer	10 mM HEPES, pH 7.4 150 mM NaCl 0.25 % NP-40
90 % sucrose	45 g Sucrose MBS until volume equals 50 ml Heat in a microwave oven (in 10-s intervals) to dissolve/melt
35 % sucrose	5.83 ml 90 % Sucrose 9.17 ml MBS/Na_2CO_3 (see below)
5 % sucrose	0.83 ml 90 % Sucrose 14.17 ml MBS/Na_2CO_3 (see below)
MBS/Na_2CO_3	250 mM Na_2CO_3 in MBS (see below)
Membrane lysis buffer	0.25 M Sucrose 1 mM EDTA 20 mM Tricine, pH 7.8

2-(*N*-morpholino)ethanesulfonic acid (MES)-buffered saline (MBS)	25 mM MES 150 mM NaCl, pH 6.0
RIPA buffer 10x	1 % NP40 0.1% SDS 50 mM Tris-HCl pH 7.4 150 mM NaCl 0.5 % $C_{24}H_{39}NaO_4$ 1 mM EDTA

3 METHODS

3.1 CELL CULTURE TECHNIQUES

3.1.1 CULTURE OF ESTABLISHED CELL LINES

3.1.1.1 Cell line and Culture conditions

Adherent human glioblastoma cell lines A172 and LN308 were cultured in T75 cm² flasks. Cells were maintained in a complete culture medium containing DMEM, supplemented with 10 % FCS, 10000 units of penicillin and 10000 µg of streptomycin per ml at 37°C in an incubator with 5 % CO_2. Before passaging the cells, the medium, PBS and trypsin were pre-warmed at 37°C. Cells were washed with PBS, followed by detaching the latter using trypsin. Fresh medium was added, and cells were collected and transferred to new flasks followed by incubation at 37°C until use.

3.1.1.2 Freezing of cells

Cells were frozen by using a cryo-preserving method. Cells from T75 cm² or T25 cm² flasks were trypsinized and collected by centrifugation. Pellets were re-suspended in freezing medium (see section 2.3.2). DMSO was added to the freezing medium to avoid ice crystals formations within the cells during the freezing procedure. 1 ml of the re-suspended solution was added to cryogenic vials with proper labeling and stored at -80°C for short-term use. For long-term storage, cryogenic vials were kept in a liquid nitrogen container.

3.2 DNA TECHNIQUES

3.2.1 POLYMERASE CHAIN REACTION (PCR)

3.2.1.1 DNA isolation from cell line

To test the mycoplasma contamination within the used cell lines, DNA was isolated from the cells in the following way: 10 x 10^5 cells / sample were collected by centrifugation for 5 min at 100 x g and 4°C. Supernatant was discarded, and the pellets were suspended in 50 µl TLB (see section 2.9.2) followed by incubation for 3 h at 56°C with smooth shaking. Afterwards, the samples were boiled for 10 min at 95°C and 100 µl of autoclaved ddH_2O was added to the boiled samples.

3.2.1.2 Mycoplasma PCR

For analyzing the mycoplasma detection by PCR, following mixture was prepared:

Table for reagent added:

Reaction component	**Amount**
H_2O	18.75 µl
10X PCR-Buffer B	2.5 µl
25 mM $MgCl_2$	1.5 µl
10 mM deoxynucleotide triphosphates (dNTP`s)	0.5 µl
Primer P1	0.25 µl
Primer P4	0.25 µl
Taq Polymerase	0.25 µl
DNA (see section 3.2.1)	1 µl

Total Volume = 25 µl

Samples were then kept in a thermo-cycler; PCR temperature was increased to 104°C, and the temperature of the PCR block was raised to 96°C for 17 min, followed by this (below) cycle which was carried out 25 times:

- Denaturation: 95°C for 1 min
- Annealing: 60°C for 1 min
- Elongation: 72°C for 1 min 30 sec

After the last cycle, the PCR block was remained at 72°C for 7 min, after which the samples were placed at 4°C.

3.2.2 AGAROSE GEL ELECTROPHORESIS

To analyze the sample after the PCR, 0.8 % agarose gel was prepared and poured in TBE buffer (see section 2.9.2) containing 0.01 µg/ml ethidium bromide. The Samples (15µl) along with 0.1 µg/µl of a 100-bp-standard were loaded on the gel. 5 V /cm current were then used to run the gel, and DNA fragments were visualized under UV-light.

3.3 IONIZING RADIATION (IR) TREATMENT

Irradiation of cells was carried out at room temperature (RT) using an X-ray machine, operated at a maximum energy of 320 kilovolt (kV) with a 1.65-mm aluminum filter

(effective photon energy approximately 90 kV), at a distance of 50 cm for 35 mm and 60 mm petri dishes whereas while using 100 mm petri dishes the distance was maintained at 75 cm. The irradiation table was kept on rotating position during exposure of radiation to ensure consistent irradiation. The dose rate of 4 Gray (Gy) was used in all experiments, except for the dose-and time-dependent cell death assay (section 3.4) where different doses starting from 2 Gy till 8 Gy were used.

3.4 PROPIDIUM IODIDE (PI) STAINING FOR CELL DEATH QUANTIFICATION

To determine the dose-dependent cell death, 1.0 x 10^5 cells were plated per 60 mm petri dish 24 h prior to irradiation. The next day, cells were treated with different doses of IR as indicated (0, 2, 4, 6 and 8 Gy) and remained in the incubator for 96 h. After 96 h medium was removed and added in a 15 ml falcon tube, cells were washed once with PBS followed by addition of trypsin to detach the cells. Cells were collected and added to the same falcon tube containing medium and centrifuged at 4°C, 500 x g for 5 min. Supernatant was discarded and the pellets were washed once with PBS followed by the centrifugation. Finally pellets were re-suspended in PBS and 0.1 µl/mg of PI was added to each sample and incubated for 10 min at RT. Samples were measured in FL-2 channel. For time-dependent cell death quantification all the procedure was performed in the same way except that the cells were plated for three different time points i.e. 76 h, 96 h and 120 h and were irradiated with 4 Gy. At each time point, staining the cells with PI was carried out.

3.5 ACID SPHINGOMYELINASE (ASM) ACTIVITY ASSAY

To determine the activity of ASM, 2.0 x 10^6 cells / plate were seeded in a 35 mm petri dish 24 h prior to irradiation. The next day, cells were treated with a 4 Gy; control cells remained non-irradiated. At indicated time point, i.e. 10 and 15 min after IR, cells were washed with PBS and lysed in 400 µl of ice-cold ASM lysis buffer (see section 2.9.2). Non-irradiated samples were treated similarly. Lysates were collected with a cell scraper and transferred into a microcentrifuge tubes followed by three sonication cycles (3 x 10 s) using a tip sonicator. [^{14}C]-labeled sphingomyelin was dried by SpeedVac centrifugation before adding to the lysates; since [^{14}C]sphingomyelin is insoluble in water, it was suspended in ASM lysis buffer, followed by a 10 min sonification for the formation of micelles. Lysates were incubated with 0.02 µCi of [^{14}C]sphingomyelin for 30 min at 37°C in a thermomixer. The reaction was stopped by the addition of 0.8 ml of $CHCl_3$:CH_3OH (2:1,v/v), followed by vigorous vortexing

and centrifugation at 800 x g for 5 min. Phases were then separated by centrifugation at maximum speed as phosphorylcholine in the upper (aqueous) phase and ceramide in the lower (organic) phase. Carefully, 250 µl aliquot from the aqueous phase were collected and added to polyethylene vials containing 4 ml of scintillation cocktail for liquid scintillation counting.

For measuring the ASM activity in presence of ROS inhibitors (apocynin and tiron), the experiment was carried out following the procedure mentioned above with slight changes. Prior to irradiation, the cells were incubated with 100 µM of respective ROS inhibitors for 30 min at 37°C. After 30 min of incubation, cells were washed once with PBS and maintained with culture medium.

ASM activity in control and gp91phox siRNA transfected cells were measured as described above. Cells were transfected with control and gp91phox siRNA as mentioned in section 3.11.

3.6 FLUORESCENCE MICROSCOPY FOR CELL SURFACE MOLECULES AND COLOCALIZATION STAINING

To determine the translocation of ASM and the clustering of ceramide on the plasma membrane, 2.0 x10^6 cells were plated per 35 mm petri dish with a round coverslip in it. Before using, 500 µl of poly-L-lysine solution were added to the coverslip and incubated for 10 min under a sterile hood, followed by washing once with PBS. The next day, cells were treated with a 4 Gy or remained untreated. At an indicated time point, 10 and 15 min after IR, cells were washed with PBS and fixed with 1 % PFA (fixing solution) (see section 2.9.3) for 10 min at RT. Non-irradiated cells were included as a control. Cells were remained unpermeablized for staining the surface molecules. To block unspecific binding sites, cells were incubated with blocking buffer (see section 2.9.3) for 15 min at RT and incubated with anti-ASM antibody or anti-ceramide antibody for 60 min at RT. Cells were then washed once with PBS and stained with fluorescent-labeled secondary antibodies Cy3-anti-rabbit IgG or anti-mouse IgM, respectively in complete darkness. Cells were washed once with washing buffer (see section 2.9.3) for 5 min and incubated with 0.1µg/ml hoechst 33342 diluted in PBS for 15 min in darkness. Cells were finally washed two times with washing buffer once with PBS and embedded in mowiol. A Leica TCS SP confocal microscope was used for the fluorescence analysis of the cell surface molecules.

To visualize the co-localized molecules, i.e. the clustering of gp91phox in ceramide-enriched membrane platforms on the plasma membrane of cells, every step was carried out as described above except for the different antibodies used. After blocking, cells were incubated with two different primary antibodies at a time, namely anti-ceramide antibody and anti-

gp91phox antibody and incubated for 60 min at RT. Cells were washed once with PBS and incubated with Cy3-anti-mouse IgM for ceramide and FITC-anti-rabbit IgG for gp91phox, respectively in complete darkness. Cells were washed once with washing buffer for 5 min and incubated with 0.1µg/ml hoechst 33342 diluted in PBS for 15 min in darkness. Cells were finally washed two times with washing buffer, once with PBS and embedded in mowiol. A leica TCS SP confocal microscope was used for the fluorescence analysis of co-localizing molecules.

For mitochondria and ceramide intracellular co-staining, cells were treated in the same way as mentioned above except that the cells were permeabilized using 0.1 % triton X-100 for 10 min at RT. Cells were incubated with anti-TIMM23 and anti-ceramide primary antibodies followed with second antibodies Cy5-anti-rabbit IgG and Cy3-anti-mouse IgM respectively. All the steps after that were followed in the same way as above.

3.7 DETERMINATION OF ROS BURST

To measure ROS burst, cells were cultured in 96-well plates (2500 cells/well) and incubated with 10 µM H_2DCFDA dissolved in DMSO for 10 min at 37°C. Cells were irradiated with 4 Gy or remained untreated and the fluorescence was determined by fluorescence micro-plate reader at excitation/emission: 485/520 nm. ROS burst using ROS inhibitors was measured in the same way as mentioned except that the cells were pre-incubated with 100 µM of ROS inhibitors apocynin and tiron for 30 min at 37°C prior to addition of H_2DCFDA and radiation treatment.

3.8 SUPEROXIDE MEASUREMENT

For measuring superoxide production, 2.0 x 10^6 cells were plated per round bottom 35 mm petri dish 24 h prior to irradiation. Cells were incubated with 5 µM DHE dissolved in PBS for 5 min at 37°C followed by irradiation at a dose of 4 Gy. For control samples cells were loaded with DHE but remained non-irradiated. Immediately after irradiation images were taken starting from 1 min till 15 min using live cell imaging technique.

For measuring mitochondrial ROS, cells were loaded with 10 µM MitoSOX dissolved in PBS for 20 min at 37°C and the procedure was followed exactly mentioned above. Images were taken after irradiation starting from 5 min till 20 min.

3.9 NADPH ACTIVITY ASSAY

To measure NADPH activity, cells were plated in 96 well-plates at a density of 2500 cells/well 24 h prior to irradiation. Protocol was followed as mentioned by NADPH assay kit from sigma manufacturer (see section 2.7) with some changes. Next day medium was removed and 95 µl working solution+ 5 µl enzyme dilution buffer + 10 µl NADPH solution at a concentration of 0.85 mg/ml were added in each well. For each solution (see section 2.9.2). Cells were incubated for 15 min at RT followed by irradiation at a dose of 4 Gy. After 10 min absorbance was measured at 550 nm using micro-plate reader. For control samples similar procedure were carried except for the irradiation.

3.10 WESTERN BLOTTING

Cells at a density of 5.0 x 10^6 were plated in 60 mm petri dishes 24 h prior to the experiment. Cells were irradiated at a dose of 4 Gy except for the control which was remained non-irradiated. After 10 and 15 min of IR, cells were washed once with cold PBS and lysed with 500 µl SDS lysis buffer (see section 2.9.1) containing complete protease inhibitor cocktail. Cells were collected with the help of cell scraper and kept in microcentrifuge tubes further incubated on ice for 20 min to ensure complete lysis of cells. Cells were then centrifuged at 800 x g for 10 min at 4°C. Cell lysates were collected as supernatant and the pellets were discarded. Protein concentration was measured from each lysates and samples were prepared by adding equal concentrations of lysates for each treatment plus SDS sample buffer (see section 2.9.1) in separate microcentrifuge tubes and boiled at 95°C for 5 min. If the sample was not used on the same day, it was kept at -20°C until further use. Each well of gel was loaded with 15-30 µg/µl protein samples. Proteins were separated using 10 % of sodium dodecyl sulfate polyacrylamide gel electrophoresis (SDS-PAGE) and transferred to nitrocellulose membranes followed by blocking with blocking buffer (see section 2.9.1) for 60 min at RT. After blocking, the membranes were incubated with primary antibody overnight at 4°C. The next day, membranes were washed 2 x 10 min using washing buffer (see section 2.9.1) and incubated 60 min with secondary antibody conjugated with horseradish peroxidase (HRP). Both primary and secondary antibodies were diluted in the respective antibodies dilution buffers (see section 2.9.1). Beta-actin was used to normalize the protein loading. To visualize the bands, enhanced chemiluminescence (ECL) immunoblotting substrate was used.

3.11 DOWNREGULATION OF gp91PHOX

For transient transfection, $1.0x10^6$ cells were seeded per well of a 6 well-plates with 2 ml culture medium. Cells were grown for 24 h to a confluence of about 60-70 %. Transfection procedure was performed according to manufacturer's description (Qiagen) (see section 2.2.3). Briefly, for each well two conditions were prepared namely control siRNA treated and gp91phox siRNA treated. For control siRNA treatment, 100 pmol of control siRNA already dissolved in RNase free buffer was added to the microcentrifuge tubes containing 100 µl of EC buffer. Similarly, for gp91phox siRNA treatment, 100 pmol of gp91phox siRNA dissolved in RNase free buffer was added to the microcentrifuge tubes containing 100 µl of EC buffer. Immediately after adding respective siRNA's to the EC buffer, 3.5 µl of enhancer was added to each microcentrifuge tubes containing (EC buffer + siRNase). The mixture was vortexed for 1 sec and incubated for 5 min at RT followed by addition of 10 µl of effectene transfection reagent. The mixture (EC buffer + siRNase + enhancer + effectene transfection reagent) was vortexed for 10 sec and incubated for 15 min at RT. Culture medium (600 µl) were added to each mixture. Medium from the wells was removed and a fresh culture medium was added followed by the addition of mixture containing (EC buffer + siRNase + enhancer + effectene transfection reagent + culture medium). After 6 h of incubation the medium was removed from each well, washed one time with PBS followed by addition of 2 ml of fresh culture medium. After 48 h, culture medium was removed and cells were used for experiments. Transient downregulation of gp91phox was checked by western blotting.

3.12 ISOLATION OF MITOCHONDRIA

Mitochondria were isolated from the cells using thermo scientific mitochondria isolation kit (see section 2.7) and the procedure was carried out exactly in the same manner mentioned by the manufacturer. Briefly, 5.0 x 10^6 cells were plated per 100 mm petri dish 24 h prior to irradiation. Next day cells were irradiated with 4 Gy and for the control samples cells were remained non-irradiated. After 10 and 15 min of irradiation, medium was removed and cells were washed once with cold PBS, scraped and collected in microcentrifuge tube. Cell pellets were collected after centrifugation at 4°C, 500 x g for 5 min followed by addition of 800 µl mitochondria isolation reagent A. Samples were incubated for 2 min on ice, 10 µl mitochondria isolation reagent B was added and incubated 5 min on ice followed by vortexing every min. Similarly, 800 µl mitochondria isolation reagent C was added and the samples were centrifuged at 700 × g for 10 min at 4°C. Supernatant was collected and centrifuged at 12,000 × g for 15 min at 4°C. Supernatant was discarded and the pellets were washed with

500 µl mitochondria isolation reagent C and finally centrifuged at 12,000 × g for 5 min at 4°C. Mitochondrial pellets were collected and resuspended in 100 µl H_2O and kept at -20°C until used.

To confirm the isolation of mitochondria western blotting was done using Translocase Of Inner Mitochondrial Membrane 23 (TIMM23) antibody and for checking contamination, other organelle markers like alpha tubulin for cytoplasm, calnexin for ER and lysosomal-associated membrane protein 1 (Lamp-1) for lysosomes were used.

3.13 DAG KINASE ASSAY FOR CERAMIDE QUANTIFICATION

The principle of DAG kinase assay implies conversion of ceramide to ceramide-1-phosphate by the transfer of [^{32}P]-phosphate from [^{32}P]γ-ATP to ceramide. To quantify the ceramide production 2.0 x 10^6 cells/plate were seeded in a 35 mm petri dish 24 h prior to irradiation. The next day, cells were treated with a 4 Gy dose of IR; control cells remained non-irradiated. At an indicated time point, i.e. 10 and 15 min after IR, cells were washed with PBS and extracted in 500 µl of $CHCl_3$: CH_3OH: 1N HCl (100:100:1). The sample if not measured on the same day was kept at -20°C otherwise 100 µl of H_2O was added per samples followed by centrifugation at maximum speed to visualize a clear separation of lower and upper phase. Three times 150 µl were taken from lower organic phase and concentrated by evaporation of the $CHCl_3$ in a SpeedVac. Detergent solution (20 µl) (see section 2.9.2) was added to the evaporated lipids followed by sonication of the samples for 10 min in a bath sonicator in order to achieve formation of micelles. Reaction was started with addition of 70 µl of DAG-kinase reaction buffer (see section 2.9.2) and the samples were incubated for 60 min at RT on a thermomixer. The reaction was stopped by adding 1 ml of $CHCl_3$:CH_3OH:1N HCl (100:100:1, v/v/v) plus 170 µl of DAG-assay buffered saline solution (see section 2.9.2) and 30 µl of a 100 mM EDTA solution per samples. Samples were vortexed and centrifuged at maximum speed. The lower organic phase were concentrated and dried in a SpeedVac. At the end 20 µl of $CHCl_3$:CH_3OH (1:1, v/v) was added to the dried lipids. Lipids were separated on a Silica G-60 TLC plate which was placed into the TLC chamber and the solvent containing $CHCl_3$:CH_3COCH_3:CH_3OH:CH_3COOH:H_2O (10:4:3:2:1, v/v/v/v/v). The TLC plate was then removed, air dried and ceramide was quantified using phosphorimager.

3.14 IMMUNOPRECIPITATION (IP)

For IP assay, 5.0 x 10^6 cells were plated per 100 mm petri dishes and kept in an incubator for 24 h prior to the experiment. The next day, cells were irradiated at 4 Gy or remained untreated. After 10 and 15 min of IR, the medium was removed followed by washing once with cold PBS. Radioimmunoprecipitation assay buffer (RIPA) (see section 2.9.4) (900 µl) was used to lyse the cells, cell lysates were collected with a cell scraper and kept in microcentrifuge tubes on ice for 30 min for the complete lysis of cells. Non-irradiated cells were treated similarly. Lysates were then centrifuged for 5 min at 800 x g and 4°C. Pellets were discarded and supernatant were kept. From each tube i.e. 0 Gy, 4 Gy 10 min and 4 Gy 15 min, 400 µl supernatant were added to separate microcentrifuge tubes. One out of each respective tube was used as control without adding antibody whereas to the other tubes, 1-2 µg of antibody were added. Lysates with and without antibody were incubated for 4 h at 4°C under rotary agitation. Next, 25 µl Protein A/G PLUS-Agarose beads were added to the all the lysates and incubated for another 45 min at 4°C under rotary agitation. Lysates were centrifuged at 800 x g for 1 min at 4°C; proteins bound to beads were collected and the supernatant was discarded. Pellets were washed 5 times with RIPA buffer followed by a centrifugation at 800 x g for 1 min at 4°C. At the last wash step, the complete supernatant was removed, and 50 µl of RIPA lysis buffer were added to the pellet. Protein samples were prepared and analyzed by western blotting. Further samples were sent for MS analysis.

3.15 CERAMIDE PULL-DOWN ASSAY

Ceramide pull-down assay was performed following the detailed prescription given by the manufacturer Echelon Biosciences (see section 2.2.4). Briefly, 5.0 x 10^6 cells per 100 mm petri dish were plated 24 h before the experiment. The next day, cells were irradiated at the dose of 4 Gy or remained untreated; 10 and 15 min after IR, cells were washed once with PBS, and 900 µl of washing/binding buffer (see section 2.9.4) were added to each of the petri dish. Non-irradiated cells were treated similarly. Cell lysates were collected with a cell scraper and centrifuged for 5 min at 800 x g at 4°C. Pellets were discarded and supernatant were kept. From each tube, i.e. 0 Gy, 4 Gy 10 min and 4 Gy 15 min, 400 µl supernatant were added to a new microcentrifuge tubes. One out of each respective tube was used as control by addition of 20 µl control beads whereas to the other tubes, 20 µl ceramide beads were added. Lysates and beads were incubated for 4 h at 4°C under rotary agitation followed by centrifugation at 400 x g for 5 min at 4°C. Supernatant were discarded and the pellets containing beads were washed with 200 µl washing/binding buffer and centrifuged at 400 x g

for 5 min at 4°C and this procedure was done for 5 times. At the last washing step, complete supernatant was removed and beads were suspended with 50 µl of washing/binding buffer and kept at -80°C until use. Samples were sent for MS analysis.

3.16 LIPID RAFT ISOLATION USING SUCROSE DENSITY GRADIENT CENTRIFUGATION

Cells were plated at a density of 5.0 x 10^6 per 100 mm petri dish 24 h prior to the experiment. The next day, cells were irradiated at 4 Gy or remained untreated, and at 10 and 15 min after IR, the medium was removed followed by washing the cells with cold PBS. PBS was completely removed and 1 ml of 500 mM Na_2CO_3 was added to each 100 mm dish. Cells were scraped and transferred to a dounce (glass-glass) homogenizer and homogenized with 60 strokes on ice. Control samples remained non-irradiated were also treated in same way. Lysate were transferred to microcentrifuge tubes and sonicated for 30 sec for three times with tip sonicator using intervals of 100 sec in between. Finally, 1 ml of cell lysates was mixed with 1 ml 90 % sucrose of which 1.3 ml (mixture of cell lysates plus 90 % sucrose) was layered in a Beckman ultracentrifuge tube followed by 1.3 ml 35 % sucrose layering and 0.6 ml 5 % sucrose with a total volume of 3.2 ml. For sucrose % (see section 2.9.4). A visible interface between the two density layers should be seen. Ultracentrifugation was performed for 24 h at 240,000 x g and 4°C in a TLA-55 rotor. After the centrifugation a faint band consisting of the buoyant lipid raft was visible between the 35 % and the 5 % sucrose interface. A volume of approximately 1 ml was collected and stored until use at -80°C. Isolation of lipid rafts was confirmed by western blotting. Further samples were sent for MS analysis.

4 RESULTS

4.1 IONIZING RADIATION (IR) INDUCES DOSE- AND TIME-DEPENDENT CELL DEATH

To determine dose-and time-dependent cell death of two human glioblastoma cell lines A172 and LN308, two different conditions were used. For dose-dependent analysis of cell death, cells were irradiated with different doses (0, 2, 4, 6, 8 Gy). Cells were harvested and stained with propidium iodide (PI) after 96 h. Similarly, for analysis of time-dependent cell death, cells were irradiated with a single dose of 4 Gy or left untreated and after 72, 96 and 120 h cells were stained with PI. In both experiments cells were stained with PI which is not able to pass intact cell membranes and PI positive cells were therefore considered to be the dead cells. The results revealed significant increase in cell death in both dose- and time-dependent manner when compared to non-irradiated cells, i.e. 0 Gy.

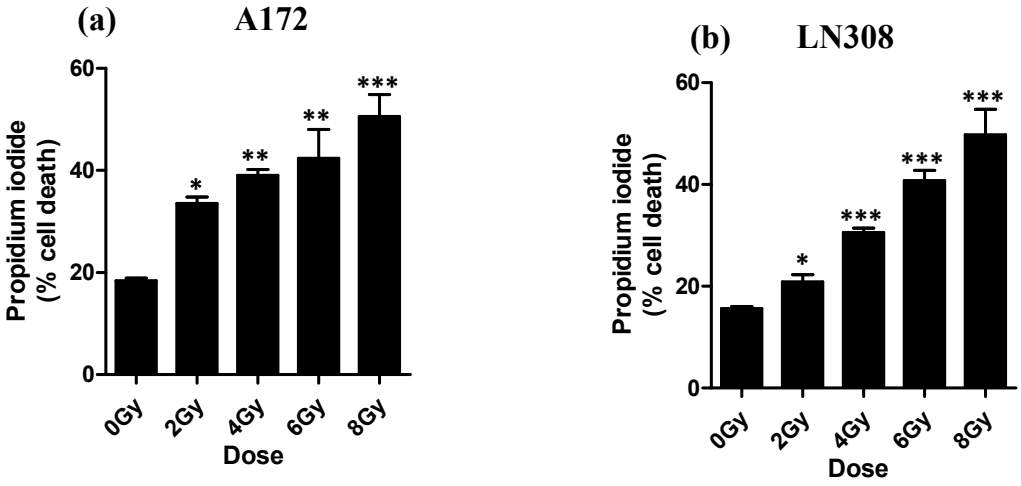

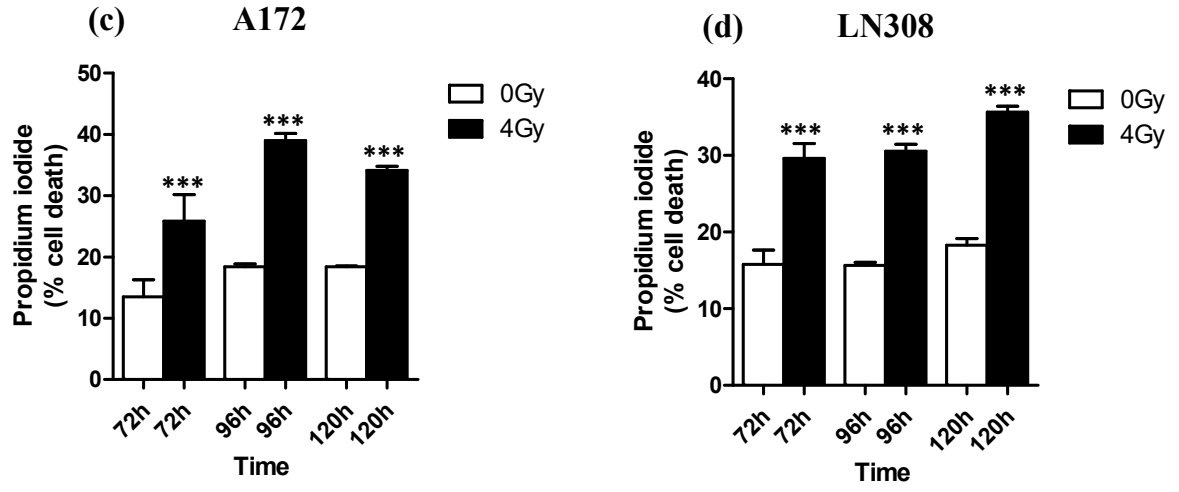

Figure 4.1: Dose- and time-dependent cell death upon IR
Cells were treated with different doses and after 96 h cells were stained with PI for dose dependent response (a) A172 and (b) LN308. Similarly cells were irradiated with a single dose of 4 Gy and after irradiated time point cells were stained with PI for time-dependent response (c) A172 and (d) LN308. Cell death was determined by FACS analysis using FL-2 channel. The data given are the mean values ± S.D. of 3 independent experiments.
Statistical significance between non-irradiated and irradiated cells was determined by analysis of variance (ANOVA) followed by a Bonferroni's selected comparisons test. *P*-values ($p \leq 0.05$, $p \leq 0.01$, $p \leq 0.001$) are indicated by an asterisk* or** or ***, respectively.

4.2 ACTIVATION OF ASM UPON IR

Many stress stimuli like bacterial infection (Grassmé et al 2003b, Zhang et al 2008), death receptors (Cifone et al 1994, Cremesti et al 2001, Perrotta et al 2010), oxidative stress (Li et al 2012, Zhang et al 2007), UV-light (Charruyer et al 2005, Kashkar et al 2005, Rotolo et al 2005, Zhang et al 2001), including irradiation (Paris et al 2001, Santana et al 1996, Sathishkumar et al 2005) are known to induce activation of ASM in variety of cell types leading to cell death pathways. To investigate whether IR is involved in inducing the activation of ASM in human glioblastoma cells, cells were irradiated with 4 Gy or remained untreated and after 10 and 15 min the enzymatic activity of ASM was measured. For A172 cells around 5-10 µg and for LN308 cells around 10-15 µg of proteins per samples were used to measure the ASM activity. The result showed a rapid activation of ASM in both cell lines after irradiation (Figure 4.2). At 10 min after irradiation, a transient increase in ASM activity is seen with slight decrease after 15 min in A172 cell lines. However, when compared to 0 Gy both 10 and 15 min irradiated cells showed an increase in ASM activity in both the cell lines.

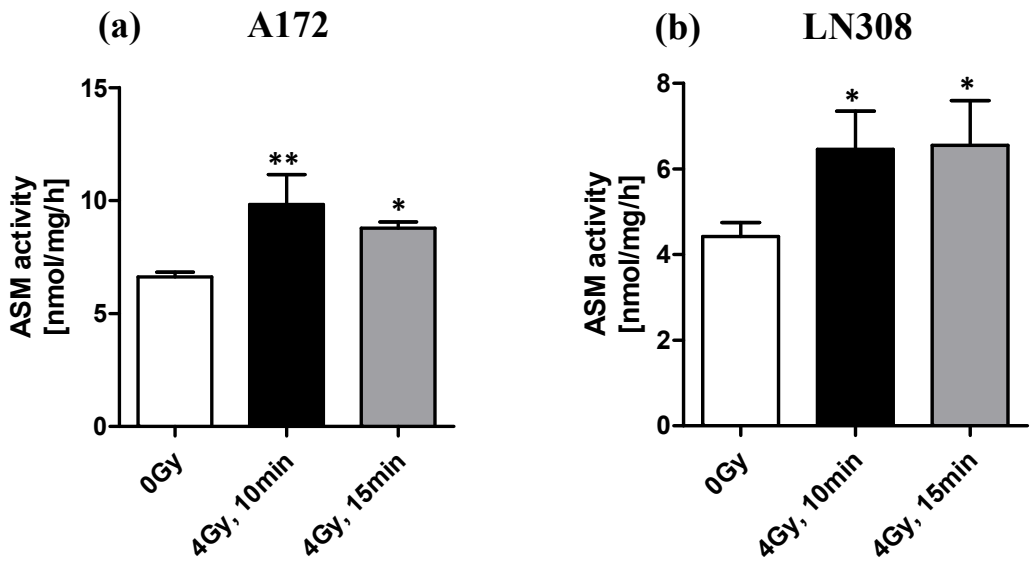

Figure 4.2: IR activates ASM
A172 (a) and LN308 (b) human glioblastoma cells were irradiated with 4 Gy or left untreated. The activity of the ASM was measured as the consumption of radioactive [^{14}C]sphingomyelin to ceramide and [^{14}C]phophorylcholine. The data given are the mean values ± S.D. of 3 independent experiments.
Statistical significance between non-irradiated and irradiated cells was determined by analysis of variance (ANOVA) followed by a Bonferroni's selected comparisons test. *P*-values ($p \leq 0.05$, $p \leq 0.01$) are indicated by an asterisk* or**, respectively.

4.3 IR-INDUCED TRANSLOCATION OF ASM FROM INTRACELLULAR PART TO OUTER LEAFLET OF CELLS

To analyze whether the observed ASM activation in the human glioblastoma cell lines is accompanied by translocation of the ASM to the outer leaflet of the cell membrane, cells grown on coverslips were irradiated with 4 Gy or left non-irradiated. After 10 and 15 min, cells were fixed and stained with an antibody specific for the ASM. The result showed ASM translocation to the cell surface/outer leaflet in irradiated cells while no translocation of ASM was observed in non-irradiated cells (Figure 4.3).

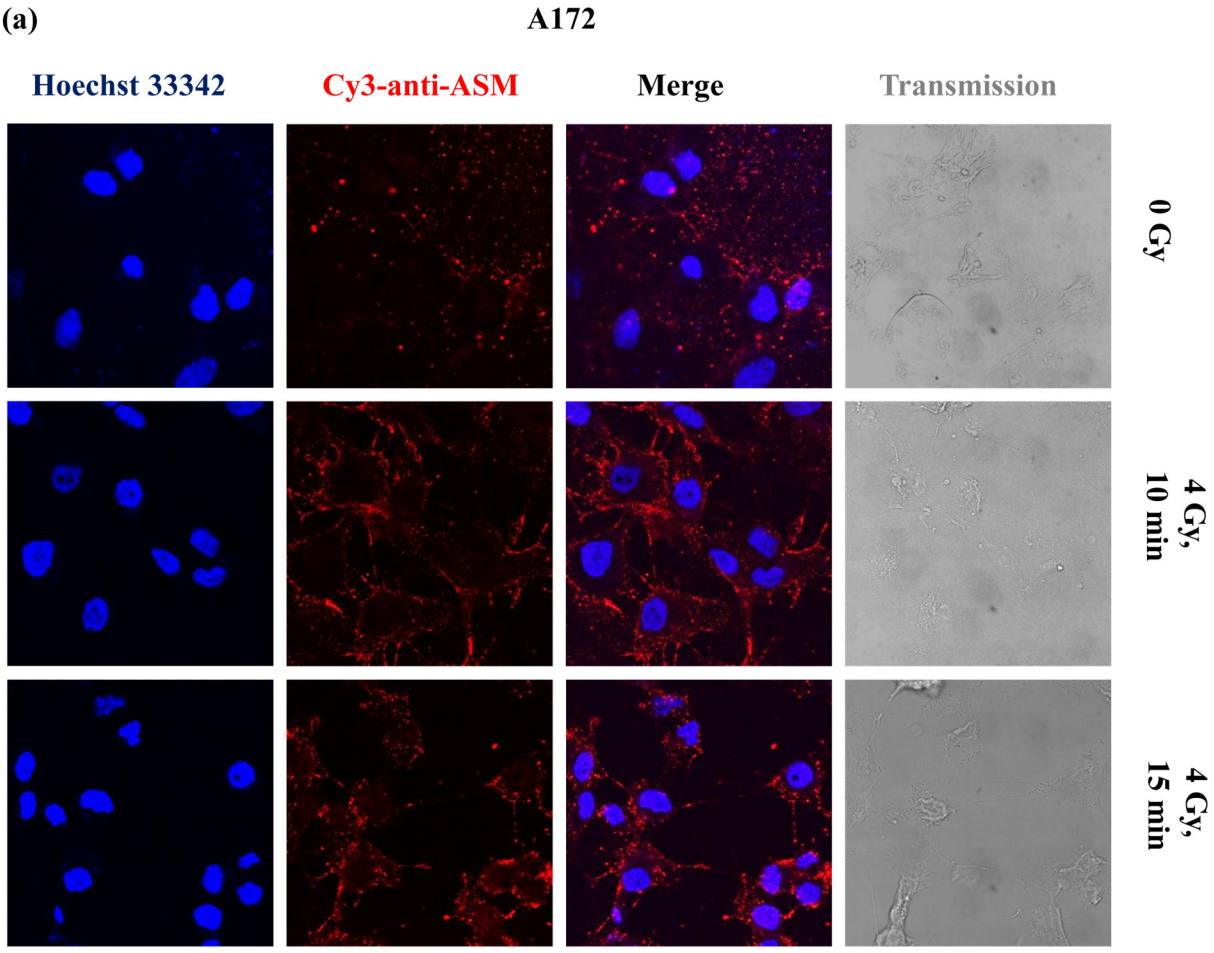
(a)
A172
Hoechst 33342
Cy3-anti-ASM
Merge
Transmission
0 Gy
4 Gy, 10 min
4 Gy, 15 min

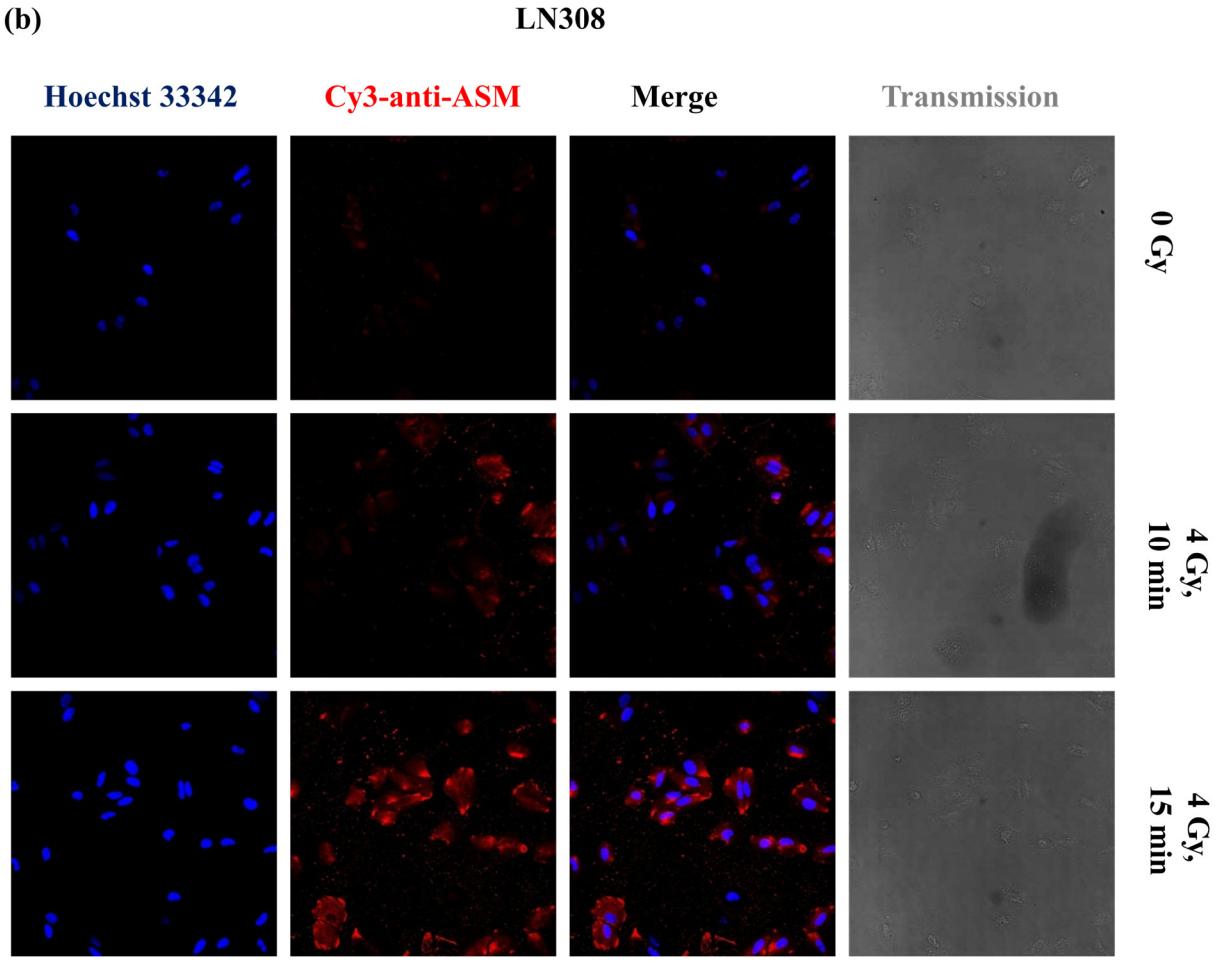

Figure 4.3: Translocation of ASM from intracellular part to outer leaflet of cells upon IR
Human glioblastoma cell lines A172 (a) and LN308 (b) were irradiated with 4 Gy or left untreated. Cells were remained unpermeabilized and stained with anti-ASM antibody followed by Cy3-labeled anti-rabbit secondary antibody. The nuclei were stained with Hoechst 33342; the merge picture panel shows the overlay of Hoechst 33342 and ASM/Cy3. The transmission light picture was taken in addition. The images are representative for 3 independent studies.

4.4 CLUSTERING OF CERAMIDE/CERAMIDE-ENRICHED MEMBRANE PLATFORMS UPON IR

Activation of ASM has been correlated with release of ceramide and formation of ceramide-enriched membrane platforms upon different stimuli. To study whether IR mediates clustering of ceramide/ceramide-enriched membrane platforms, human glioblastoma cell lines A172 and LN308 were remained non-irradiated or irradiated with 4 Gy. After 10 and 15 min, cells were fixed and immunofluorescence staining was carried out using a monoclonal anti-ceramide antibody (MID15B4) followed by a Cy3-labeled anti-mouse secondary antibody. The result revealed that ceramide accumulates in the platforms on the cell surface of both cell lines after

irradiation leading to clustering of ceramide (Figure 4.4), whereas no clustering was seen in non-irradiated cells.

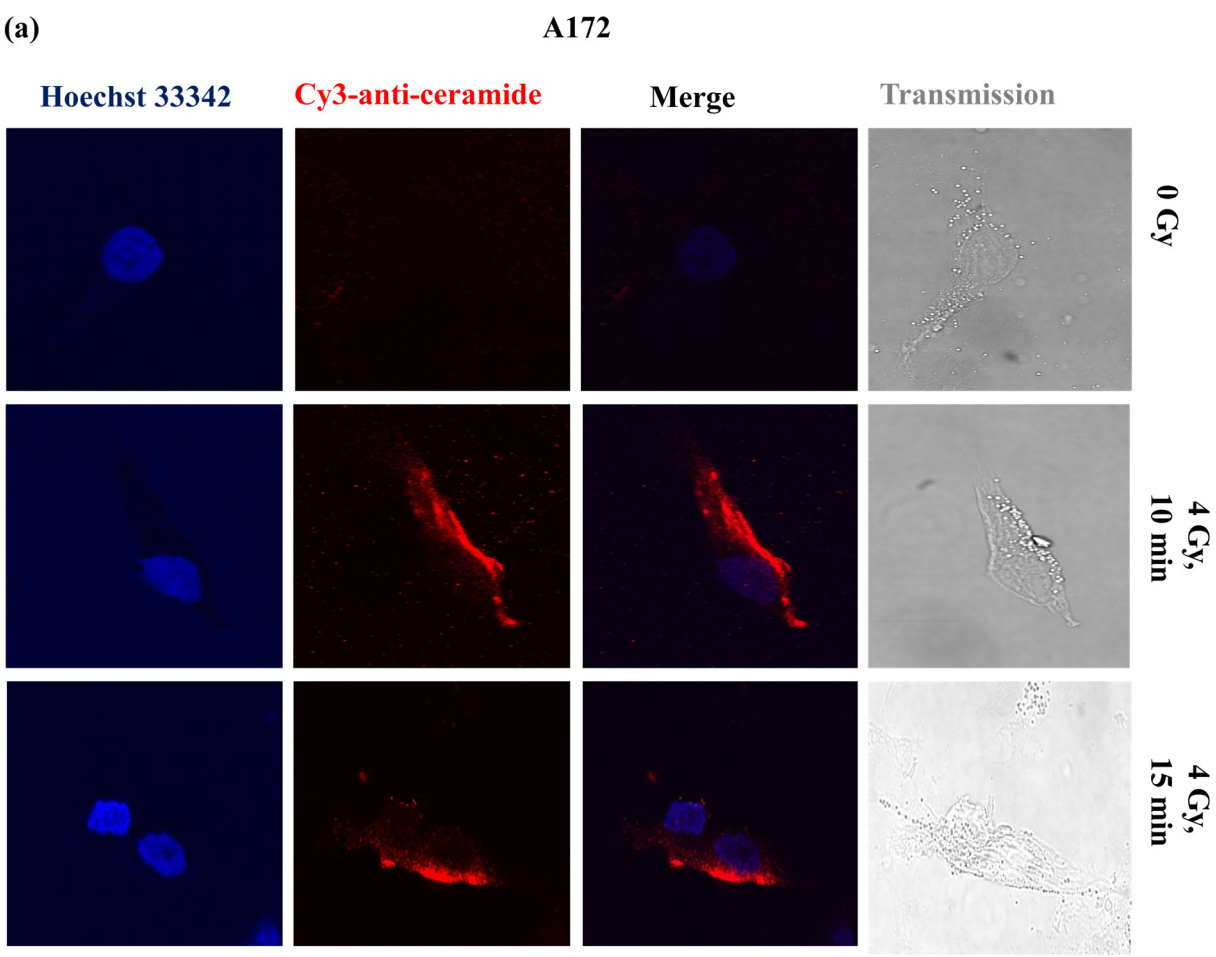

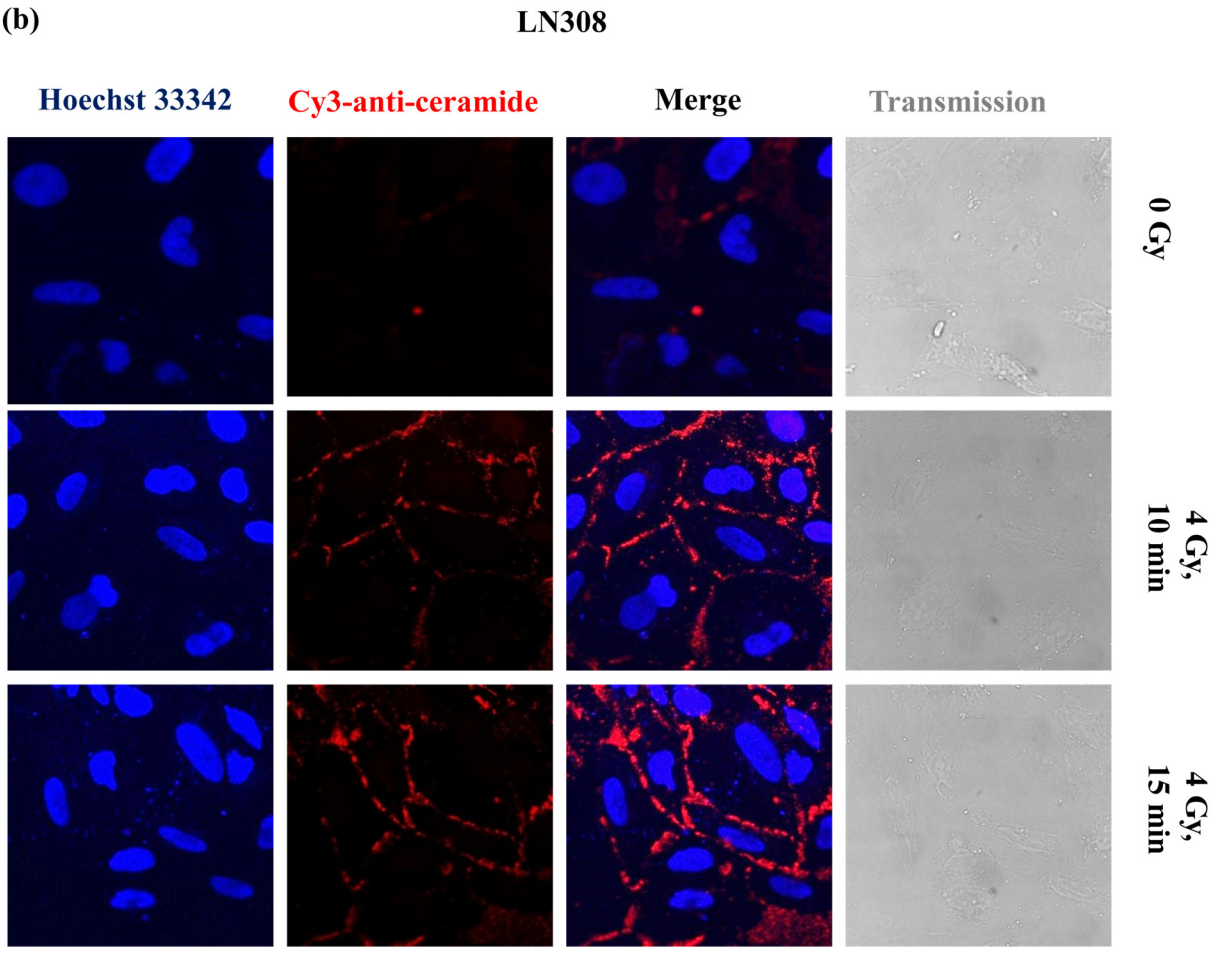

Figure 4.4: IR induces clustering of ceramide and formation of ceramide-enriched membrane platforms
Human glioblastoma cell lines A172 (a) and LN308 (b) were irradiated with 4 Gy or remained untreated. Cells were remained unpermeabilized and stained with anti-ceramide antibody (MID15B4) followed by Cy3-labeled anti-mouse secondary antibody. The nuclei were stained with Hoechst 33342; the merge picture panel shows the overlay of Hoechst 33342 and ceramide/Cy3. The transmission light picture was taken in addition. The images are representative for 3 independent studies.

4.5 ROS IS NECESSARY FOR IR-INDUCED ACTIVATION OF ASM

Previous studies have shown the role of ROS in activation of ASM in T splenocytes and macrophages (Dumitru and Gulbins 2006, Zhang et al 2008). Since IR is known to be an inducer of ROS production, it was tested whether IR-induced ROS production triggered ASM activation. To determine the ROS burst in human glioblastoma cell lines A172 and LN308, cells were pre-incubated for 10 min with 2',7'-dichlorodihydrofluorescein diacetate (H_2DCFDA), a cell-permeant fluorogenic dye that measures ROS by passively diffusing into the cells. H_2DCFDA is retained in the intracellular level after cleavage by intracellular esterases. The nonfluorescent H_2DCFDA is then converted to the highly fluorescent 2',7'-

dichlorofluorescein (DCF). Cells were remained untreated or treated with 4 Gy. IR-induced an increase of ROS burst in irradiated cells compared to non-irradiated cells. Similarly ROS production was also measured by incubating the cells with ROS inhibitors apocynin and tiron, which significantly attenuated IR–induced ROS production (Figure 4.5 a and b). Tiron is a ROS scavenger whereas apocynin is known to be an inhibitor of nicotinamide adenine dinucleotide phosphate (NADPH) oxidase activity. Apocynin inhibits the assembly of a functional NADPH-oxidase complex that is responsible for ROS production upon oxidation by myeloperoxidase (Touyz 2008).

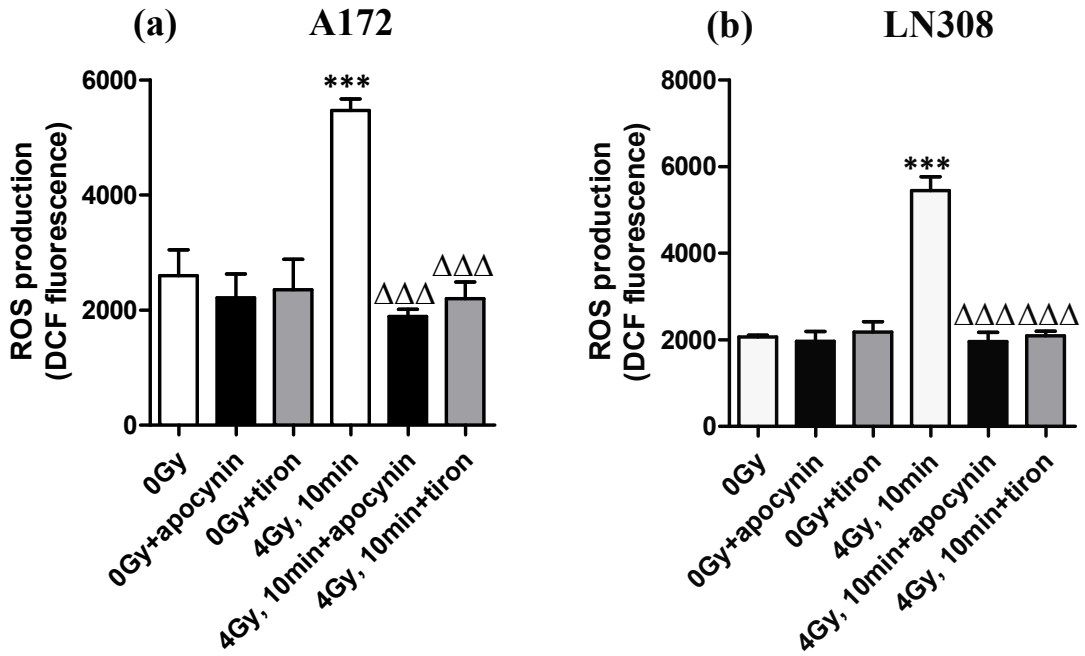

To analyse whether ROS mediates IR-induced activation of ASM, enzymatic activity of ASM was measured in human glioblastoma cell lines A172 and LN308. Cells were incubated with the ROS inhibitors apocynin and tiron prior to the 4 Gy dose of radiation treatment. This resulted in an inhibition of IR-induced ASM activation, which shows the pivotal role of ROS in the ASM activation mechanism (Figure 4.5 c and d)

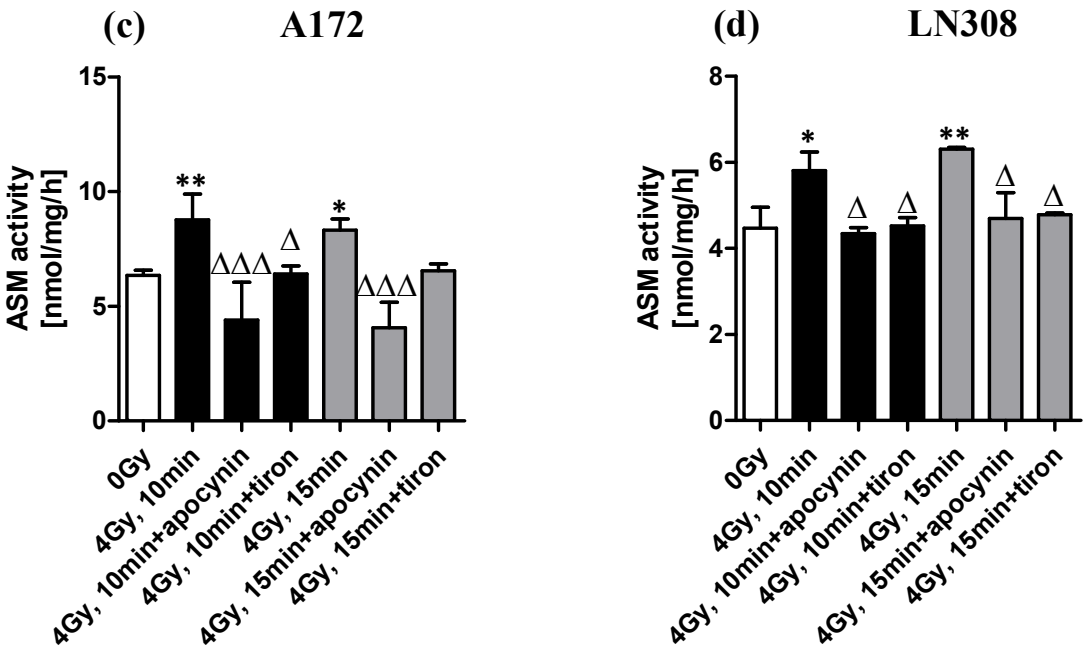

Figure 4.5: IR-induced activation of ASM is ROS dependent
Human glioblastoma cell lines A172 (a) and LN308 (b) were incubated with ROS inhibitors apocynin and tiron followed by further incubating the cells with H_2DCFDA. Cells were irradiated with 4 Gy or remained untreated and ROS was measured after 10 min using micro-plate reader. A172 (c) and LN308 (d) were incubated with ROS inhibitors apocynin and tiron followed by treating the cells with 4 Gy or remained untreated. Activity of ASM was determined as the consumption of radioactive [^{14}C]sphingomyelin to ceramide and [^{14}C]phophorylcholine. The data given are the mean values ± S.D. of 3 independent experiments.
Statistical significance between non-irradiated and irradiated cells was determined by analysis of variance (ANOVA) followed by a Bonferroni's selected comparisons test. *P*-values ($p \leq 0.05$, $p \leq 0.01$, $p \leq 0.001$) are indicated by an asterisk* or** or *** respectively or irradiated and ROS inhibitos/irradiated are indicated by delta Δ or ΔΔ or ΔΔΔ, respectively.

4.6 ACTIVATION OF ASM AND FORMATION OF CERAMIDE-ENRICHED MEMBRANE PLATFORMS UPON IRRADIATION IS DEPENDENT ON NADPH OXIDASE

4.6.1 IR INDUCES ACTIVATION OF NADPH OXIDASE AND SUPEROXIDE PRODUCTION

Previous studies have shown NADPH oxidase subunits to aggregate into ceramide-enriched membrane platforms producing superoxide to regulate signaling process (Jin et al 2008c, Zhang et al 2006). Similarly it has also been reported that radiation-induced oxidative stress is mediated by NADPH oxidase (Collins-Underwood et al 2008).

This led us to examine whether IR is involved in aggregation of gp91phox, a major membrane subunit of NADPH oxidase into ceramide-enriched membrane platforms.

IR-induced activation of NADPH oxidase was assayed by cytochrome c reduction in A172 cells. The assay mixtures consisted of cytochrome c, enzyme dilution buffer and NADPH solution (see materials). Cells were incubated with the assay mixtures for 15 min at RT followed with irradiation with 4 Gy or remained untreated. After 10 min total NADPH activity was measured at an absorbance of 550 nm using micro-plate reader. The results revealed 20 % increase in activation of NADPH oxidase in irradiated cells when compared to non-irradiated cells (Figure 4.6.1 a). As NADPH oxidase is a major source of superoxide production, next superoxide production was measured in human glioblastoma cell line A172 using dihydroethidium (DHE), a molecular probe for superoxide measurement. The substance DHE detects ROS and upon reaction with superoxide anions forms a red fluorescent product (ethidium) which intercalates with DNA. Cells were incubated for 5 min with DHE and remained non-irradiated or irradiated at a dose of 4 Gy. Superoxide production was monitored using a live cell imaging technique and images were taken starting from 1 min till 15 min. For this experiment, special round bottom petri dishes were used. The results showed increase in the fluorescence intensity for DHE dye in irradiated cells in time-dependent manner whereas no increase in the fluorescence intensity was observed in non-irradiated cells (Figure 4.6.1 b).

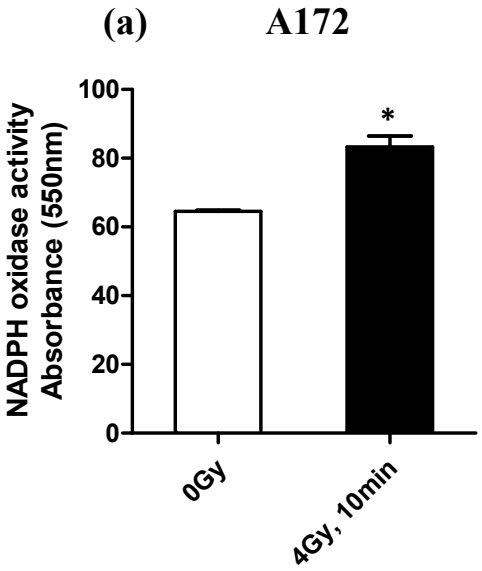

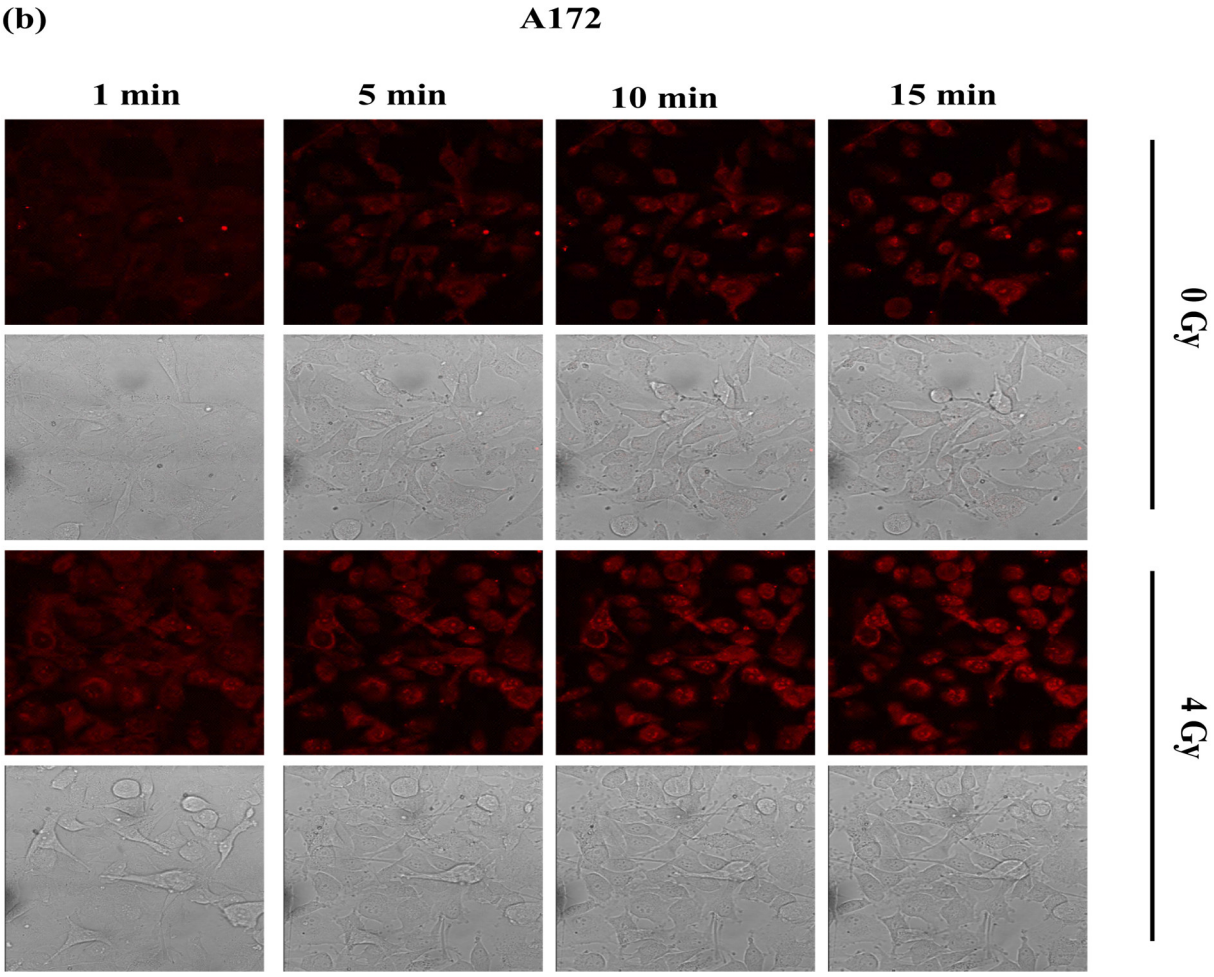

Figure 4.6.1: Increase in activation of NADPH oxidase and superoxide production upon IR
NADPH oxidase activity was measured in A172 cells by incubating the cells with cytochrome c and NADPH solution. After 15 min of incubation cells were irradiated with 4 Gy or remained untreated. The data given are the mean values ± S.D. of 3 independent experiments performed in triplicate.
Significant differences ($p \leq 0.05$, *t*-test) between non-irradiated and irradiated cells are labeled by an asterisk*.
Human glioblastoma cell line A172 (b) were incubated with DHE to measure superoxide and fluorescence intensity was recorded using live cell imaging technique. The images are representative for 3 independent studies.

4.6.2 IR-INDUCED ACTIVATION OF NADPH OXIDASE VIA CERAMIDE-ENRICHED MEMBRANE PLATFORMS

The role of ceramide-enriched membrane platforms in signaling pathway was fully elucidated showing that these platforms trap and cluster death receptors like CD95 and CD40 (Cremesti et al 2001, Grassmé et al 2001a, Grassmé et al 2001b, Grassmé et al 2002a). As a result of this trapping and clustering of receptors cell death signal is transmitted inside of the cells. Later

on, other signaling molecules like subunits of NADPH oxidase particularly gp91phox and p47phox were shown to be clustered in ceramide-enriched membrane platforms resulting in activation of ASM in endothelial cells (Bao et al 2010, Zhang et al 2007). To address the mechanism of IR-induced activation of NADPH oxidase with the involvement of ceramide-enriched membrane platforms, it was examine whether ceramide-enriched membrane platforms are involved in aggregation of gp91phox, a major membrane subunit of NADPH oxidase. Immunofluorescence co-staining of ceramide and gp91phox was performed. Human glioblastoma cell lines A172 and LN308 were remained non-irradiated or irradiated with 4 Gy. After 10 and 15 min, cells were fixed and remained unpermeabilized followed by staining the cells with monoclonal anti-ceramide antibody (MID15B4) and gp91phox antibody. Similarly, Cy3-labeled anti-mouse and FITC- labeled anti-rabbit secondary antibodies were used. The results showed that gp91phox aggregates/clusters in and co-localizes with ceramide-enriched platforms (Figure 4.6.2) and this phenomenon was absent in non-irradiated cells.

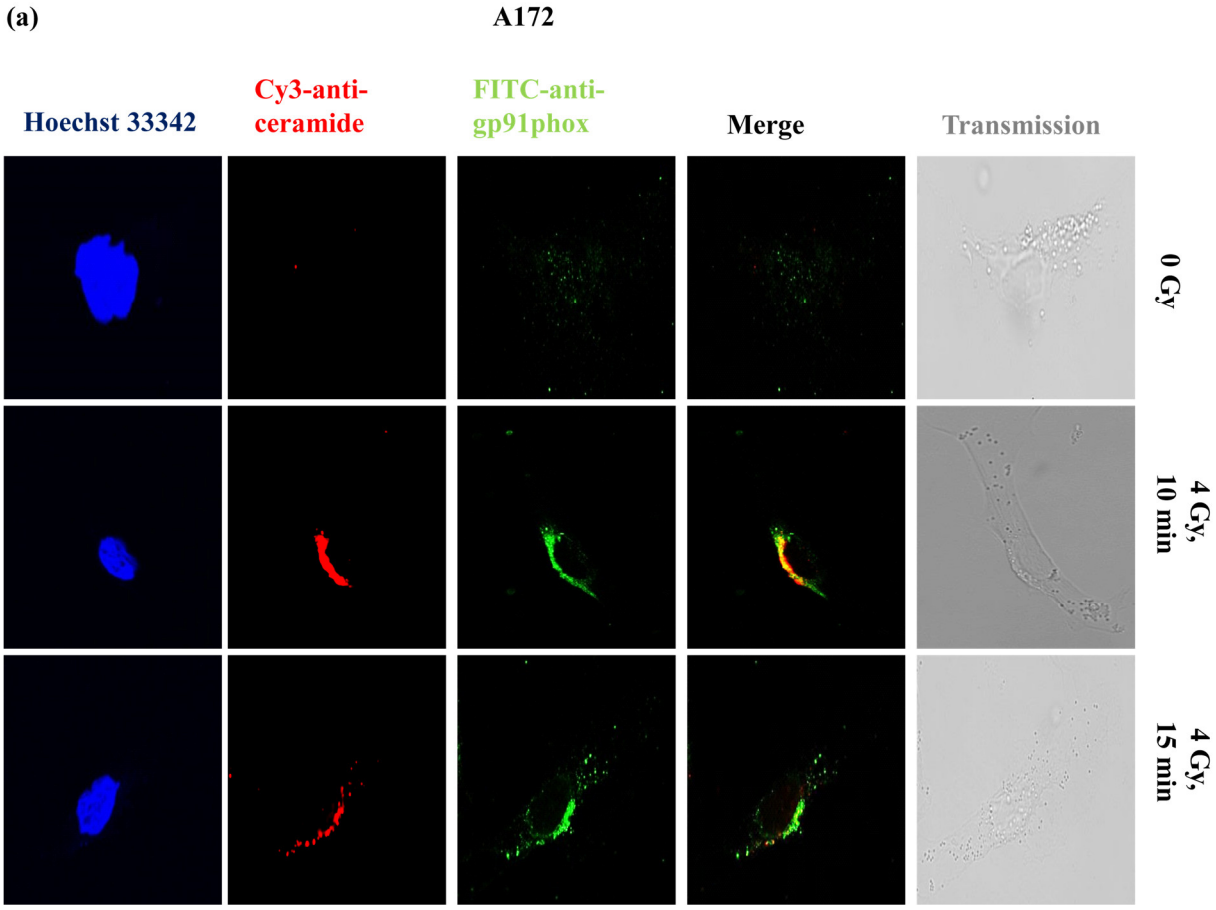

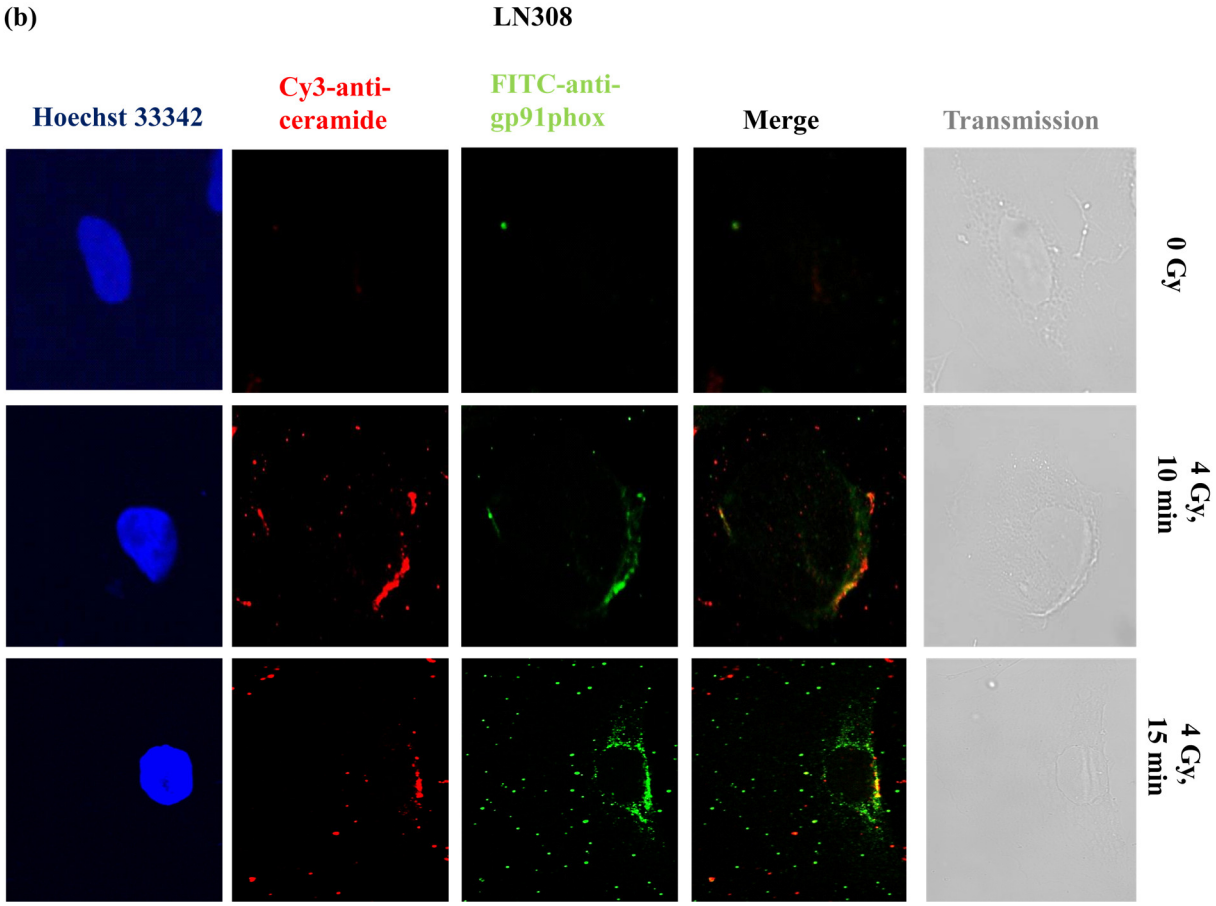

Figure 4.6.2: NADPH oxidase subunit gp91phox clusters in ceramide-enriched membrane platforms upon irradiation
Human glioblastoma cell lines A172 (a) and LN308 (b) were irradiated with 4 Gy or left untreated and fixed. Cells were remained unpermeabilized and stained with anti-ceramide (MID15B4) and gp91phox antibodies followed by Cy3-labeled anti-mouse and FITC-labeled anti-rabbit secondary antibodies. The nuclei were stained with Hoechst 33342; the merge picture panel shows the overlay of ceramide/Cy3 and gp91phox/FITC. The transmission light picture was taken in addition. The images are representative for 3 independent studies.

4.6.3 INVOLVEMENT OF GP91PHOX IN IR-INDUCED ACTIVATION OF ASM

Previously it was shown that adipokines (visfatin), a Pre-B colony Enhancing Factor (PBEF) known to be involved in the early development of B lymphocytes (Samal et al 1994) stimulates ceramide production via activation of ASM and induces NADPH oxidase activation through the formation of lipid raft (LR) signaling platforms in glomerular endothelial cells (GECs). Silencing of ASM gene or using ASM inhibitor amitriptyline or silencing of gp91phox gene or using NADPH oxidase inhibitor, diphenyleneiodonium chloride (DPI) attenuated the co-localization of gp91phox and LR showing the existence of feed forward loop. Thus, the study elucidated the role of ASM to form redox signaling platforms by aggregation and activation of NADPH oxidase subunits gp91phox (Boini et al

2010). Similarly Zhang and coworker showed using NADPH oxidase inhibitor DPI resulted in blockade of Asm activation and formation of ceramide-enriched membrane platforms in macrophages upon *P. aeruginosa* stimulation (Zhang et al 2008).

To explore the involvement of gp91phox upon activation of ASM during radiation, one of the human glioblastoma cell lines A172 were transfected with either gp91phox siRNA or control siRNA. The result demonstrated that transfecting the cells with gp91phox siRNA for 48 h resulted in around 50 % downregulation of gp91phox protein expression which was confirmed by western blotting using antibody against gp91phox (Figure 4.6.3 a). Normalization of control siRNA and gp91phox siRNA with loading control beta-actin was carried out using imageJ program (Figure 4.6.3 b). Further enzymatic activity of ASM was measured in gp91phox as well as control siRNA transfected cells which was treated with 4 Gy or remained untreated. This result showed inhibition of ASM activity in gp91phox siRNA transfected cells compared to control siRNA transfected cells upon irradiation (Figure 4.6.3c).

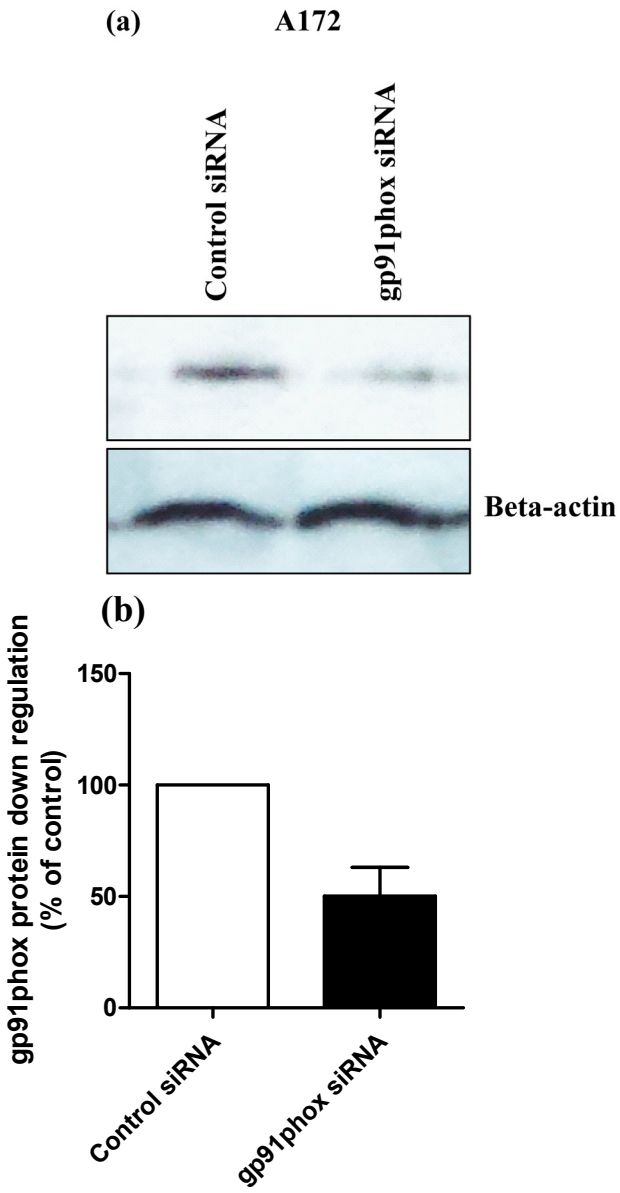

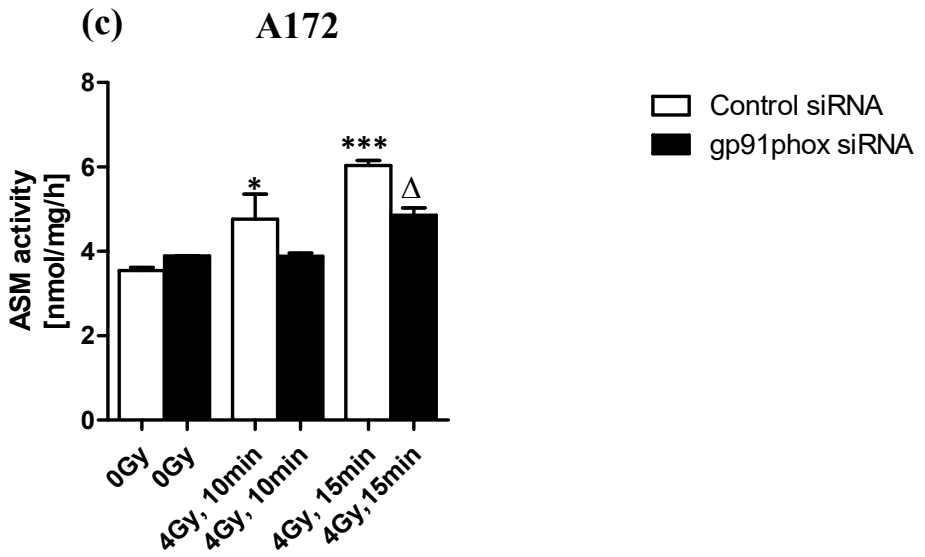

Figure 4.6.3: IR induced activation of ASM is NADPH oxidase dependent
A172 cells were transfected with control or gp91phox siRNA followed by western blotting to confirm the downregulation of gp91phox protein (65 kDa) (a).
The images are representative for 2 independent studies.
Normalization of gp91phox and control siRNA transfected protein level to loading control beta-actin was confirmed using program imageJ (b). A172 cells were transfected with gp91phox and control siRNA followed with 4 Gy dose of irradiation or remained untreated. ASM activity was measured as the consumption of radioactive [^{14}C]sphingomyelin to ceramide and [^{14}C]phophorylcholine (c). The data given are the mean values ± S.D. of 3 independent experiments.
Statistical significance between non-irradiated (control siRNA) and irradiated (control siRNA) or irradiated (control siRNA) and irradiated (gp91phox siRNA) was determined by analysis of variance (ANOVA) followed by a Bonferroni's selected comparisons test. *P*-values ($p \leq 0.05$, $p \leq 0.001$) between non-irradiated (control siRNA) and irradiated (control siRNA) are indicated by an asterisk* or *** and irradiated (control siRNA) and irradiated (gp91phox siRNA) are indicated by delta Δ respectively.

4.7 MITOCHONDRIAL ROS AND CERAMIDE PRODUCTION IN IRRADIATED HUMAN GLIOBLASTOMA CELLS

Several studies have shown the role of radiation in production of mitochondrial ceramide leading to cell death (Dai et al 2004, Lee et al 2011). To investigate whether IR targets organelles other than plasma membrane for generation of ceramide/ceramide-enriched membrane platforms upon irradiation in human glioblastoma cell lines, studies targeting mitochondria was performed. Mitochondrial ROS was measured in A172 cells using MitoSOX red, a mitochondrial superoxide indicator. MitoSOX red is a fluorogenic dye that targets mitochondria as it can permeates live cells. It is rapidly oxidized by superoxide and

upon binding to nucleic acid the oxidized product is highly fluorescent. Irradiating the cells with 4 Gy in presence of MitoSOX for 20 min resulted in rapid production of mitochondrial superoxide. Images were taken through live cell imaging technique starting from 5 min till 20 min which showed a time-dependent ROS increase in irradiated cells. No such increase was observed in non-irradiated cells (Figure 4.7 a). Next a co-staining of ceramide and mitochondrial marker TIMM23 was performed. For this A172 cells were remained non-irradiated or irradiated with 4 Gy and after 10 and 15 min, cells were fixed and permeabilized. Cells were stained with monoclonal anti-ceramide (MID15B4) and TIMM23 antibodies followed by Cy3-labeled anti-mouse and Cy5-labeled anti-rabbit antibodies. The result revealed the co-localization of ceramide in mitochondria in irradiated cells. Compared to the irradiated cells no co-localization was seen in non-irradiated cells (Figure 4.7 b).

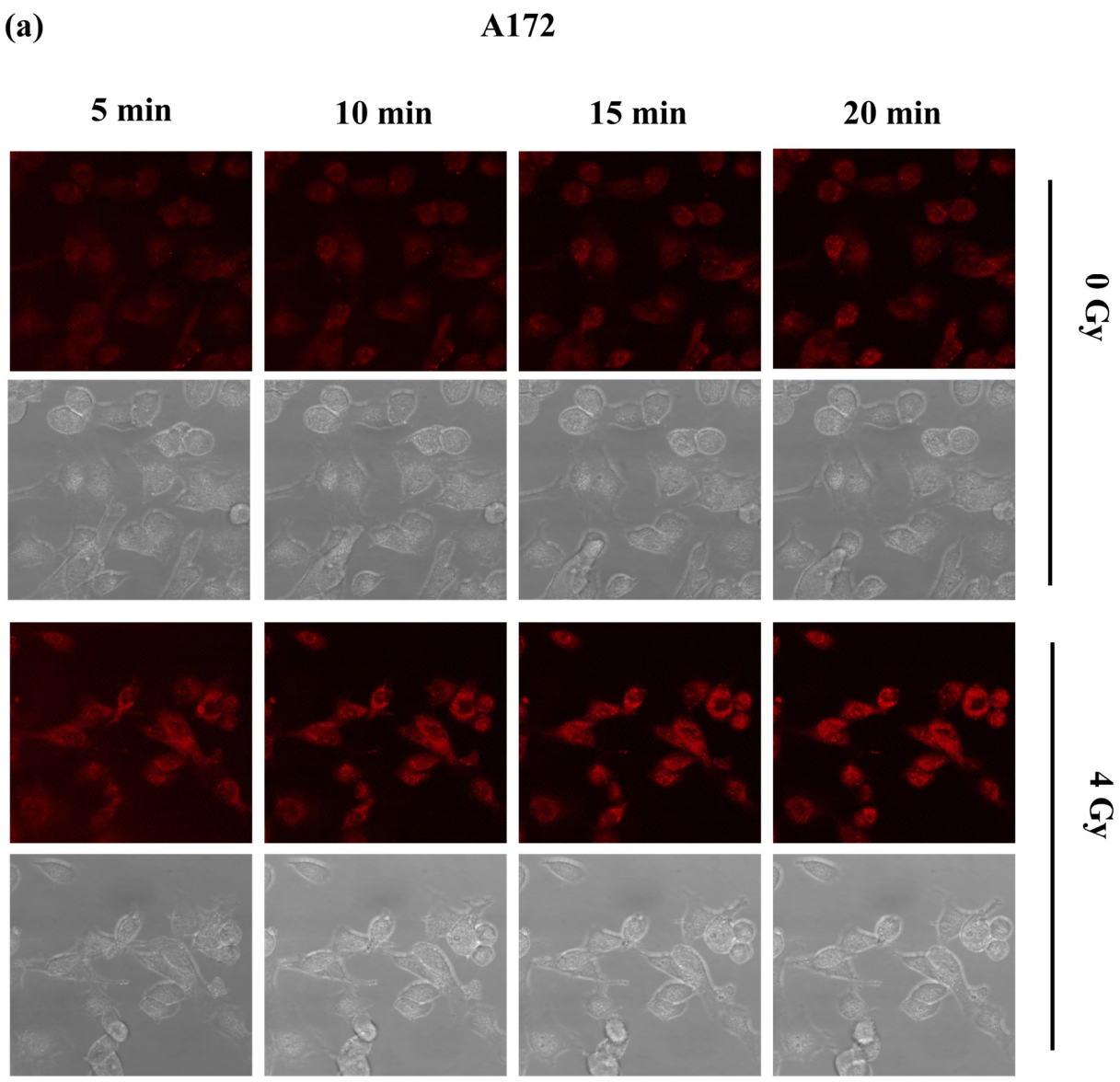

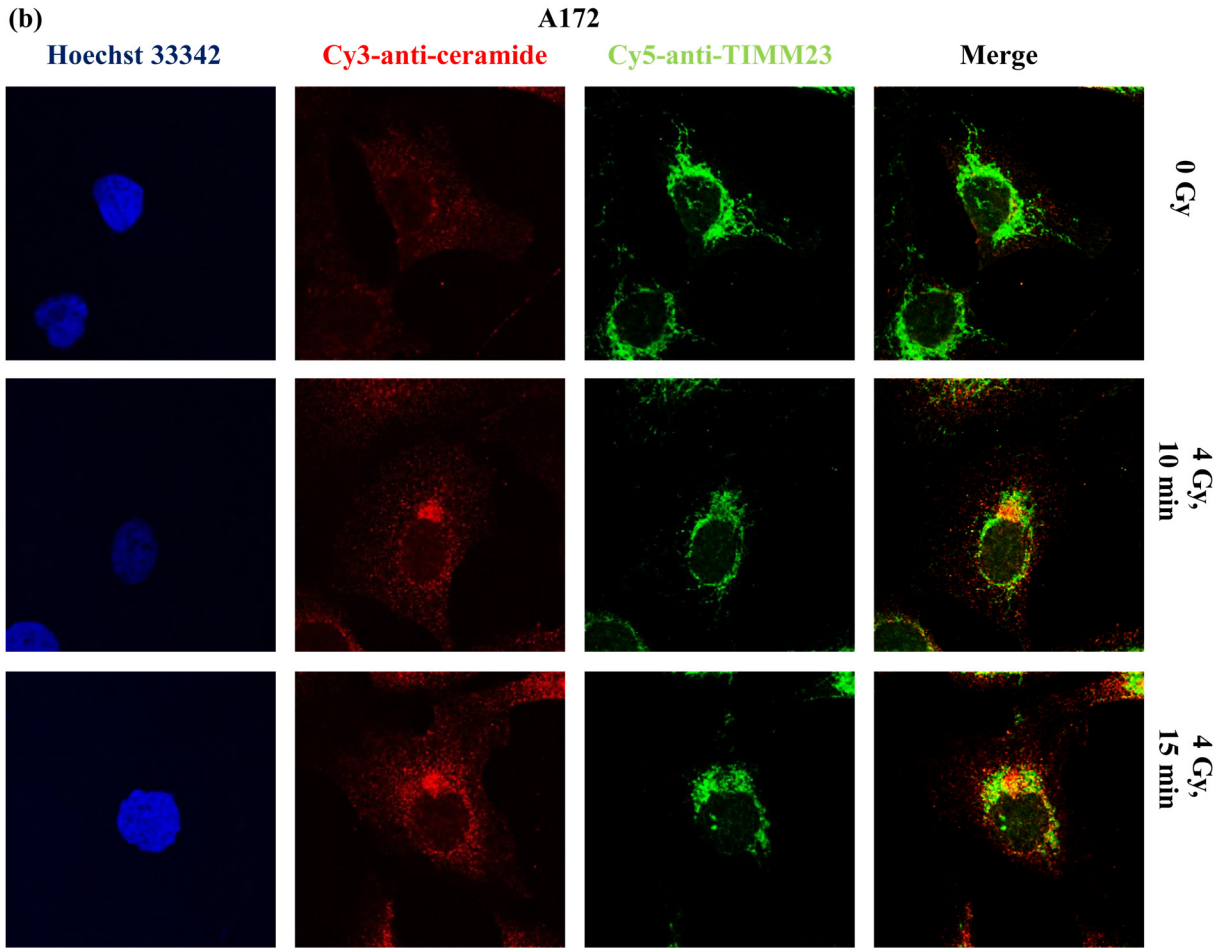

To make a quantitative analysis for mitochondrial ceramide production, diacylglycerol (DAG) kinase assay in mitochondrial-enriched fractions isolated from human glioblastoma A172 and LN308 cells was performed. For this, human glioblastoma cell lines A172 and LN308 were irradiated with 4 Gy or remained untreated and after 10 and 15 min cells were collected. Mitochondria were isolated using mitochondrial isolation kit (see materials). Western blotting was used to confirm enrichment of mitochondria using mitochondrial marker TIMM23. Similarly, to verify that the isolated mitochondrial fractions are free from contaminations various other organelles markers like alpha-tubulin for cytoplasm, calnexin for endoplasmic reticulum (ER) and lysosomal-associated membrane protein 1 (Lamp-1) for lysosomes were used. As a result, isolated mitochondrial fractions were found to be negative when tested with all the other organelle markers except for ER marker calnexin, which showed a slight band positive for isolated fractions within the mitochondrial fraction (Figure 4.7 c and d). Once isolated mitochondrial fractions were confirmed, ceramide DAG-kinase assay was performed in those fractions. Ceramide (C16 and C24 species) was separated from other lipids with the

use of thin-layer chromatography (TLC) (Figure 4.7 e and f). Quantification of TLC plates was performed using phosphorimager (Fujifilm) (Figure 4.7. g and h).

Results from scanned TLC plates showed a small increase in ceramide level at 10 and 15 min after irradiation in both cell lines when compared to non-irradiated cells. Despite ceramide increase was clearly visible, it has to be mentioned that after quantification of ceramide levels the increase was not statistically significant. The next point to be noticed would be that a clear increase of mitochondrial ceramide is observed in fluorescence microscopy with a very less amount of ceramide seen in non-irradiated cells because the setting for microscope were minimized to see if there is any difference between irradiated and non-irradiated cells. The settings were kept exactly the same for both the treated as well as non-irradiated samples. The results from DAG kinase assay might be the ceramide from mitochondria as well as ER as contamination in isolated mitochondrial fractions was observed.

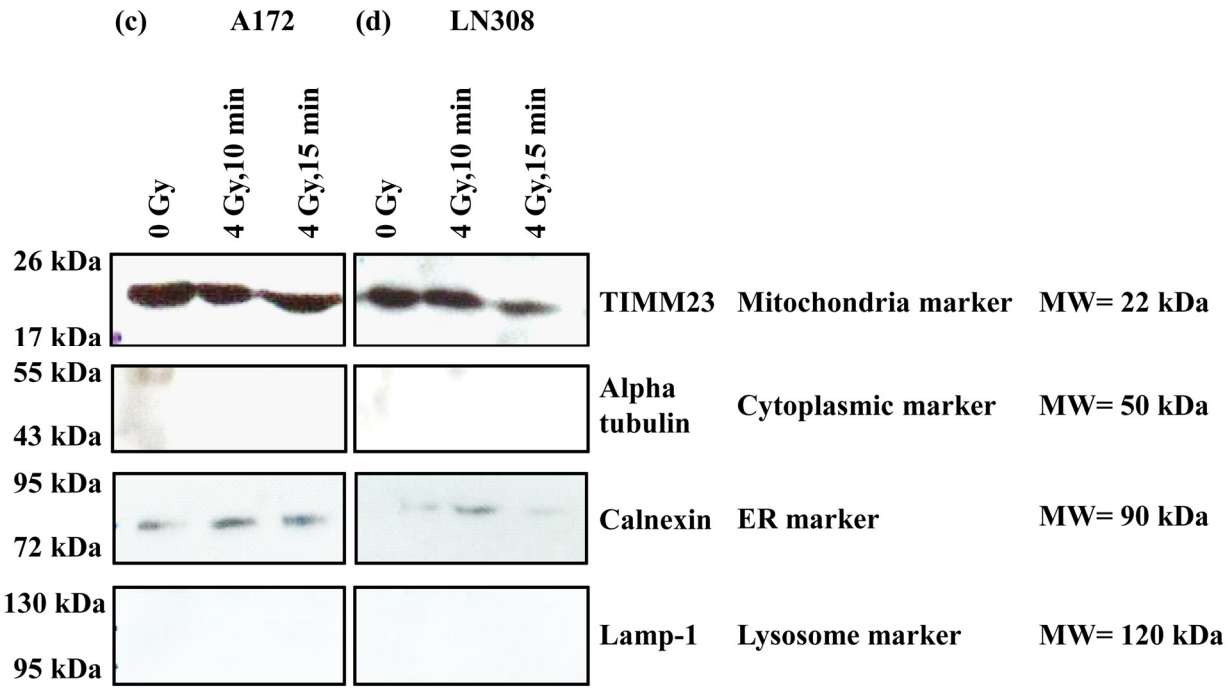

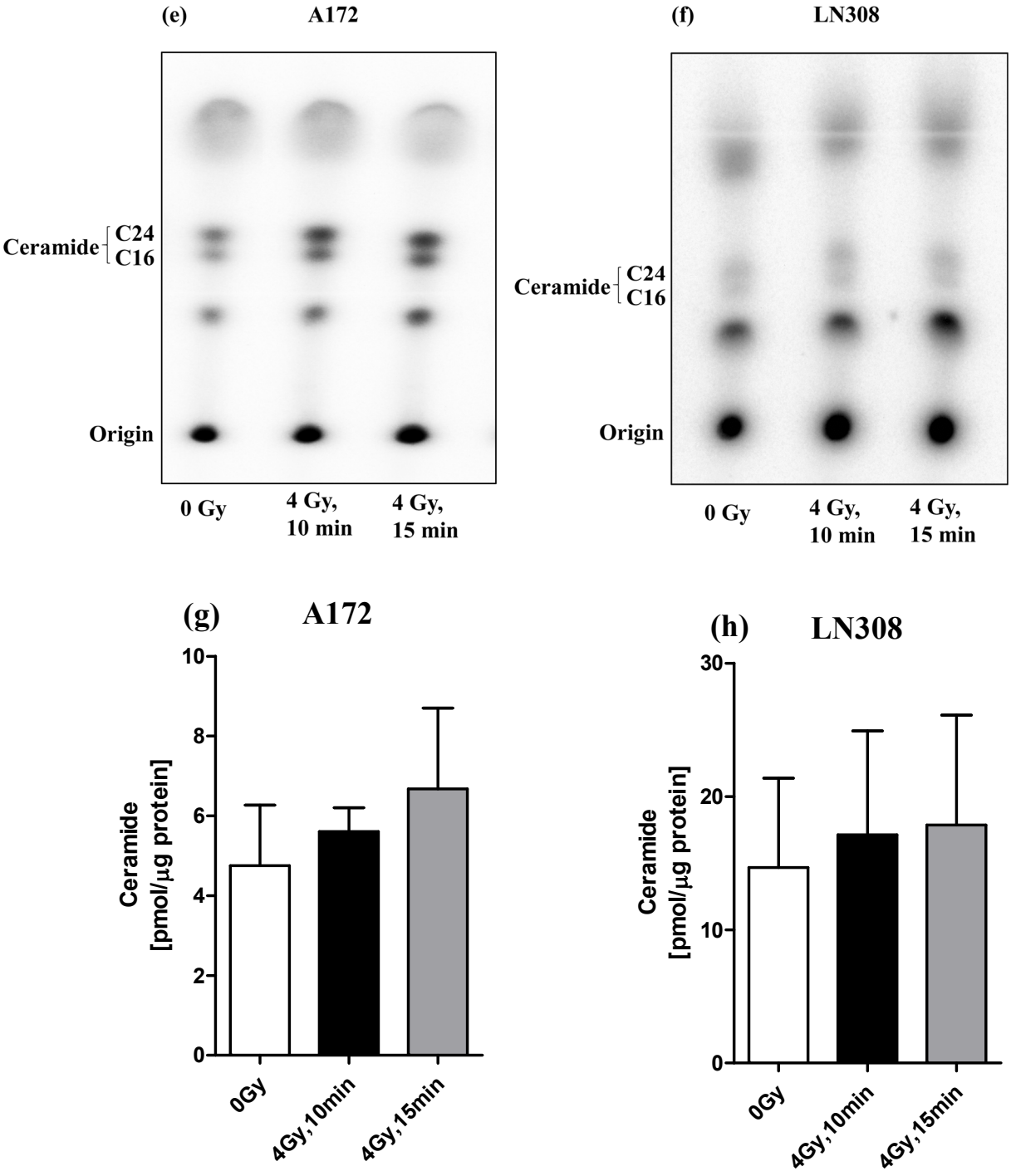

Figure 4.7: IR results in production of mitochondrial ROS and ceramide

Human glioblastoma cells A172 (a) were irradiated with 4 Gy or remained non-irradiated in presence of mitochondrial indicator MitoSOX. Live cell imaging technique was used to monitor the mitochondrial ROS production. The transmission light picture was taken in addition. The images are representative for 3 independent studies.

Co-staining for ceramide and mitochondria in untreated and irradiated A172 cells (b) were performed using antibodies against ceramide and mitochondria (TIMM23) followed by Cy3-labeled anti-mouse and Cy5-labeled anti-rabbit antibodies. To view intracellular ceramide,

cells were fixed and permeabilized. The nuclei were stained with Hoechst 33342; the merge picture panel shows the overlay of ceramide/Cy3 and TIMM23/Cy5. The images are representative for 3 independent studies.
Isolation of mitochondrial fraction in A172 (c) and LN308 (d) cells were analyzed by western blotting with antibody to TIMM23 (mitochondria marker) 22 kDa and contamination was checked with antibodies to alpha tubulin (cytoplasm marker) 50 kDa, calnexin (ER marker) 90 kDa and Lamp-1 (lysosomes marker) 120 kDa. The images are representative for 3 independent studies.
Human glioblastoma cell lines A172 (e) and LN308 (f) were treated with 4 Gy or remained untreated and cellular ceramide was determined by DAG-kinase assay. The assay is used to determine the cellular ceramide amount by the phosphorylation of ceramide to ceramide-1-phosphate in the presence of [^{32}P]γ-ATP. The TLC shows the C16 and C24 species of ceramide. The images are representative for 3 independent studies.

4.8 IDENTIFICATION OF VARIOUS INTERACTING PARTNERS OF ASM, CERAMIDE AND LIPID RAFT AFTER IR

Although a massive knowledge about ASM/ceramide-regulated pathways has increased in the past decade, molecular mechanisms of ASM/ceramide action remain poorly understood, primarily due to limited information about ASM/ceramide-binding proteins. In the present study, liquid chromatography–mass spectrometry/mass spectrometry (LC-MS/MS) was used to identify potential ASM/ceramide-interacting proteins in A172 human glioblastoma cells. In addition lipid raft-binding proteins were also identified. First, to identify ASM interacting proteins, human glioblastoma cells A172 and LN308 were irradiated with 4 Gy or remained untreated. After 10 and 15 min cells were lysed and ASM (65 kDa) was immunoprecipitated using protein A/G PLUS-Agarose beads. Immunoprecipitation results was confirmed by western blotting using ASM antibody (Figure 4.8 a and b). The samples from A172 cells were further subjected to LC-MS/MS. The purification resulted in identification of different proteins. One of the most important proteins found in 10 min irradiated samples was flotillin-1. Flotillin-1 is a subtype of flotillins which are categorized as plasma membrane proteins forming detergent-resistant domains known as lipid raft. No flotillin-1 protein was present in non-irradiated samples. Similarly various cytoskeleton proteins namely desmocollin-3, f-actin-capping protein subunit alpha-2, talin-1 was also identified in irradiated samples.
To identify proteins interacting with ceramide in A172 cells, cells were irradiated with 4 Gy or remained untreated. After 10 and 15 min, cells were lysed and ceramide was pulled down using ceramide beads. To prove non-specific binding of beads to lysates, samples with control beads were also included. Samples were further subjected to LC-MS/MS. As a result, different proteins were identified. The identified proteins are known to be involved in various

cellular processes including apoptosis, cellular stress, cell cycle, cell differentiation and signaling. One of the important proteins identified in 15 min irradiated samples was caveolin-1. Caveolin-1 is known to play an important role in cell growth by modulating the activity of various molecules involved in growth factor signaling (Shack et al 2003). Caveolin-1 is known to be a tumor suppressor protein that inactivates several signaling molecules involved in survival pathways by interacting with them. No caveolin-1 protein was present in non-irradiated samples.

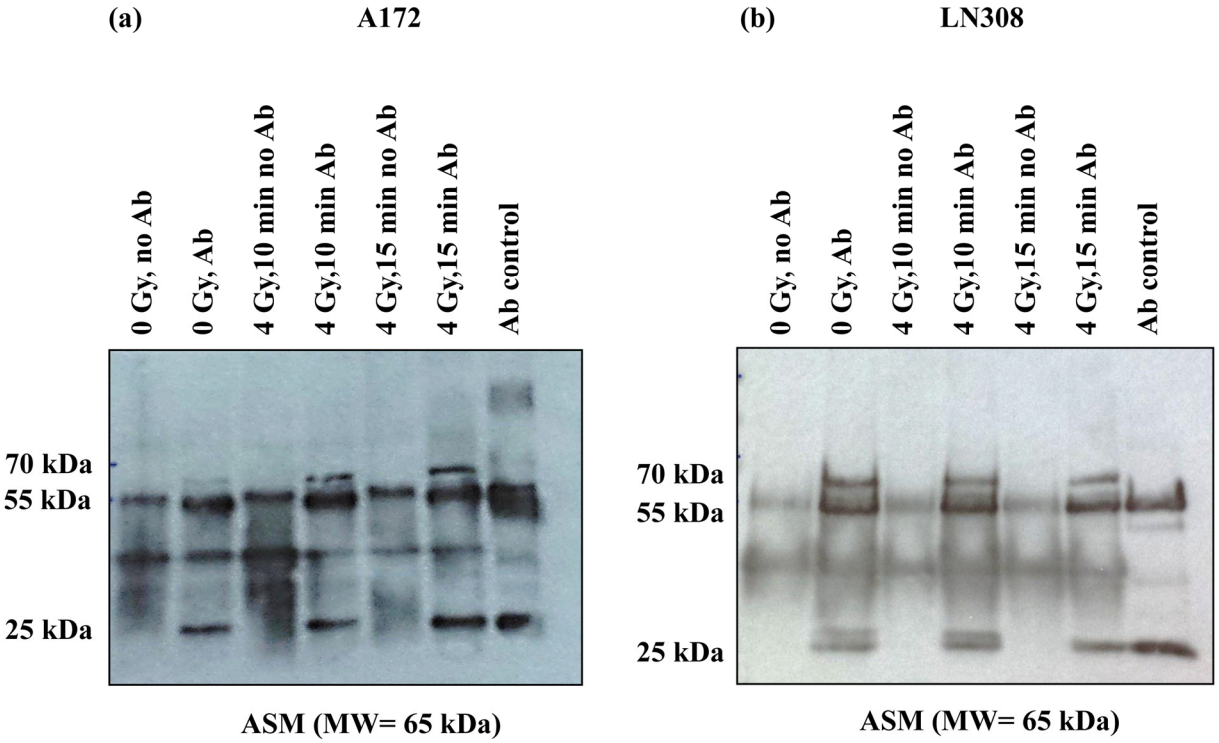

Ab= antibody

For determination of proteins interacting with lipid rafts, isolation of lipid rafts was performed with A172 and LN308 cells using sucrose density gradient technique. Cells were irradiated with 4 Gy or remained untreated. After 10 and 15 min cells were lysed and homogenized with 60 strokes in a dounce homogenizer. A layer of sucrose and samples was loaded in centrifuge tube. The sucrose gradient samples were spun for 24 h and lipid raft fractions were harvested by collecting 0.5 ml fractions, beginning at the top of the gradient. Isolated lipid raft was confirmed by western blotting using antibody against flotillin-1 (47 kDa), a marker for lipid raft. The results showed a clear band positive for flotillin-1 (Figure 4.8 c and d). To be sure that the isolated fractions were free of contamination, mitochondrial marker COXIV (17 kDa) was used and by western blotting it was revealed that the fraction was negative for COXIV (Figure 4.8 e and f). The samples from A172 cells were further subjected to LC-MS/MS and more than 500 different proteins were identified. Since caveolins and flotillins are known to

be lipid raft proteins, caveolin-1 and flotillin-1, 2 proteins were identified in both irradiated and non-irradiated samples. Various proteins involved in lysosomal trafficking of ASM namely dysferlin (Han et al 2012) and sortilin (Jin et al 2008b) were also identified in irradiated samples.

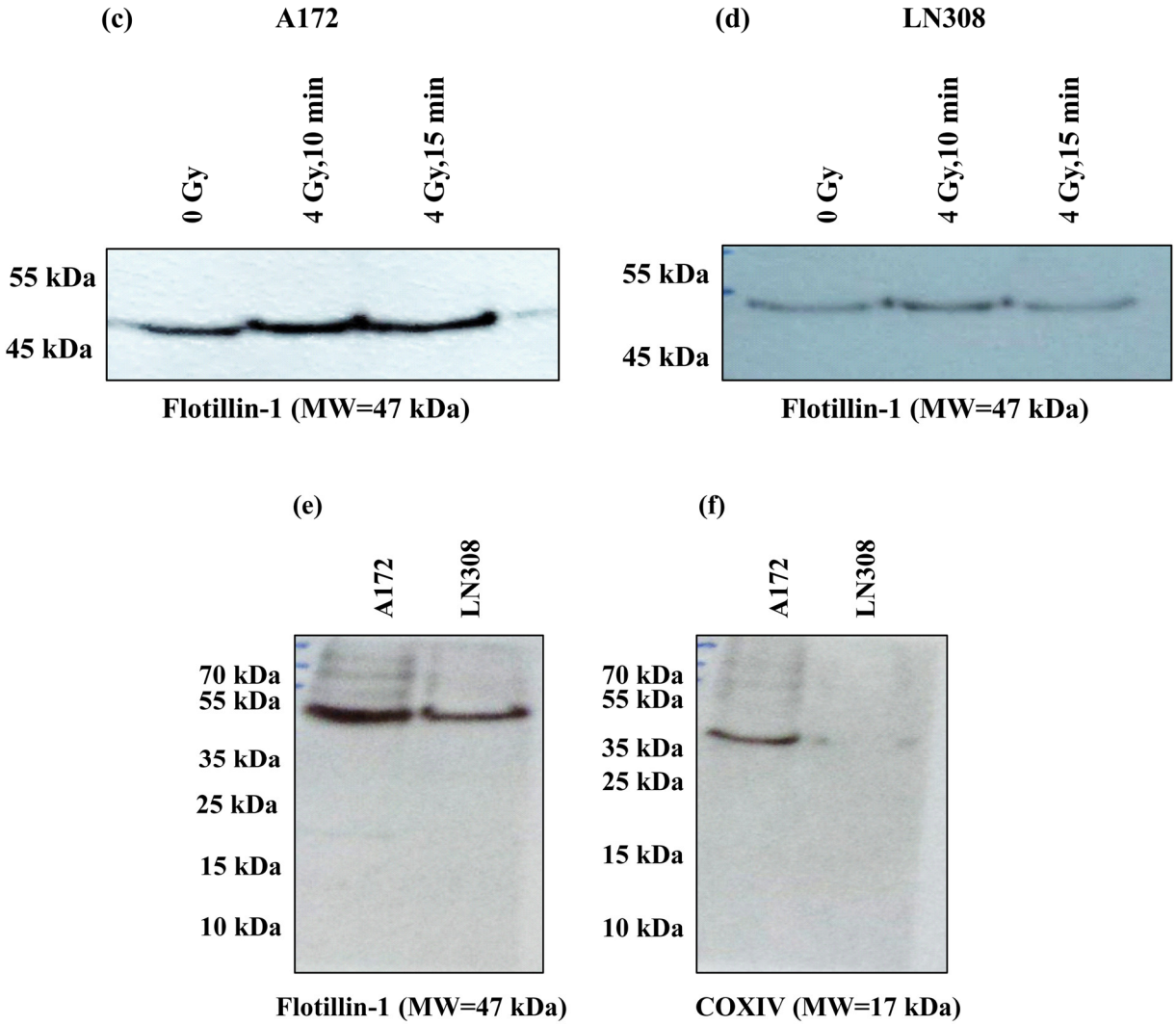

Figure 4.8: Confirmation of ASM immunoprecipitation and lipid raft isolation
Human glioblastoma cells A172 (a) and LN308 (b) were irradiated with 4 Gy or left non-irradiated for immunoprecipitation of ASM. Cells were incubated with protein A/G PLUS-Agarose beads and ASM antibody. The results were confirmed by western blotting.
The images are representative for 3 independent studies.
For isolation of lipid rafts, human glioblastoma cell lines A172 (c) and LN308 (d) cells were irradiated with 4 Gy or left untreated followed by sucrose density gradient technique. To confirm that the isolation of lipid rafts, western blotting was performed using lipid raft marker flotillin-1 (47 kDa) and the fraction was found to be positive for this marker (e). To check if the lipid raft fractions were free of contamination, the same blot already checked before for flotillin-1 was probed with antibody against mitochondrial marker COXIV (17 kDa) in A172 and LN308 (f) which was found to be negative. The images are representative for 3 independent studies.

5 DISCUSSION

5.1 ACTIVATION AND TRANSLOCATION OF ASM

ASM activity can be measured in cells lysates by radioactively or fluorescently sphingomyelin labeled. ASM activity assay using radioactive [^{14}C]sphingomyelin is measured as a rate of consumption of [^{14}C]sphingomyelin to ceramide and [^{14}C]phosphorylcholine. Ceramide being insoluble in water remains in lower organic phase whereas [^{14}C]phosphorylcholine being easily soluble in water is separated from the substrate [^{14}C]sphingomyelin and ceramide. For three forms i.e. acid, neutral and alkaline, sphingomyelin serves as a substrate (Hannun 1996). Another method for measuring ASM activity is fluorescence-based, high-performance liquid chromatographic assay (He et al 2002, He et al 2003) where sphingomyelin is hydrolyzed to phosphorylcholine and ceramide in presence of sphingomyelinase. Dephosphorylation of phosphorylcholine by alkaline phosphatase results in generation of choline which is used for production of hydrogen peroxide. The reaction is catalyzed by enzyme choline oxidase. Hydrogen peroxide then reacts with amplex red reagent after addition of peroxidase resulting in a fluorescent product (He et al 2002).

In the present study ASM enzymatic activity was measured as the consumption of radioactive [^{14}C]sphingomyelin to ceramide and phosphorylcholine. Two different human glioblastoma cell lines A172 and LN308 were remained untreated or treated with 4 Gy. Transient activation of ASM within 10 and 15 min after irradiation was observed. Our results relates to some of the earlier findings which showed irradiation induces activation of ASM in different cell types (Paris et al 2001, Santana et al 1996, Sathishkumar et al 2005). To check if ASM activation is accompanied by its translocation to the outer leaflet of the cell membrane as shown in different studies (Grassmé et al 2001a, Perrotta et al 2010), immunofluorescence staining was performed. Cells were remained unpermeabilized to view ASM in plasma membrane before and after 4 Gy. Result showed that ASM was translocated to the plasma membrane of irradiated cells whereas no such translocation was observed in non-irradiated cells. ASM is known to be activated upon various stress stimuli for example upon bacterial infection (Grassmé et al 2003b, Zhang et al 2008), death receptors (Cifone et al 1994, Cremesti et al 2001, Grassmé et al 2001a, Perrotta et al 2010) oxidative stress (Li et al 2012, Zhang et al 2007), UV-light (Charruyer et al 2005, Kashkar et al 2005, Rotolo et al 2005, Zhang et al 2001), irradiation (Paris et al 2001, Santana et al 1996, Sathishkumar et al 2005). Activation

of ASM has been correlated with its translocation from lysosome to plasma membrane (Grassmé et al 2001a, Perrotta et al 2010). Lymphocytes stimulated with CD95 resulted in translocation of ASM to the outer surface of plasma membrane. Further clustering of CD95 in sphingolipid-rich membrane rafts was also observed leading to apoptosis induction whilst ASM-deficient lymphocytes prevented CD95 clustering and apoptosis upon stimulation. Translocation of ASM onto the cell surface upon CD95 stimulation was detected using confocal as well as scanning electron microscopy and the activity of ASM was measured using radioactive method (Grassmé et al 2001a). In human glioma cells U373, ASM activated and translocated upon CD95-activating antibodies CH11 stimulation. Activation of ASM within 5 min of treatment was observed and around 30 min the condition returned to control level. Activity of ASM was measured by radioactive technique whereas for translocation of ASM, three different techniques were used: cell surface biotinylation assay, flow cytometry and immunofluorescence. ASM translocation upon CD95 treatment was found to be dependent on SNARE (soluble *N*-ethylmaleimide-sensitive-factor activating protein receptor) protein syntaxin 4 (Perrotta et al 2010).

5.2 MECHANISM OF THE ASM ACTIVATION

In this study it was shown that IR-induced a rapid activation of ASM in human glioblastoma cells A172 and LN308 which was found to be dependent on ROS production, since inhibition of ROS using two different ROS inhibitors apocynin and tiron prevented the activation of ASM. It should be mentioned that apocynin and tiron did not completely block ASM activation because of incomplete block of ROS. Our results relates to the finding from Dumitru and colleagues where using ROS inhibitors tiron and N-acetyl cysteine prevented activation of ASM upon TNF-related apoptosis-inducing ligand (TRAIL) stimulation (Dumitru and Gulbins 2006). Similarly upon *Pseudomonas aeruginosa* (*P. aeruginosa)* infection in macrophages, ROS scavengers were able to block activation and translocation of ASM further blocking formation of ceramide-enriched membrane platforms (Zhang et al 2008). In neutrophils ceramide derived from ASM was found to be mediated by ROS which further resulted in CD95 clustering finally leading to apoptosis (Scheel-Toellner et al 2004). Not only the role of ROS in ASM activation has been studied but some findings have shown that ROS mediates the translocation and activation of ASM at the plasma membrane. Studies with U937 cells showed ROS regulated activation and translocation of ASM to membrane rafts resulting in ceramide-enriched membrane platforms formation and this event was blocked using ROS scavengers pyrrolidinedithiocarbamate (PDTC) (Charruyer et al 2005).

Similarly, Jurkat cells when stimulated with hydrogen peroxide showed activation and translocation of ASM to membrane rafts (Li et al 2012). Some of the studies have demonstrated that ASM once activated can plays a crucial role in production of ROS showing the existence of a feed forward loop between ROS and ASM. Using ASM inhibitors on hepatocytes resulted in blockade of ROS production (Reinehr et al 2005). Studies on macrophages and endothelial cells revealed an involvement of ASM in generation of ROS (Hatanaka et al 1998, Zhang et al 2007).

Further studies showed that activation and translocation of ASM is dependent on ROS generating enzyme NADPH oxidase. NADPH oxidase is one of the primary sources for superoxide production (Karupiah et al 2000). A study from Zhang and colleagues clearly demonstrated that NADPH oxidase regulates the activity of Asm upon *P. aeruginosa* stimulation in macrophages. *P. aeruginosa* rapidly activates Asm and ceramide-enriched membrane platforms formation while inhibition of NADPH oxidase using diphenyleneiodonium chloride (DPI) resulted in blockade of this process (Zhang et al 2008). Similar to this finding, the present study showed that irradiation of human glioblastoma cells A172 and LN308 leads to rapid activation of ASM which was observed to be ROS dependent. However to check if the generated ROS is originated from NADPH oxidase complex further studies were carried. To elucidate the mechanism if NADPH oxidase has a role in ASM activation, total NADPH oxidase activity was measured upon irradiation in A172 cells which showed a 20 % increase in activity. Down regulating of gp91phox using siRNA, one of the important subunit of NADPH oxidase in generating superoxide, resulted in the inhibition of ASM activation in A172 cells compared with control siRNA transfected cells. However no complete block of ASM activation was observed which might be because the gp91phox protein was down regulated only around 50 %.

5.3 CLUSTERING OF SIGNALING MOLECULES IN CERAMIDE-ENRICHED MEMBRANE PLATFORMS

In this study clustering of gp91phox in ceramide-enriched membrane platforms/domains was demonstrated in human glioblastoma cells A172 and LN308 upon irradiation. The results were confirmed by immunofluorescence staining using confocal microscopy. Since surface molecules can be easily disrupted if detergents are used during staining process, therefore it is very important to avoid detergents during the fixing process. For detecting surface localization of gp91phox in ceramide-enriched membrane platforms, antibodies against ceramide and gp91phox were used in combination with secondary antibodies. When two

different molecules or antigens are needed to be imaged in confocal microscopy sequential scanning (from LeicaSP5 software) was performed because it helps to avoid the interference of artifacts and crosstalk between various fluorescent channels used. Sequential scanning allows detecting multiple fluorophores in one sample by intensifying the image quality and avoids crosstalk by recording in a sequential order rather than a synchronal acquisition.

The role of ceramide-enriched membrane platforms in signaling pathway was fully elucidated showing that these platforms trap and cluster death receptors like CD95 and CD40 (Cremesti et al 2001, Grassmé et al 2001a, Grassmé et al 2002b). An apoptotic "signalosome" is formed as a result of this trapping and clustering of receptors resulting in transmitting and amplifying cell death signal inside the cells. Later other signaling molecules like subunits of NADPH oxidase particularly gp91phox and p47phox were shown to be clustered in ceramide-enriched membrane platforms resulting in activation of ASM in endothelial cells (Bao et al 2010, Zhang et al 2007). NADPH oxidase known to be one of the important superoxide radical generators was found to be concentrated and activated in lipid raft platforms in endothelial cells forming redox lipid rafts (Zhang et al 2006). It was recognized that for formation of these redox lipid rafts ASM/ceramide play a crucial role and there exists a feed forward loop where ROS produced by NADPH oxidase complex activates ASM in endothelial cells (Zhang et al 2007). In endothelial cells, activation of NADPH oxidase within ceramide-enriched membrane platforms was shown upon various stress stimuli like Fas-L (Zhang et al 2007), endostatin (Jin et al 2008c), TRAIL (Li et al 2013b). Upon irradiation, rat brain microvascular endothelial cells showed activation of NADPH oxidase which resulted in production of intracellular ROS and increased expression of subunits like Nox4, p22phox, and p47phox. Pharmacologic and genetic inhibition of NADPH oxidase was able to block total intracellular ROS induced by radiation (Collins-Underwood et al 2008). However it has to be noted that the mechanism underlying radiation mediated activation of NADPH oxidase complex has still to be elucidated.

At present the role of ceramide-enriched membrane platforms in activation of NADPH oxidase activation remains unanswered. It can be hypothesized that there might be strong interactions among the subunits of NADPH oxidase once they are aggregated in ceramide-enriched membrane platforms thereby enhancing the provocation of ROS.

5.4 CERAMIDE PRODUCTION

Several quantitative methods have been developed for measuring total cellular ceramide like high-performance liquid chromatography (HPLC) analysis (Couch et al 1997, Iwamori et al 1979, Previati et al 1996, Yano et al 1998), high performance thin layer chromatography (HPTLC) analysis (Motta et al 1994), evaporative light-scattering detection (McNabb et al 1999) or using radioactive precursors for labeling of cells (Allan 2000, Tepper and Van Blitterswijk 2000). Another widely used technique to measure ceramide is mass spectrometry (MS) (Allan 2000, Couch et al 1997, Gu et al 1997, Kalhorn and Zager 1999, Karlsson et al 1998, Liebisch et al 1999, Mano et al 1997, Watts et al 1999). One of the best used method for ceramide quantification is the diacylglycerol (DAG) kinase assay. The advantage of the DAG kinase assay over other technique involves the measurement of total mass levels of ceramide and the use of crude lipid extracts in the assay. Processing a large number of samples in a rapid manner also provides a great advantage of this assay over other standard techniques.

The highly hydrophobic ceramide is extracted in organic solvent from the cells. Cells are lysed in a solution containing equal amount of methanol and chloroform. Hydrochloric acid is added to the cell lysates for acidification and to extract the shorter acyl chain ceramide-1-phosphates or hydroxylated ceramides. DAG kinase is one of the fastest ways to measure total cellular ceramide, remains to have an advantage over other techniques.

Ceramide level is known to be increased in various cell lines upon different stress stimuli for example with several chemotherapeutic drugs (Grammatikos et al 2007, Lacour et al 2004), irradiation (Santana et al 1996), different pathogens (Esen et al 2001, Grassmé et al 1997, Grassmé et al 2003b, Jan et al 2000), TNF family of ligands and receptors (Cremesti et al 2001, Dumitru and Gulbins 2006, Grassmé et al 2001a, Grassmé et al 2001b). However in glioma cells ceramide is known to be rapidly consumed by ceramide degrading enzyme ceramide glycosyltransferase/glucosylceramide synthase (GCS). It was reported that in glioma cells upon gemcitabine treatment failure of ceramide accumulation was observed which was found to be the result of ceramide consumption by glycosyltransferase enzyme. Pharmacologic or genetic inhibition of this enzyme reversed the event resulting in accumulation of ceramide in those cells (Dumitru et al 2009).

For measuring local ceramide in compartment of human glioblastoma cells, mitochondria were isolated before and after irradiation using mitochondrial isolation kit following detergent/reagent based method. Various kits are available for isolating mitochondria which include reagent based and dounce homogenizer method. Even though the traditional dounce homogenization method might help to retain more mitochondrial fraction than compared to

reagent based method, the latter method provides an advantage to process several samples together. As mentioned in the kit instruction, using reagent based isolation method around six samples can be processed at a time in comparison to dounce homogenization method where only one samples at a time can be prepared. Once mitochondria were isolated TIMM23 (mitochondrial marker) was used to confirmed the isolation of mitochondria using western blotting. Similarly to check if the isolated fractions are free of contamination different organelle markers were used like alpha tubulin for cytoplasm, calnexin for endoplasmic reticulum (ER) and Lamp-1 for lysosomes. The fractions isolated were found to be negative for markers of cytoplasm and lysosomes but positive for ER marker. This might be because various tethering proteins exists that connect ER and mitochondria compartments by localizing both sides. One of such proteins is mitofusin 2 which was found to interconnect ER and mitochondria during Ca^{2+} signaling (de Brito and Scorrano 2008). Another protein reported for connecting ER and mitochondria is chaperone glucose-regulated protein 75 (grp75). It was demonstrated that the voltage-dependent anion channel (VDAC) of the outer mitochondrial membrane is associated with ER and mitochondrial Ca^{2+} channels through grp75 (Szabadkai et al 2006).

After isolation of mitochondria from the cells, ceramide DAG kinase assay was performed. C16 and C24 ceramide species were separated from other lipids with the use of thin-layer chromatography (TLC). Results from scanned TLC plate showed a small increase in ceramide in both cell lines. Quantification of TLC was performed using phosphorimager which showed a slight increase in ceramide but without statistical significance. As, mentioned earlier isolated mitochondrial fractions were found to be contaminated with ER, ceramide is known to be synthesized in ER (Stiban et al 2008) and it can be assume that the result from DAG kinase assay might show the ceramide synthesized in ER too. As ER synthesized ceramide might be equally produced in both irradiated as well as non-irradiated cells. So it could be that even if there is a small amount of increase in mitochondrial ceramide in irradiated cells it could hardly be seen or no difference in ceramide level could be seen. Another method used to measured cellular ceramide was immunofluorescence staining using antibodies against ceramide and mitochondria (TIMM23). The result showed an increase in mitochondrial ceramide in irradiated cells with no or very less amount of ceramide in non-irradiated cells. The settings for laser intensity in confocal microscopy were kept to minimal so that if there is a difference in irradiated and non-irradiated cells it could be visualized easily however same settings were applied for both irradiated as well as non-irradiated cells.

Increase in mitochondrial ceramide was reported before in HeLa cells upon UV irradiation (Dai et al 2004) and IR (Lee et al 2011). For identifying the amount of ceramide increased in mitochondria Lee and coworkers irradiated cells with 10 Gy and isolated mitochondrial ceramide-rich macrodomains (MCRM) using differential centrifugation via a discontinuous sucrose gradient. Ceramide was measured using DAG kinase assay 33 h after treated with radiation. To confirm the results confocal microscopy was performed to measure cellular ceramide using mitotracker red and ceramide antibody (Lee et al 2011).

5.5 INTERACTING PARTNERS OF ASM, CERAMIDE AND LIPID RAFTS

Previous studies have shown that lysosomal ASM trafficking to plasma membrane is an important event resulting in clustering of membrane raft particularly shown by stimulation of coronary arterial endothelial cells (CAECs) with Fas ligand (FasL) (Bao et al 2010, Jin et al 2008b, Shao et al 2003). FasL induced activation of ASM and generation of ceramide further leading to lipid raft platforms formation (Zhang et al 2007). These studies showed a direct link of ASM with production of ceramide and generation of lipid raft platforms. So our study aimed to identify some interacting partners of ASM, ceramide and lipid raft. For this, three different experiments were performed namely ASM immunoprecipitation (IP) assay, ceramide pull-down assay and lipid raft isolation. For all the three methods the same initial step was performed i.e. irradiating cells with 4 Gy or remained untreated followed by lysing the cells at 10 and 15 min. IP is one of the best known techniques to precipitate protein of interest using specific antibody. Monoclonal or polyclonal antibodies used against the particular protein require a solid support like protein A/G PLUS-Agarose beads. Incubating with gentle agitation allows the protein of interest to bind with the antibody immobilized on the beads. To prove nonspecific binding of proteins, one sample was kept without adding antibodies from each particular treatment. Cells were lysed using RIPA buffer. RIPA buffer is the most efficient lysis buffer that solubilizes proteins eluding protein degradation and resulting in minimal low background effect. Once ASM was precipitated, western blotting was used to confirm the IP. It should be noted that IP technique can be troubleshooting various times for example non-specific binding of proteins to the beads is one of them. In this condition pre-clearing step should be used, this step starts with addition of beads to the cell lysates followed by incubation for 30-60 min. This will allow the end result to have lower background level and better signal in comparison to noise signal. Another important point that needs to be considered during IP is antigen degrading during the process. To avoid this, fresh protease inhibitors should be added to buffer for lysing the cells. Beyond these two hindrances

many more like incomplete washing, too much antibodies used, too many cells or too much protein in lysates can also be problematic.

Similarly for ceramide pull-down assay, ceramide beads were used and to prove for nonspecific binding samples, control beads were included. For lipid raft isolation a method was adapted from (Ostrom and Insel 2006) with slight modification. Several ways to prepare lipid rafts using detergent or detergent-free methods has been described till date (Schnitzer et al 1995, Smart et al 1995, Song et al 1996). To isolate lipid rafts membranes from a variety of cells, detergent-free method have been frequently used as the method being more reproducible and provides higher inner leaflet-membrane lipids fractions when compared to detergent based method (Pike 2004). In this study lipid rafts was isolated using detergent-free method using sucrose gradient of 45 %, 35 % and 5 %. On the basis of their density lipid rafts are distributed at the interface between the 35 % and 5 % sucrose layer after ultracentrifugation for 24 h.

Three different conditions for the samples were prepared 0 Gy, 4 Gy 10 min and 4 Gy 15 min. After samples were prepared from all the three different methods i.e. ASM IP, ceramide pull-down assay and lipid raft isolation, mass spectrometry (MS) analysis was performed to identify the interacting partners of ASM, ceramide and lipid raft. MS remains to be one of the best used techniques in the biological research. It can be used for both qualitative and quantitative studies. It possesses various advantages like providing information by measuring molecular weight accurately, analyzing amino acid, oligonucleotide sequencing and also identifies protein structures. However one of the major disadvantages of this technique arises when a compound with multiple functional groups has to be analyzed (Ashcroft 2013).

Various proteins were identified from ASM IP samples; flotillin-1 is one of the proteins identified in the samples of 4 Gy 10 min but was not present in non-irradiated samples. Flotillin-1 is a subtype of flotillins which are categorized as plasma membrane proteins forming detergent-resistant domains known as lipid raft. Besides localizing at plasma membrane these proteins are trafficking between different compartments by a so far unknown mechanism (Langhorst et al 2008). The role of flotillin-1 has been reported in signaling event (Fork et al 2014) and flotillins are also known to interact with various cytoskeletal proteins (Affentranger et al 2011, Ludwig et al 2010). Recently it was demonstrated that translocation of ASM further leads to its co-localization within flotillin-1 enriched lipid raft (Wei et al 2013). The findings in this study support our hypothesis that upon IR, ASM is translocated to plasma membrane where it gets concentrated in flotillin-1 enriched lipid raft since the protein was identified only in the irradiated samples. Similarly various cytoskeletal proteins were

identified in the samples after 4 Gy 10 and 15 min including desmocollin-3, f-actin-capping protein subunit alpha-2, talin-1. It has been reported that plasma membrane is linked with actin cytoskeleton with the involvement of various lipid and proteins (Saarikangas et al 2010, Sechi and Wehland 2000).

From ceramide pull-down assay, at 4 Gy after 10 min samples, only three proteins different than 0 Gy were identified namely proliferating cell nuclear antigen (PCNA)-interacting partner, elongation factor Tu mitochondrial, low-density lipoprotein receptor-related protein 5. Ceramide is known to initiate apoptotic signaling process by inhibiting activation of Akt with dephosphorylation at Ser473 (Schubert et al 2000). Additionally ceramide is also known to lower the expression of PCNA and hindering nuclear import of some important proteins like cyclin A resulting in inhibition of cell proliferation (Faustino et al 2008). Similarly it was shown that this whole process was regulated by syntaxin 4 (Perrotta et al 2010). Syntaxin 4 silencing resulted in inhibition of ASM, preventing Akt dephosphorylation finally resulting in decrease PCNA thus cells became more proliferative and survived (Perrotta et al 2010). In 4 Gy, 15 min samples various interesting proteins were identified including caveolin-1. Caveolin-1 proteins are one of the forms of caveolae. Caveolae are the vesicles that get incorporated in plasma membrane (Severs 1988) and exist in two forms caveolin-1 and 2. Caveolin-1 is known to be regulated by lipid raft (Kagawa et al 2015) and is mostly expressed on all cells types except most of the tumor cells where it is reported to be absent or down regulated (Koleske et al 1995, Lee et al 1998, Racine et al 1999). It is very intriguing that caveolin-1 is known to be absent in tumor cells but in our study caveolin-1 was identified in malignant tumor cells. Caveolin-1 is known to play an important role in cell growth by modulating the activity of various molecules involved in growth factor signaling (Shack et al 2003). It is correlated to be a tumor suppressor that inactivates several signaling molecules involved in survival pathways by interacting with them for example: epidermal growth factor receptor (Engelman et al 1998), ERK (Engelman et al 1998, Galbiati et al 1998), mitogen/extracellular signal-regulated kinase 1 (Engelman et al 1998, Galbiati et al 1998), platelet-derived growth factor receptor (Yamamoto et al 1998), Raf (Engelman et al 1998), Src (Li et al 1996). All these finding suggests that caveolin-1 plays important role in mediating cell death however this fact remain controversial. In Rat-1 fibroblasts caveolin-1 resulted in ceramide-induced cell death (Zundel et al 2000) and in LNCaP cells caveolin-1 was able to suppress c-myc-induced apoptosis (Timme et al 2000). Various Ras related Rab and Rap proteins were also identified in 4 Gy, 15 min samples namely Ras-related protein, Rab-1A, Rab-1B, Rab-2A, Rab-5C, Rab-6A, Rab-10, Rab 11B, Rab-14, Rab-18, Rab-32 and

Rap-1b-like protein. Various Ras proteins are known to be involved in cytoskeletal rearrangement (D'Souza-Schorey et al 1997), vesicular trafficking (Conklin et al 2010) and signaling pathways (Van Aelst et al 1996). Similarly many cytoskeletal membrane proteins like vesicle-associated membrane protein-associated protein B/C, transmembrane protein 109, Thy-1 membrane glycoprotein, CD59 glycoprotein were also detected in irradiated samples.

From the isolated lipid raft caveolin-1 and flotillin 1, 2 were present in both irradiated as well as non-irradiated samples. Some reports have suggested that for expression of caveolae, flotillin is an important factor. When flotillin-1 was down regulated a decrease of the expression of caveolin-1 was observed. This study was performed on endothelial cells where association of flotillin-1 and caveolin-1 remained essential for signaling process (Vassilieva et al 2009). Apart from membrane proteins various other membrane-associated proteins like Ras-related protein Rab-11A, Rab-31, Rab11 family-interacting protein 5, Ras GTPase-activating protein-binding protein 1, Ras GTPase-activating-like protein IQGAP3, Rho GTPase-activating protein 1 was also identified in irradiated samples. Actin cytoskeleton plays an important role in maintaining the organization of lipid raft (Simpson-Holley et al 2002), similarly in this study various cytoskeletal proteins were identified including filamin-C, F-actin-capping protein subunit alpha-1, F-actin-capping protein subunit alpha-2, twinfilin-1, dynactin subunit 2, plakophilin-2, profilin-2 in irradiated samples. Apart from flotillin and caveolin another protein identified in lipid raft samples before and after irradiation was raftlin (raft-linking protein). Raftlin is known to be an essential protein for organizing and maintaining the structure of lipid raft and regulates the signal transduction process (Saeki et al 2003). Two important proteins that were identified in irradiated samples of lipid rafts were dysferlin and sortilin which are known to be involved in lysosomal trafficking of ASM to plasma membrane. Dysferlin is involved in fusion of lysosomes to plasma membrane through its C2A domain (Han et al 2012). Lysosome fusion is one of the most important mechanisms resulting in membrane raft clustering. Upon FasL ligand in bovine coronary arterial endothelial cells (CAECs) dysferlin was found to be clustered in membrane raft when visualized by confocal microscopy however knockdown of this particular protein using siRNA prevented the clustering of membrane raft which demonstrated the importance of dysferlin in regulating membrane rafts (Han et al 2012). Similarly another important protein sortilin was reported to be involved in lysosomal targeting of ASM in the formation of lipid raft redox signaling (Jin et al 2008b). Upon FasL stimulation in CAECs, ASM was found to be targeted on lysosomal membrane via sortilin which was detected by confocal microscopy and fluorescence resonance energy transfer (FRET). FasL stimulated targeting of ASM was

abrogated when CAECs were transfected with siRNA of sortilin resulting in deterioration of LRs clustering and formation of LR-redox signaling platforms (Jin et al 2008b).

6 SUMMARY

Treating malignant glioblastoma with radiation therapy in combination with chemotherapy is one of the most promising outcomes. The present study aimed to elucidate the underlying mechanism of IR induced activation of ASM and production of ceramide in glioblastoma. We focused on the initial event that involves the activation of ASM and production of ceramide upon irradiation in human glioblastoma cells. Irradiation of human glioblastoma cells resulted in rapid activation and translocation of ASM to plasma membrane which resulted in clustering of ceramide and formation of ceramide-enriched membrane platforms. We addressed the mechanism of ASM activation which was found to be dependent on reactive oxygen species (ROS) production.

Ceramide enriched-membrane platforms are known to actively cluster signaling molecule including death receptors CD95 and CD40 (Cremesti et al 2001, Grassmé et al 2001a, Grassmé et al 2001b, Grassmé et al 2002a) or subunits of NADPH oxidase like gp91phox and p47phox (Bao et al 2010, Zhang et al 2007). Similar to these observations we found that upon irradiation gp91phox clustered in ceramide enriched-membrane platforms and further using gp91phox siRNA, inhibition in IR-induced activation of ASM was seen. This result relates to the finding from Zhang and colleagues showing NADPH oxidase-derived ROS regulate Asm-initiated redox signaling in a positive feedback manner (Zhang et al 2008).

Lastly we identified various interacting partners of ASM, ceramide and lipid rafts using LC-MS/MS technique. Flotillin-1 and caveolin-1 proteins were identified in irradiated samples which suggest that upon irradiation, ASM translocated to plasma membrane leads to generation of ceramide and further co-localization of ASM and ceramide in lipid raft platforms takes place. Various other proteins were identified in irradiated samples of lipid rafts including dysferlin and sortilin whose role in ASM trafficking from lysosome to plasma membrane has already been described earlier upon different stimuli other than radiation (Han et al 2012, Jin et al 2008b).

7 REFERENCES

1 Abdel Shakor AB, Kwiatkowska K, Sobota A (2004). Cell surface ceramide generation precedes and controls FcgammaRII clustering and phosphorylation in rafts. *The Journal of biological chemistry* **279:** 36778-36787.

2 Affentranger S, Martinelli S, Hahn J, Rossy J, Niggli V (2011). Dynamic reorganization of flotillins in chemokine-stimulated human T-lymphocytes. *BMC cell biology* **12:** 28.

3 Alfadda AA, Sallam RM (2012). Reactive oxygen species in health and disease. *Journal of biomedicine & biotechnology* **2012:** 936486.

4 Allan D (2000). Lipid metabolic changes caused by short-chain ceramides and the connection with apoptosis. *The Biochemical journal* **345 Pt 3:** 603-610.

5 Alonso MA, Millan J (2001). The role of lipid rafts in signalling and membrane trafficking in T lymphocytes. *Journal of cell science* **114:** 3957-3965.

6 Amberger-Murphy V (2009). Hypoxia helps glioma to fight therapy. *Current cancer drug targets* **9:** 381-390.

7 Ames BN, Shigenaga MK, Hagen TM (1995). Mitochondrial decay in aging. *Biochimica et biophysica acta* **1271:** 165-170.

8 Amir M, Liu K, Zhao E, Czaja MJ (2012). Distinct functions of JNK and c-Jun in oxidant-induced hepatocyte death. *Journal of cellular biochemistry* **113:** 3254-3265.

9 Anderson RA, Marchesi VT (1985). Regulation of the association of membrane skeletal protein 4.1 with glycophorin by a polyphosphoinositide. *Nature* **318:** 295-298.

10 Ardestani S, Deskins DL, Young PP (2013). Membrane TNF-alpha-activated programmed necrosis is mediated by Ceramide-induced reactive oxygen species. *Journal of molecular signaling* **8:** 12.

11 Ashcroft AE (2013). An Introduction to Mass Spectrometry.

12 Assari T (2006). Chronic Granulomatous Disease; fundamental stages in our understanding of CGD. *Medical immunology* **5:** 4.

13 Avota E, Gulbins E, Schneider-Schaulies S (2011). DC-SIGN mediated sphingomyelinase-activation and ceramide generation is essential for enhancement of viral uptake in dendritic cells. *PLoS pathogens* **7:** e1001290.

14 Babior BM (1999). NADPH oxidase: an update. *Blood* **93:** 1464-1476.

15 Babizhayev MA, Strokov IA, Nosikov VV, Savel'yeva EL, Sitnikov VF, Yegor EY *et al* (2014). The Role of Oxidative Stress in Diabetic Neuropathy: Generation of Free Radical Species in the Glycation Reaction and Gene Polymorphisms Encoding Antioxidant Enzymes to Genetic Susceptibility to Diabetic Neuropathy in Population of Type I Diabetic Patients. *Cell biochemistry and biophysics*.

16 Bao JX, Jin S, Zhang F, Wang ZC, Li N, Li PL (2010). Activation of membrane NADPH oxidase associated with lysosome-targeted acid sphingomyelinase in coronary endothelial cells. *Antioxidants & redox signaling* **12:** 703-712.

17 Bao S, Wu Q, McLendon RE, Hao Y, Shi Q, Hjelmeland AB *et al* (2006). Glioma stem cells promote radioresistance by preferential activation of the DNA damage response. *Nature* **444:** 756-760.

18 Bartke N, Hannun YA (2009). *Journal of lipid research* **50 Suppl:** S91-96.

19 Baskar R, Lee KA, Yeo R, Yeoh KW (2012). Cancer and radiation therapy: current advances and future directions. *International journal of medical sciences* **9:** 193-199.

20 Basu S, Bayoumy S, Zhang Y, Lozano J, Kolesnick R (1998). BAD enables ceramide to signal apoptosis via Ras and Raf-1. *The Journal of biological chemistry* **273:** 30419-30426.

21 Beak SM, Lee YS, Kim JA (2004). NADPH oxidase and cyclooxygenase mediate the ultraviolet B-induced generation of reactive oxygen species and activation of nuclear factor-kappaB in HaCaT human keratinocytes. *Biochimie* **86:** 425-429.
22 Belyakov OV, Folkard M, Mothersill C, Prise KM, Michael BD (2002). Bystander-induced apoptosis and premature differentiation in primary urothelial explants after charged particle microbeam irradiation. *Radiation protection dosimetry* **99:** 249-251.
23 Bezombes C, Grazide S, Garret C, Fabre C, Quillet-Mary A, Muller S *et al* (2004). Rituximab antiproliferative effect in B-lymphoma cells is associated with acid-sphingomyelinase activation in raft microdomains. *Blood* **104:** 1166-1173.
24 Bishop AL, Hall A (2000). Rho GTPases and their effector proteins. *The Biochemical journal* **348 Pt 2:** 241-255.
25 Boini KM, Zhang C, Xia M, Han WQ, Brimson C, Poklis JL *et al* (2010). Visfatin-induced lipid raft redox signaling platforms and dysfunction in glomerular endothelial cells. *Biochimica et biophysica acta* **1801:** 1294-1304.
26 Bollinger CR, Teichgraber V, Gulbins E (2005). Ceramide-enriched membrane domains. *Biochimica et biophysica acta* **1746:** 284-294.
27 Boucher LM, Wiegmann K, Futterer A, Pfeffer K, Machleidt T, Schutze S *et al* (1995). CD28 signals through acidic sphingomyelinase. *The Journal of experimental medicine* **181:** 2059-2068.
28 Brady RO, Kanfer JN, Mock MB, Fredrickson DS (1966). The metabolism of sphingomyelin. II. Evidence of an enzymatic deficiency in Niemann-Pick diseae. *Proceedings of the National Academy of Sciences of the United States of America* **55:** 366-369.
29 Brenner B, Koppenhoefer U, Weinstock C, Linderkamp O, Lang F, Gulbins E (1997). Fas- or ceramide-induced apoptosis is mediated by a Rac1-regulated activation of Jun N-terminal kinase/p38 kinases and GADD153. *The Journal of biological chemistry* **272:** 22173-22181.
30 Brown DA, London E (1998). Functions of lipid rafts in biological membranes. *Annual review of cell and developmental biology* **14:** 111-136.
31 Brown DA, London E (2000). Structure and function of sphingolipid- and cholesterol-rich membrane rafts. *The Journal of biological chemistry* **275:** 17221-17224.
32 Brown DA (2006). Lipid rafts, detergent-resistant membranes, and raft targeting signals. *Physiology* **21:** 430-439.
33 Cai W, Andres DA (2014). mTORC2 is required for rit-mediated oxidative stress resistance. *PloS one* **9:** e115602.
34 Calzadilla P, Sapochnik D, Cosentino S, Diz V, Dicelio L, Calvo JC *et al* (2011). N-acetylcysteine reduces markers of differentiation in 3T3-L1 adipocytes. *International journal of molecular sciences* **12:** 6936-6951.
35 Cao J, Xu D, Wang D, Wu R, Zhang L, Zhu H *et al* (2009). ROS-driven Akt dephosphorylation at Ser-473 is involved in 4-HPR-mediated apoptosis in NB4 cells. *Free radical biology & medicine* **47:** 536-547.
36 Castillo SS, Levy M, Thaikoottathil JV, Goldkorn T (2007). Reactive nitrogen and oxygen species activate different sphingomyelinases to induce apoptosis in airway epithelial cells. *Experimental cell research* **313:** 2680-2686.
37 Chalfant CE, Kishikawa K, Mumby MC, Kamibayashi C, Bielawska A, Hannun YA (1999). Long chain ceramides activate protein phosphatase-1 and protein phosphatase-2A. Activation is stereospecific and regulated by phosphatidic acid. *The Journal of biological chemistry* **274:** 20313-20317.
38 Chalfant CE, Rathman K, Pinkerman RL, Wood RE, Obeid LM, Ogretmen B *et al* (2002). De novo ceramide regulates the alternative splicing of caspase 9 and Bcl-x in

A549 lung adenocarcinoma cells. Dependence on protein phosphatase-1. *The Journal of biological chemistry* **277:** 12587-12595.

39 Chang D, Chen F, Zhang F, McKay BC, Ljungman M (1999). Dose-dependent effects of DNA-damaging agents on p53-mediated cell cycle arrest. *Cell growth & differentiation : the molecular biology journal of the American Association for Cancer Research* **10:** 155-162.

40 Charruyer A, Grazide S, Bezombes C, Muller S, Laurent G, Jaffrezou JP (2005). *The Journal of biological chemistry* **280:** 19196-19204.

41 Chen Q, Chai YC, Mazumder S, Jiang C, Macklis RM, Chisolm GM *et al* (2003). The late increase in intracellular free radical oxygen species during apoptosis is associated with cytochrome c release, caspase activation, and mitochondrial dysfunction. *Cell death and differentiation* **10:** 323-334.

42 Cheng JC, Bai A, Beckham TH, Marrison ST, Yount CL, Young K *et al* (2013). Radiation-induced acid ceramidase confers prostate cancer resistance and tumor relapse. *The Journal of clinical investigation* **123:** 4344-4358.

43 Cheng Y, Nilsson A, Tomquist E, Duan RD (2002). Purification, characterization, and expression of rat intestinal alkaline sphingomyelinase. *Journal of lipid research* **43:** 316-324.

44 Chung HS, Park SR, Choi EK, Park HJ, Griffin RJ, Song CW *et al* (2003). Role of sphingomyelin-MAPKs pathway in heat-induced apoptosis. *Experimental & molecular medicine* **35:** 181-188.

45 Cifone MG, De Maria R, Roncaioli P, Rippo MR, Azuma M, Lanier LL *et al* (1994). Apoptotic signaling through CD95 (Fas/Apo-1) activates an acidic sphingomyelinase. *The Journal of experimental medicine* **180:** 1547-1552.

46 Claus RA, Bunck AC, Bockmeyer CL, Brunkhorst FM, Losche W, Kinscherf R *et al* (2005). Role of increased sphingomyelinase activity in apoptosis and organ failure of patients with severe sepsis. *FASEB journal : official publication of the Federation of American Societies for Experimental Biology* **19:** 1719-1721.

47 Cohen AW, Hnasko R, Schubert W, Lisanti MP (2004). Role of caveolae and caveolins in health and disease. *Physiological reviews* **84:** 1341-1379.

48 Collins-Underwood JR, Zhao W, Sharpe JG, Robbins ME (2008). NADPH oxidase mediates radiation-induced oxidative stress in rat brain microvascular endothelial cells. *Free radical biology & medicine* **45:** 929-938.

49 Conklin MW, Ada-Nguema A, Parsons M, Riching KM, Keely PJ (2010). R-Ras regulates beta1-integrin trafficking via effects on membrane ruffling and endocytosis. *BMC cell biology* **11:** 14.

50 Couch LH, Churchwell MI, Doerge DR, Tolleson WH, Howard PC (1997). Identification of ceramides in human cells using liquid chromatography with detection by atmospheric pressure chemical ionization-mass spectrometry. *Rapid communications in mass spectrometry : RCM* **11:** 504-512.

51 Cremesti A, Paris F, Grassmé H, Holler N, Tschopp J, Fuks Z *et al* (2001). Ceramide enables fas to cap and kill. *The Journal of biological chemistry* **276:** 23954-23961.

52 Cremesti AE, Goni FM, Kolesnick R (2002). Role of sphingomyelinase and ceramide in modulating rafts: do biophysical properties determine biologic outcome? *FEBS letters* **531:** 47-53.

53 Crompton NE (1998). Programmed cellular response to ionizing radiation damage. *Acta oncologica* **37:** 129-142.

54 Czaja MJ, Liu H, Wang Y (2003). Oxidant-induced hepatocyte injury from menadione is regulated by ERK and AP-1 signaling. *Hepatology* **37:** 1405-1413.

55 D'Angelo G, Polishchuk E, Di Tullio G, Santoro M, Di Campli A, Godi A *et al* (2007). Glycosphingolipid synthesis requires FAPP2 transfer of glucosylceramide. *Nature* **449:** 62-67.

56 D'Souza-Schorey C, Boshans RL, McDonough M, Stahl PD, Van Aelst L (1997). A role for POR1, a Rac1-interacting protein, in ARF6-mediated cytoskeletal rearrangements. *The EMBO journal* **16:** 5445-5454.

57 Dai Q, Liu J, Chen J, Durrant D, McIntyre TM, Lee RM (2004). Mitochondrial ceramide increases in UV-irradiated HeLa cells and is mainly derived from hydrolysis of sphingomyelin. *Oncogene* **23:** 3650-3658.

58 Dang PM, Babior BM, Smith RM (1999). NADPH dehydrogenase activity of p67PHOX, a cytosolic subunit of the leukocyte NADPH oxidase. *Biochemistry* **38:** 5746-5753.

59 de Brito OM, Scorrano L (2008). Mitofusin 2 tethers endoplasmic reticulum to mitochondria. *Nature* **456:** 605-610.

60 del Pozo MA, Alderson NB, Kiosses WB, Chiang HH, Anderson RG, Schwartz MA (2004). Integrins regulate Rac targeting by internalization of membrane domains. *Science* **303:** 839-842.

61 Deng X, Yin X, Allan R, Lu DD, Maurer CW, Haimovitz-Friedman A *et al* (2008). Ceramide biogenesis is required for radiation-induced apoptosis in the germ line of C. elegans. *Science* **322:** 110-115.

62 Devasagayam TP, Tilak JC, Boloor KK, Sane KS, Ghaskadbi SS, Lele RD (2004). Free radicals and antioxidants in human health: current status and future prospects. *The Journal of the Association of Physicians of India* **52:** 794-804.

63 Ding Z, Liu S, Wang X, Khaidakov M, Dai Y, Mehta JL (2013). Oxidant stress in mitochondrial DNA damage, autophagy and inflammation in atherosclerosis. *Scientific reports* **3:** 1077.

64 Dobrowsky RT, Kamibayashi C, Mumby MC, Hannun YA (1993). Ceramide activates heterotrimeric protein phosphatase 2A. *The Journal of biological chemistry* **268:** 15523-15530.

65 Doehner W, Bunck AC, Rauchhaus M, von Haehling S, Brunkhorst FM, Cicoira M *et al* (2007). Secretory sphingomyelinase is upregulated in chronic heart failure: a second messenger system of immune activation relates to body composition, muscular functional capacity, and peripheral blood flow. *European heart journal* **28:** 821-828.

66 Dreschers S, Franz P, Dumitru C, Wilker B, Jahnke K, Gulbins E (2007). Infections with human rhinovirus induce the formation of distinct functional membrane domains. *Cellular physiology and biochemistry : international journal of experimental cellular physiology, biochemistry, and pharmacology* **20:** 241-254.

67 Duan RD, Cheng Y, Hansen G, Hertervig E, Liu JJ, Syk I *et al* (2003). Purification, localization, and expression of human intestinal alkaline sphingomyelinase. *Journal of lipid research* **44:** 1241-1250.

68 Dumitru CA, Gulbins E (2006). TRAIL activates acid sphingomyelinase via a redox mechanism and releases ceramide to trigger apoptosis. *Oncogene* **25:** 5612-5625.

69 Dumitru CA, Carpinteiro A, Trarbach T, Hengge UR, Gulbins E (2007). Doxorubicin enhances TRAIL-induced cell death via ceramide-enriched membrane platforms. *Apoptosis : an international journal on programmed cell death* **12:** 1533-1541.

70 Dumitru CA, Weller M, Gulbins E (2009). Ceramide metabolism determines glioma cell resistance to chemotherapy. *Journal of cellular physiology* **221:** 688-695.

71 Edelmann B, Bertsch U, Tchikov V, Winoto-Morbach S, Perrotta C, Jakob M *et al* (2011). Caspase-8 and caspase-7 sequentially mediate proteolytic activation of acid sphingomyelinase in TNF-R1 receptosomes. *The EMBO journal* **30:** 379-394.

72 El-Aal HAHMA (2012). Lipid Peroxidation End-Products as a Key of Oxidative Stress: Effect of Antioxidant on Their Production and Transfer of Free Radicals: http://www.intechopen.com/books/lipid-peroxidation/lipid-peroxidation-end-products-as-a-key-of-oxidative-stress-effect-of-antioxidant-on-their-producti.

73 Engelman JA, Chu C, Lin A, Jo H, Ikezu T, Okamoto T *et al* (1998). Caveolin-mediated regulation of signaling along the p42/44 MAP kinase cascade in vivo. A role for the caveolin-scaffolding domain. *FEBS letters* **428:** 205-211.

74 Esen M, Schreiner B, Jendrossek V, Lang F, Fassbender K, Grassmé H *et al* (2001). Mechanisms of Staphylococcus aureus induced apoptosis of human endothelial cells. *Apoptosis : an international journal on programmed cell death* **6:** 431-439.

75 Facchino S, Abdouh M, Bernier G (2011). Brain cancer stem cells: current status on glioblastoma multiforme. *Cancers* **3:** 1777-1797.

76 Fang F, Gong PS, Zhao HG, Bi YJ, Zhao G, Gong SL *et al* (2013). Mitochondrial modulation of apoptosis induced by low-dose radiation in mouse testicular cells. *Biomedical and environmental sciences : BES* **26:** 820-830.

77 Faustino RS, Cheung P, Richard MN, Dibrov E, Kneesch AL, Deniset JF *et al* (2008). Ceramide regulation of nuclear protein import. *Journal of lipid research* **49:** 654-662.

78 Fensome AC, Rodrigues-Lima F, Josephs M, Paterson HF, Katan M (2000). A neutral magnesium-dependent sphingomyelinase isoform associated with intracellular membranes and reversibly inhibited by reactive oxygen species. *The Journal of biological chemistry* **275:** 1128-1136.

79 Ferlinz K, Hurwitz R, Vielhaber G, Suzuki K, Sandhoff K (1994). Occurrence of two molecular forms of human acid sphingomyelinase. *The Biochemical journal* **301 (Pt 3):** 855-862.

80 Ferlinz K, Hurwitz R, Moczall H, Lansmann S, Schuchman EH, Sandhoff K (1997). Functional characterization of the N-glycosylation sites of human acid sphingomyelinase by site-directed mutagenesis. *European journal of biochemistry / FEBS* **243:** 511-517.

81 Ferlinz K, Kopal G, Bernardo K, Linke T, Bar J, Breiden B *et al* (2001). Human acid ceramidase: processing, glycosylation, and lysosomal targeting. *The Journal of biological chemistry* **276:** 35352-35360.

82 Finkel T, Holbrook NJ (2000). Oxidants, oxidative stress and the biology of ageing. *Nature* **408:** 239-247.

83 Fiorini C, Cordani M, Gotte G, Picone D, Donadelli M (2015). Onconase induces autophagy sensitizing pancreatic cancer cells to gemcitabine and activates Akt/mTOR pathway in a ROS-dependent manner. *Biochimica et biophysica acta* **1854:** 549-560.

84 Fork C, Hitzel J, Nichols BJ, Tikkanen R, Brandes RP (2014). Flotillin-1 facilitates toll-like receptor 3 signaling in human endothelial cells. *Basic research in cardiology* **109:** 439.

85 Forrester HB, Vidair CA, Albright N, Ling CC, Dewey WC (1999). Using computerized video time lapse for quantifying cell death of X-irradiated rat embryo cells transfected with c-myc or c-Ha-ras. *Cancer research* **59:** 931-939.

86 Fowler S (1969). Lysosomal localization of sphingomyelinase in rat liver. *Biochimica et biophysica acta* **191:** 481-484.

87 Friedman M, Ryan US, Davenport WC, Chaney EL, Strickland DL, Kwock L (1986). Reversible alterations in cultured pulmonary artery endothelial cell monolayer morphology and albumin permeability induced by ionizing radiation. *Journal of cellular physiology* **129:** 237-249.

88 Fuks Z, Persaud RS, Alfieri A, McLoughlin M, Ehleiter D, Schwartz JL *et al* (1994). Basic fibroblast growth factor protects endothelial cells against radiation-induced programmed cell death in vitro and in vivo. *Cancer research* **54:** 2582-2590.

89 Fuks Z, Alfieri A, Haimovitz-Friedman A, Seddon A, Cordon-Cardo C (1995). Intravenous basic fibroblast growth factor protects the lung but not mediastinal organs against radiation-induced apoptosis in vivo. *The cancer journal from Scientific American* **1:** 62-72.

90 Funato K, Riezman H (2001). Vesicular and nonvesicular transport of ceramide from ER to the Golgi apparatus in yeast. *The Journal of cell biology* **155:** 949-959.

91 Furukawa S, Fujita T, Shimabukuro M, Iwaki M, Yamada Y, Nakajima Y *et al* (2004). Increased oxidative stress in obesity and its impact on metabolic syndrome. *The Journal of clinical investigation* **114:** 1752-1761.

92 Gabrys D, Greco O, Patel G, Prise KM, Tozer GM, Kanthou C (2007). Radiation effects on the cytoskeleton of endothelial cells and endothelial monolayer permeability. *International journal of radiation oncology, biology, physics* **69:** 1553-1562.

93 Galbiati F, Volonte D, Engelman JA, Watanabe G, Burk R, Pestell RG *et al* (1998). Targeted downregulation of caveolin-1 is sufficient to drive cell transformation and hyperactivate the p42/44 MAP kinase cascade. *The EMBO journal* **17:** 6633-6648.

94 Garcia-Barros M, Paris F, Cordon-Cardo C, Lyden D, Rafii S, Haimovitz-Friedman A *et al* (2003). Tumor response to radiotherapy regulated by endothelial cell apoptosis. *Science* **300:** 1155-1159.

95 Garcia-Ruiz C, Colell A, Mari M, Morales A, Calvo M, Enrich C *et al* (2003). Defective TNF-alpha-mediated hepatocellular apoptosis and liver damage in acidic sphingomyelinase knockout mice. *The Journal of clinical investigation* **111:** 197-208.

96 Garcia-Saez AJ, Schwille P (2010). Stability of lipid domains. *FEBS letters* **584:** 1653-1658.

97 Gassert E, Avota E, Harms H, Krohne G, Gulbins E, Schneider-Schaulies S (2009). Induction of membrane ceramides: a novel strategy to interfere with T lymphocyte cytoskeletal reorganisation in viral immunosuppression. *PLoS pathogens* **5:** e1000623.

98 Ghoti H, Amer J, Winder A, Rachmilewitz E, Fibach E (2007). Oxidative stress in red blood cells, platelets and polymorphonuclear leukocytes from patients with myelodysplastic syndrome. *European journal of haematology* **79:** 463-467.

99 Giussani P, Bassi R, Anelli V, Brioschi L, De Zen F, Riccitelli E *et al* (2012). Glucosylceramide synthase protects glioblastoma cells against autophagic and apoptotic death induced by temozolomide and Paclitaxel. *Cancer investigation* **30:** 27-37.

100 Górska M, Baranczuk E, Dobrzyn A (2003). Secretory Zn2+-dependent sphingomyelinase activity in the serum of patients with type 2 diabetes is elevated. *Hormone and metabolic research = Hormon- und Stoffwechselforschung = Hormones et metabolisme* **35:** 506-507.

101 Graber D, Salvayre R, Levade T (1994). Accurate differentiation of neuronopathic and nonneuronopathic forms of Niemann-Pick disease by evaluation of the effective residual lysosomal sphingomyelinase activity in intact cells. *Journal of neurochemistry* **63:** 1060-1068.

102 Gramatzki D, Herrmann C, Happold C, Becker KA, Gulbins E, Weller M *et al* (2013). Glioma cell death induced by irradiation or alkylating agent chemotherapy is independent of the intrinsic ceramide pathway. *PloS one* **8:** e63527.

103 Grammatikos G, Teichgraber V, Carpinteiro A, Trarbach T, Weller M, Hengge UR *et al* (2007). Overexpression of acid sphingomyelinase sensitizes glioma cells to chemotherapy. *Antioxidants & redox signaling* **9:** 1449-1456.

104 Grassmé H, Gulbins E, Brenner B, Ferlinz K, Sandhoff K, Harzer K *et al* (1997). Acidic sphingomyelinase mediates entry of N. gonorrhoeae into nonphagocytic cells. *Cell* **91:** 605-615.

105 Grassmé H, Kirschnek S, Riethmueller J, Riehle A, von Kurthy G, Lang F *et al* (2000). CD95/CD95 ligand interactions on epithelial cells in host defense to Pseudomonas aeruginosa. *Science* **290:** 527-530.
106 Grassmé H, Jekle A, Riehle A, Schwarz H, Berger J, Sandhoff K *et al* (2001a). CD95 signaling via ceramide-rich membrane rafts. *The Journal of biological chemistry* **276:** 20589-20596.
107 Grassmé H, Schwarz H, Gulbins E (2001b). Molecular mechanisms of ceramide-mediated CD95 clustering. *Biochemical and biophysical research communications* **284:** 1016-1030.
108 Grassmé H, Bock J, Kun J, Gulbins E (2002a). Clustering of CD40 ligand is required to form a functional contact with CD40. *The Journal of biological chemistry* **277:** 30289-30299.
109 Grassmé H, Jendrossek V, Bock J, Riehle A, Gulbins E (2002b). Ceramide-rich membrane rafts mediate CD40 clustering. *Journal of immunology* **168:** 298-307.
110 Grassmé H, Cremesti A, Kolesnick R, Gulbins E (2003a). Ceramide-mediated clustering is required for CD95-DISC formation. *Oncogene* **22:** 5457-5470.
111 Grassmé H, Jendrossek V, Riehle A, von Kurthy G, Berger J, Schwarz H *et al* (2003b). Host defense against Pseudomonas aeruginosa requires ceramide-rich membrane rafts. *Nature medicine* **9:** 322-330.
112 Grassmé H, Riehle A, Wilker B, Gulbins E (2005). Rhinoviruses infect human epithelial cells via ceramide-enriched membrane platforms. *The Journal of biological chemistry* **280:** 26256-26262.
113 Grills IS, Yan D, Martinez AA, Vicini FA, Wong JW, Kestin LL (2003). Potential for reduced toxicity and dose escalation in the treatment of inoperable non-small-cell lung cancer: a comparison of intensity-modulated radiation therapy (IMRT), 3D conformal radiation, and elective nodal irradiation. *International journal of radiation oncology, biology, physics* **57:** 875-890.
114 Gu M, Kerwin JL, Watts JD, Aebersold R (1997). Ceramide profiling of complex lipid mixtures by electrospray ionization mass spectrometry. *Analytical biochemistry* **244:** 347-356.
115 Gulbins E, Bissonnette R, Mahboubi A, Martin S, Nishioka W, Brunner T *et al* (1995). FAS-induced apoptosis is mediated via a ceramide-initiated RAS signaling pathway. *Immunity* **2:** 341-351.
116 Gulbins E, Szabo I, Baltzer K, Lang F (1997). Ceramide-induced inhibition of T lymphocyte voltage-gated potassium channel is mediated by tyrosine kinases. *Proceedings of the National Academy of Sciences of the United States of America* **94:** 7661-7666.
117 Gupta N, Nodzenski E, Khodarev NN, Yu J, Khorasani L, Beckett MA *et al* (2001). Angiostatin effects on endothelial cells mediated by ceramide and RhoA. *EMBO reports* **2:** 536-540.
118 Gusman J, Malonne H, Atassi G (2001). A reappraisal of the potential chemopreventive and chemotherapeutic properties of resveratrol. *Carcinogenesis* **22:** 1111-1117.
119 Ha H, Kwak HB, Lee SW, Jin HM, Kim HM, Kim HH *et al* (2004). Reactive oxygen species mediate RANK signaling in osteoclasts. *Experimental cell research* **301:** 119-127.
120 Haimovitz-Friedman A, Kan CC, Ehleiter D, Persaud RS, McLoughlin M, Fuks Z *et al* (1994). Ionizing radiation acts on cellular membranes to generate ceramide and initiate apoptosis. *The Journal of experimental medicine* **180:** 525-535.
121 Haines GA, Hendry JH, Daniel CP, Morris ID (2002). Germ cell and dose-dependent DNA damage measured by the comet assay in murine spermatozoaa after testicular X-irradiation. *Biology of reproduction* **67:** 854-861.

122 Hall A (1998). Rho GTPases and the actin cytoskeleton. *Science* **279:** 509-514.
123 Han WQ, Xia M, Xu M, Boini KM, Ritter JK, Li NJ *et al* (2012). Lysosome fusion to the cell membrane is mediated by the dysferlin C2A domain in coronary arterial endothelial cells. *Journal of cell science* **125:** 1225-1234.
124 Hanada K, Palacpac NM, Magistrado PA, Kurokawa K, Rai G, Sakata D *et al* (2002). Plasmodium falciparum phospholipase C hydrolyzing sphingomyelin and lysocholinephospholipids is a possible target for malaria chemotherapy. *The Journal of experimental medicine* **195:** 23-34.
125 Hannun YA (1996). Functions of ceramide in coordinating cellular responses to stress. *Science* **274:** 1855-1859.
126 Harder T, Simons K (1997). Caveolae, DIGs, and the dynamics of sphingolipid-cholesterol microdomains. *Current opinion in cell biology* **9:** 534-542.
127 Hatanaka Y, Fujii J, Fukutomi T, Watanabe T, Che W, Sanada Y *et al* (1998). Reactive oxygen species enhances the induction of inducible nitric oxide synthase by sphingomyelinase in RAW264.7 cells. *Biochimica et biophysica acta* **1393:** 203-210.
128 Hauck CR, Grassmé H, Bock J, Jendrossek V, Ferlinz K, Meyer TF *et al* (2000). Acid sphingomyelinase is involved in CEACAM receptor-mediated phagocytosis of Neisseria gonorrhoeae. *FEBS letters* **478:** 260-266.
129 He X, Chen F, McGovern MM, Schuchman EH (2002). A fluorescence-based, high-throughput sphingomyelin assay for the analysis of Niemann-Pick disease and other disorders of sphingomyelin metabolism. *Analytical biochemistry* **306:** 115-123.
130 He X, Chen F, Dagan A, Gatt S, Schuchman EH (2003). A fluorescence-based, high-performance liquid chromatographic assay to determine acid sphingomyelinase activity and diagnose types A and B Niemann-Pick disease. *Analytical biochemistry* **314:** 116-120.
131 Hein PA, Gladstone DJ, Bellerive MR, Hug EB (2005). Importance of protocol target definition on the ability to spare normal tissue: an IMRT and 3D-CRT planning comparison for intraorbital tumors. *International journal of radiation oncology, biology, physics* **62:** 1540-1548.
132 Heinrich M, Wickel M, Schneider-Brachert W, Sandberg C, Gahr J, Schwandner R *et al* (1999). Cathepsin D targeted by acid sphingomyelinase-derived ceramide. *The EMBO journal* **18:** 5252-5263.
133 Heinrich M, Neumeyer J, Jakob M, Hallas C, Tchikov V, Winoto-Morbach S *et al* (2004). Cathepsin D links TNF-induced acid sphingomyelinase to Bid-mediated caspase-9 and -3 activation. *Cell death and differentiation* **11:** 550-563.
134 Helliwell SB, Schmidt A, Ohya Y, Hall MN (1998). The Rho1 effector Pkc1, but not Bni1, mediates signalling from Tor2 to the actin cytoskeleton. *Current biology : CB* **8:** 1211-1214.
135 Hertervig E, Nilsson A, Cheng Y, Duan RD (2003). Purified intestinal alkaline sphingomyelinase inhibits proliferation without inducing apoptosis in HT-29 colon carcinoma cells. *Journal of cancer research and clinical oncology* **129:** 577-582.
136 Ho CC, Huang PH, Huang HY, Chen YH, Yang PC, Hsu SM (2002). Up-regulated caveolin-1 accentuates the metastasis capability of lung adenocarcinoma by inducing filopodia formation. *The American journal of pathology* **161:** 1647-1656.
137 Hofmann K, Tomiuk S, Wolff G, Stoffel W (2000). Cloning and characterization of the mammalian brain-specific, Mg2+-dependent neutral sphingomyelinase. *Proceedings of the National Academy of Sciences of the United States of America* **97:** 5895-5900.
138 Holmstrom KM, Finkel T (2014). Cellular mechanisms and physiological consequences of redox-dependent signalling. *Nature reviews Molecular cell biology* **15:** 411-421.

139 Horinouchi K, Erlich S, Perl DP, Ferlinz K, Bisgaier CL, Sandhoff K *et al* (1995). Acid sphingomyelinase deficient mice: a model of types A and B Niemann-Pick disease. *Nature genetics* **10:** 288-293.
140 Hsieh CT, Chuang JH, Yang WC, Yin Y, Lin Y (2014). Ceramide inhibits insulin-stimulated Akt phosphorylation through activation of Rheb/mTORC1/S6K signaling in skeletal muscle. *Cellular signalling* **26:** 1400-1408.
141 Hunt MA, Zelefsky MJ, Wolden S, Chui CS, LoSasso T, Rosenzweig K *et al* (2001). Treatment planning and delivery of intensity-modulated radiation therapy for primary nasopharynx cancer. *International journal of radiation oncology, biology, physics* **49:** 623-632.
142 Hurwitz R, Ferlinz K, Vielhaber G, Moczall H, Sandhoff K (1994). Processing of human acid sphingomyelinase in normal and I-cell fibroblasts. *The Journal of biological chemistry* **269:** 5440-5445.
143 Huwiler A, Brunner J, Hummel R, Vervoordeldonk M, Stabel S, van den Bosch H *et al* (1996). Ceramide-binding and activation defines protein kinase c-Raf as a ceramide-activated protein kinase. *Proceedings of the National Academy of Sciences of the United States of America* **93:** 6959-6963.
144 Huwiler A, Fabbro D, Pfeilschifter J (1998). Selective ceramide binding to protein kinase C-alpha and -delta isoenzymes in renal mesangial cells. *Biochemistry* **37:** 14556-14562.
145 Huwiler A, Johansen B, Skarstad A, Pfeilschifter J (2001). Ceramide binds to the CaLB domain of cytosolic phospholipase A2 and facilitates its membrane docking and arachidonic acid release. *FASEB journal : official publication of the Federation of American Societies for Experimental Biology* **15:** 7-9.
146 Ito Y, Yoshida H, Nakano K, Kobayashi K, Yokozawa T, Hirai K *et al* (2002). Caveolin-1 overexpression is an early event in the progression of papillary carcinoma of the thyroid. *British journal of cancer* **86:** 912-916.
147 Iwamori M, Costello C, Moser HW (1979). Analysis and quantitation of free ceramide containing nonhydroxy and 2-hydroxy fatty acids, and phytosphingosine by high-performance liquid chromatography. *Journal of lipid research* **20:** 86-96.
148 Jan JT, Chatterjee S, Griffin DE (2000). Sindbis virus entry into cells triggers apoptosis by activating sphingomyelinase, leading to the release of ceramide. *Journal of virology* **74:** 6425-6432.
149 Jang M, Cai L, Udeani GO, Slowing KV, Thomas CF, Beecher CW *et al* (1997). Cancer chemopreventive activity of resveratrol, a natural product derived from grapes. *Science* **275:** 218-220.
150 Jenkins RW, Idkowiak-Baldys J, Simbari F, Canals D, Roddy P, Riner CD *et al* (2011). A novel mechanism of lysosomal acid sphingomyelinase maturation: requirement for carboxyl-terminal proteolytic processing. *The Journal of biological chemistry* **286:** 3777-3788.
151 Jia SJ, Jin S, Zhang F, Yi F, Dewey WL, Li PL (2008). Formation and function of ceramide-enriched membrane platforms with CD38 during M1-receptor stimulation in bovine coronary arterial myocytes. *American journal of physiology Heart and circulatory physiology* **295:** H1743-1752.
152 Jin J, Hou Q, Mullen TD, Zeidan YH, Bielawski J, Kraveka JM *et al* (2008a). Ceramide generated by sphingomyelin hydrolysis and the salvage pathway is involved in hypoxia/reoxygenation-induced Bax redistribution to mitochondria in NT-2 cells. *The Journal of biological chemistry* **283:** 26509-26517.
153 Jin S, Yi F, Zhang F, Poklis JL, Li PL (2008b). Lysosomal targeting and trafficking of acid sphingomyelinase to lipid raft platforms in coronary endothelial cells. *Arteriosclerosis, thrombosis, and vascular biology* **28:** 2056-2062.

154 Jin S, Zhang Y, Yi F, Li PL (2008c). Critical role of lipid raft redox signaling platforms in endostatin-induced coronary endothelial dysfunction. *Arteriosclerosis, thrombosis, and vascular biology* **28:** 485-490.
155 Joiner MC, van der Kogel A (2009). Basic Clinical Radiobiology Fourth Edition. CRC Press.
156 Kagawa Y, Yasumoto Y, Sharifi K, Ebrahimi M, Islam A, Miyazaki H *et al* (2015). Fatty acid-binding protein 7 regulates function of caveolae in astrocytes through expression of caveolin-1. *Glia* **63:** 780-794.
157 Kalhorn T, Zager RA (1999). Renal cortical ceramide patterns during ischemic and toxic injury: assessments by HPLC-mass spectrometry. *The American journal of physiology* **277:** F723-733.
158 Kaliberov SA, Buchsbaum DJ (2012). Chapter seven--Cancer treatment with gene therapy and radiation therapy. *Advances in cancer research* **115:** 221-263.
159 Kanzaki H, Shinohara F, Kajiya M, Kodama T (2013). The Keap1/Nrf2 protein axis plays a role in osteoclast differentiation by regulating intracellular reactive oxygen species signaling. *The Journal of biological chemistry* **288:** 23009-23020.
160 Karahatay S, Thomas K, Koybasi S, Senkal CE, Elojeimy S, Liu X *et al* (2007). Clinical relevance of ceramide metabolism in the pathogenesis of human head and neck squamous cell carcinoma (HNSCC): attenuation of C(18)-ceramide in HNSCC tumors correlates with lymphovascular invasion and nodal metastasis. *Cancer letters* **256:** 101-111.
161 Karlsson AA, Michelsen P, Odham G (1998). Molecular species of sphingomyelin: determination by high-performance liquid chromatography/mass spectrometry with electrospray and high-performance liquid chromatography/tandem mass spectrometry with atmospheric pressure chemical ionization. *Journal of mass spectrometry : JMS* **33:** 1192-1198.
162 Karupiah G, Hunt NH, King NJ, Chaudhri G (2000). NADPH oxidase, Nramp1 and nitric oxide synthase 2 in the host antimicrobial response. *Reviews in immunogenetics* **2:** 387-415.
163 Kashiwagi K, Shirai Y, Kuriyama M, Sakai N, Saito N (2002a). Importance of C1B domain for lipid messenger-induced targeting of protein kinase C. *The Journal of biological chemistry* **277:** 18037-18045.
164 Kashiwagi M, Ohba M, Chida K, Kuroki T (2002b). Protein kinase C eta (PKC eta): its involvement in keratinocyte differentiation. *Journal of biochemistry* **132:** 853-857.
165 Kashkar H, Wiegmann K, Yazdanpanah B, Haubert D, Kronke M (2005). Acid sphingomyelinase is indispensable for UV light-induced Bax conformational change at the mitochondrial membrane. *The Journal of biological chemistry* **280:** 20804-20813.
166 Kato K, Hida Y, Miyamoto M, Hashida H, Shinohara T, Itoh T *et al* (2002). Overexpression of caveolin-1 in esophageal squamous cell carcinoma correlates with lymph node metastasis and pathologic stage. *Cancer* **94:** 929-933.
167 Kawano M, Kumagai K, Nishijima M, Hanada K (2006). Efficient trafficking of ceramide from the endoplasmic reticulum to the Golgi apparatus requires a VAMP-associated protein-interacting FFAT motif of CERT. *The Journal of biological chemistry* **281:** 30279-30288.
168 Kim SK, Ahn KH, Jeon HJ, Lee DH, Jung SY, Jung KM *et al* (2010). Purification of neutral sphingomyelinase 2 from bovine brain and its calcium-dependent activation. *Journal of neurochemistry* **112:** 1088-1097.
169 Kohama T, Olivera A, Edsall L, Nagiec MM, Dickson R, Spiegel S (1998). Molecular cloning and functional characterization of murine sphingosine kinase. *The Journal of biological chemistry* **273:** 23722-23728.

170 Koleske AJ, Baltimore D, Lisanti MP (1995). Reduction of caveolin and caveolae in oncogenically transformed cells. *Proceedings of the National Academy of Sciences of the United States of America* **92:** 1381-1385.
171 Kolesnick RN, Kronke M (1998). Regulation of ceramide production and apoptosis. *Annual review of physiology* **60:** 643-665.
172 Kondo T (2013). Radiation-induced cell death and its mechanisms.
173 Korzeniowski M, Shakor AB, Makowska A, Drzewiecka A, Bielawska A, Kwiatkowska K *et al* (2007). Fc gamma RII activation induces cell surface ceramide production which participates in the assembly of the receptor signaling complex. *Cellular physiology and biochemistry : international journal of experimental cellular physiology, biochemistry, and pharmacology* **20:** 347-356.
174 Kowluru A, Kowluru RA (2014). Phagocyte-like NADPH oxidase [Nox2] in cellular dysfunction in models of glucolipotoxicity and diabetes. *Biochemical pharmacology* **88:** 275-283.
175 Koybasi S, Senkal CE, Sundararaj K, Spassieva S, Bielawski J, Osta W *et al* (2004). Defects in cell growth regulation by C18:0-ceramide and longevity assurance gene 1 in human head and neck squamous cell carcinomas. *The Journal of biological chemistry* **279:** 44311-44319.
176 Krut O, Wiegmann K, Kashkar H, Yazdanpanah B, Kronke M (2006). Novel tumor necrosis factor-responsive mammalian neutral sphingomyelinase-3 is a C-tail-anchored protein. *The Journal of biological chemistry* **281:** 13784-13793.
177 Lacour S, Hammann A, Grazide S, Lagadic-Gossmann D, Athias A, Sergent O *et al* (2004). Cisplatin-induced CD95 redistribution into membrane lipid rafts of HT29 human colon cancer cells. *Cancer research* **64:** 3593-3598.
178 Lambert AJ, Brand MD (2009). Reactive oxygen species production by mitochondria. *Methods in molecular biology* **554:** 165-181.
179 Lang PA, Schenck M, Nicolay JP, Becker JU, Kempe DS, Lupescu A *et al* (2007). Liver cell death and anemia in Wilson disease involve acid sphingomyelinase and ceramide. *Nature medicine* **13:** 164-170.
180 Langhorst MF, Reuter A, Jaeger FA, Wippich FM, Luxenhofer G, Plattner H *et al* (2008). Trafficking of the microdomain scaffolding protein reggie-1/flotillin-2. *European journal of cell biology* **87:** 211-226.
181 Lansmann S, Ferlinz K, Hurwitz R, Bartelsen O, Glombitza G, Sandhoff K (1996). Purification of acid sphingomyelinase from human placenta: characterization and N-terminal sequence. *FEBS letters* **399:** 227-231.
182 Lansmann S, Schuette CG, Bartelsen O, Hoernschemeyer J, Linke T, Weisgerber J *et al* (2003). Human acid sphingomyelinase. *European journal of biochemistry / FEBS* **270:** 1076-1088.
183 Lassing I, Lindberg U (1985). Specific interaction between phosphatidylinositol 4,5-bisphosphate and profilactin. *Nature* **314:** 472-474.
184 Law B, Rossie S (1995). The dimeric and catalytic subunit forms of protein phosphatase 2A from rat brain are stimulated by C2-ceramide. *The Journal of biological chemistry* **270:** 12808-12813.
185 Leach JK, Van Tuyle G, Lin PS, Schmidt-Ullrich R, Mikkelsen RB (2001). Ionizing radiation-induced, mitochondria-dependent generation of reactive oxygen/nitrogen. *Cancer research* **61:** 3894-3901.
186 Lean JM, Jagger CJ, Kirstein B, Fuller K, Chambers TJ (2005). Hydrogen peroxide is essential for estrogen-deficiency bone loss and osteoclast formation. *Endocrinology* **146:** 728-735.
187 Lee CT, Bilton SD, Famiglietti RM, Riley BA, Mahajan A, Chang EL *et al* (2005a). Treatment planning with protons for pediatric retinoblastoma, medulloblastoma, and

pelvic sarcoma: how do protons compare with other conformal techniques? *International journal of radiation oncology, biology, physics* **63:** 362-372.

188 Lee H, Rotolo JA, Mesicek J, Penate-Medina T, Rimner A, Liao WC *et al* (2011). Mitochondrial ceramide-rich macrodomains functionalize Bax upon irradiation. *PloS one* **6:** e19783.

189 Lee NK, Choi YG, Baik JY, Han SY, Jeong DW, Bae YS *et al* (2005b). A crucial role for reactive oxygen species in RANKL-induced osteoclast differentiation. *Blood* **106:** 852-859.

190 Lee SW, Reimer CL, Oh P, Campbell DB, Schnitzer JE (1998). Tumor cell growth inhibition by caveolin re-expression in human breast cancer cells. *Oncogene* **16:** 1391-1397.

191 Lepple-Wienhues A, Belka C, Laun T, Jekle A, Walter B, Wieland U *et al* (1999). Stimulation of CD95 (Fas) blocks T lymphocyte calcium channels through sphingomyelinase and sphingolipids. *Proceedings of the National Academy of Sciences of the United States of America* **96:** 13795-13800.

192 Lewanski CR, Gullick WJ (2001). Radiotherapy and cellular signalling. *The Lancet Oncology* **2:** 366-370.

193 Li CM, Hong SB, Kopal G, He X, Linke T, Hou WS *et al* (1998). Cloning and characterization of the full-length cDNA and genomic sequences encoding murine acid ceramidase. *Genomics* **50:** 267-274.

194 Li HF, Kim JS, Waldman T (2009). Radiation-induced Akt activation modulates radioresistance in human glioblastoma cells. *Radiation oncology* **4:** 43.

195 Li S, Couet J, Lisanti MP (1996). Src tyrosine kinases, Galpha subunits, and H-Ras share a common membrane-anchored scaffolding protein, caveolin. Caveolin binding negatively regulates the auto-activation of Src tyrosine kinases. *The Journal of biological chemistry* **271:** 29182-29190.

196 Li WF, Zhang L, Li HY, Zheng SS, Zhao L (2014). WISP-1 contributes to fractionated irradiation-induced radioresistance in esophageal carcinoma cell lines and mice. *PloS one* **9:** e94751.

197 Li X, Gulbins E, Zhang Y (2012). Oxidative stress triggers Ca-dependent lysosome trafficking and activation of acid sphingomyelinase. *Cellular physiology and biochemistry : international journal of experimental cellular physiology, biochemistry, and pharmacology* **30:** 815-826.

198 Li X, Fang P, Mai J, Choi ET, Wang H, Yang XF (2013a). Targeting mitochondrial reactive oxygen species as novel therapy for inflammatory diseases and cancers. *Journal of hematology & oncology* **6:** 19.

199 Li X, Han WQ, Boini KM, Xia M, Zhang Y, Li PL (2013b). TRAIL death receptor 4 signaling via lysosome fusion and membrane raft clustering in coronary arterial endothelial cells: evidence from ASM knockout mice. *Journal of molecular medicine* **91:** 25-36.

200 Liang JM, Xu HY, Zhang XJ, Li X, Zhang HB, Ge PF (2013). Role of mitochondrial function in the protective effects of ischaemic postconditioning on ischaemia/reperfusion cerebral damage. *The Journal of international medical research* **41:** 618-627.

201 Liebisch G, Drobnik W, Reil M, Trumbach B, Arnecke R, Olgemoller B *et al* (1999). Quantitative measurement of different ceramide species from crude cellular extracts by electrospray ionization tandem mass spectrometry (ESI-MS/MS). *Journal of lipid research* **40:** 1539-1546.

202 Liu B, Hannun YA (1997). Inhibition of the neutral magnesium-dependent sphingomyelinase by glutathione. *The Journal of biological chemistry* **272:** 16281-16287.

203 Liu H, Sugiura M, Nava VE, Edsall LC, Kono K, Poulton S *et al* (2000). Molecular cloning and functional characterization of a novel mammalian sphingosine kinase type 2 isoform. *The Journal of biological chemistry* **275:** 19513-19520.
204 Liu Q, He X, Liu Y, Du B, Wang X, Zhang W *et al* (2008). NADPH oxidase-mediated generation of reactive oxygen species: A new mechanism for X-ray-induced HeLa cell death. *Biochemical and biophysical research communications* **377:** 775-779.
205 Ludwig A, Otto GP, Riento K, Hams E, Fallon PG, Nichols BJ (2010). Flotillin microdomains interact with the cortical cytoskeleton to control uropod formation and neutrophil recruitment. *The Journal of cell biology* **191:** 771-781.
206 Luo H, Yang A, Schulte BA, Wargovich MJ, Wang GY (2013). Resveratrol induces premature senescence in lung cancer cells via ROS-mediated DNA damage. *PloS one* **8:** e60065.
207 Mahdy AE, Cheng JC, Li J, Elojeimy S, Meacham WD, Turner LS *et al* (2009). Acid ceramidase upregulation in prostate cancer cells confers resistance to radiation: AC inhibition, a potential radiosensitizer. *Molecular therapy : the journal of the American Society of Gene Therapy* **17:** 430-438.
208 Mandala SM (2001). Sphingosine-1-Phosphate Phosphatases. *Prostaglandins* **64:** 143-156.
209 Mano N, Oda Y, Yamada K, Asakawa N, Katayama K (1997). Simultaneous quantitative determination method for sphingolipid metabolites by liquid chromatography/ionspray ionization tandem mass spectrometry. *Analytical biochemistry* **244:** 291-300.
210 Mao C, Obeid LM (2008). Ceramidases: regulators of cellular responses mediated by ceramide, sphingosine, and sphingosine-1-phosphate. *Biochimica et biophysica acta* **1781:** 424-434.
211 Mareková M, Vavrova J, Vokurkova D (2003). Monitoring of premitotic and postmitotic apoptosis in gamma-irradiated HL-60 cells by the mitochondrial membrane protein-specific monoclonal antibody APO2.7. *General physiology and biophysics* **22:** 191-200.
212 Mascayano C, Espinosa V, Sepulveda-Boza S, Hoobler EK, Perry S, Diaz G *et al* (2014). Enzymatic Studies of Isoflavonoids as Selective and Potent Inhibitors of Human Leukocyte 5-Lipo-Oxygenase. *Chemical biology & drug design*.
213 Mathias S, Younes A, Kan CC, Orlow I, Joseph C, Kolesnick RN (1993). Activation of the sphingomyelin signaling pathway in intact EL4 cells and in a cell-free system by IL-1 beta. *Science* **259:** 519-522.
214 Mathias S, Pena LA, Kolesnick RN (1998). Signal transduction of stress via ceramide. *The Biochemical journal* **335 (Pt 3):** 465-480.
215 McCollister BD, Myers JT, Jones-Carson J, Voelker DR, Vazquez-Torres A (2007). Constitutive acid sphingomyelinase enhances early and late macrophage killing of Salmonella enterica serovar Typhimurium. *Infection and immunity* **75:** 5346-5352.
216 McNabb TJ, Cremesti AE, Brown PR, Fischl AS (1999). The separation and direct detection of ceramides and sphingoid bases by normal-phase high-performance liquid chromatography and evaporative light-scattering detection. *Analytical biochemistry* **276:** 242-250.
217 Megha, London E (2004). Ceramide selectively displaces cholesterol from ordered lipid domains (rafts): implications for lipid raft structure and function. *The Journal of biological chemistry* **279:** 9997-10004.
218 Mencarelli C, Martinez-Martinez P (2013). *Cellular and molecular life sciences : CMLS* **70:** 181-203.
219 Michel C, van Echten-Deckert G, Rother J, Sandhoff K, Wang E, Merrill AH, Jr. (1997). Characterization of ceramide synthesis. A dihydroceramide desaturase

introduces the 4,5-trans-double bond of sphingosine at the level of dihydroceramide. *The Journal of biological chemistry* **272:** 22432-22437.

220 Mikkelsen RB, Wardman P (2003). Biological chemistry of reactive oxygen and nitrogen and radiation-induced signal transduction mechanisms. *Oncogene* **22:** 5734-5754.

221 Miller ME, Adhikary S, Kolokoltsov AA, Davey RA (2012). Ebolavirus requires acid sphingomyelinase activity and plasma membrane sphingomyelin for infection. *Journal of virology* **86:** 7473-7483.

222 Morgan WF, Sowa MB (2005). Effects of ionizing radiation in nonirradiated cells. *Proceedings of the National Academy of Sciences of the United States of America* **102:** 14127-14128.

223 Morita Y, Perez GI, Paris F, Miranda SR, Ehleiter D, Haimovitz-Friedman A *et al* (2000). Oocyte apoptosis is suppressed by disruption of the acid sphingomyelinase gene or by sphingosine-1-phosphate therapy. *Nature medicine* **6:** 1109-1114.

224 Motta S, Monti M, Sesana S, Mellesi L, Ghidoni R, Caputo R (1994). Abnormality of water barrier function in psoriasis. Role of ceramide fractions. *Archives of dermatology* **130:** 452-456.

225 Müller G, Ayoub M, Storz P, Rennecke J, Fabbro D, Pfizenmaier K (1995). PKC zeta is a molecular switch in signal transduction of TNF-alpha, bifunctionally regulated by ceramide and arachidonic acid. *The EMBO journal* **14:** 1961-1969.

226 Murphy MP (2009). How mitochondria produce reactive oxygen species. *The Biochemical journal* **417:** 1-13.

227 Nagashima T, Matsutani M, Nakamura O, Tanaka Y (1989). [Regrowth pattern of glioblastoma multiforme after radiotherapy]. *Gan no rinsho Japan journal of cancer clinics* **35:** 1272-1276.

228 Natarajan R, Fisher BJ, Jones DG, Fowler AA, 3rd (2002). Atypical mechanism of NF-kappaB activation during reoxygenation stress in microvascular endothelium: a role for tyrosine kinases. *Free radical biology & medicine* **33:** 962.

229 Ng K-H (2003). Non-ionizing radiations–sources, biological effects, emissions and exposures.

230 Novotna B, Bagryantseva Y, Siskova M, Neuwirtova R (2009). Oxidative DNA damage in bone marrow cells of patients with low-risk myelodysplastic syndrome. *Leukemia research* **33:** 340-343.

231 Ogawa K, Utsunomiya T, Mimori K, Tanaka F, Haraguchi N, Inoue H *et al* (2006). Differential gene expression profiles of radioresistant pancreatic cancer cell lines established by fractionated irradiation. *International journal of oncology* **28:** 705-713.

232 Ogretmen B, Hannun YA (2004). Biologically active sphingolipids in cancer pathogenesis and treatment. *Nature reviews Cancer* **4:** 604-616.

233 Okado-Matsumoto A, Fridovich I (2002). Amyotrophic lateral sclerosis: a proposed mechanism. *Proceedings of the National Academy of Sciences of the United States of America* **99:** 9010-9014.

234 Olavarria VH, Recabarren P, Fredericksen F, Villalba M, Yanez A (2015). ISAV infection promotes apoptosis of SHK-1 cells through a ROS/p38 MAPK/Bad signaling pathway. *Molecular immunology* **64:** 1-8.

235 Orient A, Donko A, Szabo A, Leto TL, Geiszt M (2007). Novel sources of reactive oxygen species in the human body. *Nephrology, dialysis, transplantation : official publication of the European Dialysis and Transplant Association - European Renal Association* **22:** 1281-1288.

236 Ostrom RS, Insel PA (2006). Methods for the study of signaling molecules in membrane lipid rafts and caveolae. *Methods in molecular biology* **332:** 181-191.

237 Padgett LE, Burg AR, Lei W, Tse HM (2015). Loss of NADPH oxidase-derived superoxide skews macrophage phenotypes to delay type 1 diabetes. *Diabetes* **64:** 937-946.
238 Palacino JJ, Sagi D, Goldberg MS, Krauss S, Motz C, Wacker M *et al* (2004). Mitochondrial dysfunction and oxidative damage in parkin-deficient mice. *The Journal of biological chemistry* **279:** 18614-18622.
239 Paravicini TM, Touyz RM (2008). NADPH oxidases, reactive oxygen species, and hypertension: clinical implications and therapeutic possibilities. *Diabetes care* **31 Suppl 2:** S170-180.
240 Paris F, Fuks Z, Kang A, Capodieci P, Juan G, Ehleiter D *et al* (2001). Endothelial apoptosis as the primary lesion initiating intestinal radiation damage in mice. *Science* **293:** 293-297.
241 Parolini I, Sargiacomo M, Lisanti MP, Peschle C (1996). Signal transduction and glycophosphatidylinositol-linked proteins (lyn, lck, CD4, CD45, G proteins, and CD55) selectively localize in Triton-insoluble plasma membrane domains of human leukemic cell lines and normal granulocytes. *Blood* **87:** 3783-3794.
242 Peña LA, Fuks Z, Kolesnick RN (2000). Radiation-induced apoptosis of endothelial cells in the murine central nervous system: protection by fibroblast growth factor and sphingomyelinase deficiency. *Cancer research* **60:** 321-327.
243 Perez WI, Soto Y, Ortiz C, Matta J, Melendez E (2015). Ferrocenes as potential chemotherapeutic drugs: synthesis, cytotoxic activity, reactive oxygen species production and micronucleus assay. *Bioorganic & medicinal chemistry* **23:** 471-479.
244 Perrotta C, Bizzozero L, Cazzato D, Morlacchi S, Assi E, Simbari F *et al* (2010). Syntaxin 4 is required for acid sphingomyelinase activity and apoptotic function. *The Journal of biological chemistry* **285:** 40240-40251.
245 Pescio LG, Favale NO, Marquez MG, Sterin-Speziale NB (2012). Glycosphingolipid synthesis is essential for MDCK cell differentiation. *Biochimica et biophysica acta* **1821:** 884-894.
246 Peters LJ, Withers HR, Thames HD, Jr., Fletcher GH (1982). Tumor radioresistance in clinical radiotherapy. *International journal of radiation oncology, biology, physics* **8:** 101-108.
247 Pewzner-Jung Y, Ben-Dor S, Futerman AH (2006). When do Lasses (longevity assurance genes) become CerS (ceramide synthases)?: Insights into the regulation of ceramide synthesis. *The Journal of biological chemistry* **281:** 25001-25005.
248 Pfeiffer A, Bottcher A, Orso E, Kapinsky M, Nagy P, Bodnar A *et al* (2001). Lipopolysaccharide and ceramide docking to CD14 provokes ligand-specific receptor clustering in rafts. *European journal of immunology* **31:** 3153-3164.
249 Pike LJ (2004). Lipid rafts: heterogeneity on the high seas. *The Biochemical journal* **378:** 281-292.
250 Predescu S, Knezevic I, Bardita C, Neamu RF, Brovcovych V, Predescu D (2013). Platelet activating factor-induced ceramide micro-domains drive endothelial NOS activation and contribute to barrier dysfunction. *PloS one* **8:** e75846.
251 Previati M, Bertolaso L, Tramarin M, Bertagnolo V, Capitani S (1996). Low nanogram range quantitation of diglycerides and ceramide by high-performance liquid chromatography. *Analytical biochemistry* **233:** 108-114.
252 Prise KM, Folkard M, Michael BD (2003). Bystander responses induced by low LET radiation. *Oncogene* **22:** 7043-7049.
253 Pritsos CA (2000). Cellular distribution, metabolism and regulation of the xanthine oxidoreductase enzyme system. *Chemico-biological interactions* **129:** 195-208.

254 Qiu H, Edmunds T, Baker-Malcolm J, Karey KP, Estes S, Schwarz C *et al* (2003). Activation of human acid sphingomyelinase through modification or deletion of C-terminal cysteine. *The Journal of biological chemistry* **278:** 32744-32752.
255 Quintern LE, Weitz G, Nehrkorn H, Tager JM, Schram AW, Sandhoff K (1987). Acid sphingomyelinase from human urine: purification and characterization. *Biochimica et biophysica acta* **922:** 323-336.
256 Quintern LE, Schuchman EH, Levran O, Suchi M, Ferlinz K, Reinke H *et al* (1989). Isolation of cDNA clones encoding human acid sphingomyelinase: occurrence of alternatively processed transcripts. *The EMBO journal* **8:** 2469-2473.
257 Racine C, Belanger M, Hirabayashi H, Boucher M, Chakir J, Couet J (1999). Reduction of caveolin 1 gene expression in lung carcinoma cell lines. *Biochemical and biophysical research communications* **255:** 580-586.
258 Rada B, Leto TL (2008). Oxidative innate immune defenses by Nox/Duox family NADPH oxidases. *Contributions to microbiology* **15:** 164-187.
259 Radford IR (1986). Evidence for a general relationship between the induced level of DNA double-strand breakage and cell-killing after X-irradiation of mammalian cells. *International journal of radiation biology and related studies in physics, chemistry, and medicine* **49:** 611-620.
260 Rajagopalan V, Canals D, Luberto C, Snider J, Voelkel-Johnson C, Obeid LM *et al* (2015). Critical determinants of mitochondria-associated neutral sphingomyelinase (MA-nSMase) for mitochondrial localization. *Biochimica et biophysica acta* **1850:** 628-639.
261 Reinehr R, Becker S, Eberle A, Grether-Beck S, Haussinger D (2005). Involvement of NADPH oxidase isoforms and Src family kinases in CD95-dependent hepatocyte apoptosis. *The Journal of biological chemistry* **280:** 27179-27194.
262 Ribas J, Mattiolo P, Boix J (2015). Pharmacological modulation of reactive oxygen species in cancer treatment. *Current drug targets* **16:** 31-37.
263 Riebeling C, Allegood JC, Wang E, Merrill AH, Jr., Futerman AH (2003). Two mammalian longevity assurance gene (LAG1) family members, trh1 and trh4, regulate dihydroceramide synthesis using different fatty acyl-CoA donors. *The Journal of biological chemistry* **278:** 43452-43459.
264 Rodriguez-Lafrasse C, Alphonse G, Aloy MT, Ardail D, Gerard JP, Louisot P *et al* (2002). Increasing endogenous ceramide using inhibitors of sphingolipid metabolism maximizes ionizing radiation-induced mitochondrial injury and apoptotic cell killing. *International journal of cancer Journal international du cancer* **101:** 589-598.
265 Romiti E, Meacci E, Tani M, Nuti F, Farnararo M, Ito M *et al* (2000). Neutral/alkaline and acid ceramidase activities are actively released by murine endothelial cells. *Biochemical and biophysical research communications* **275:** 746-751.
266 Rotolo JA, Zhang J, Donepudi M, Lee H, Fuks Z, Kolesnick R (2005). Caspase-dependent and -independent activation of acid sphingomyelinase signaling. *The Journal of biological chemistry* **280:** 26425-26434.
267 Rousseau M, Gaugler MH, Rodallec A, Bonnaud S, Paris F, Corre I (2011). RhoA GTPase regulates radiation-induced alterations in endothelial cell adhesion and migration. *Biochemical and biophysical research communications* **414:** 750-755.
268 Saad AF, Meacham WD, Bai A, Anelli V, Elojeimy S, Mahdy AE *et al* (2007). The functional effects of acid ceramidase overexpression in prostate cancer progression and resistance to chemotherapy. *Cancer biology & therapy* **6:** 1455-1460.
269 Saarikangas J, Zhao H, Lappalainen P (2010). Regulation of the actin cytoskeleton-plasma membrane interplay by phosphoinositides. *Physiological reviews* **90:** 259-289.
270 Saddoughi SA, Song P, Ogretmen B (2008). Roles of bioactive sphingolipids in cancer biology and therapeutics. *Sub-cellular biochemistry* **49:** 413-440.

271 Saeki K, Miura Y, Aki D, Kurosaki T, Yoshimura A (2003). The B cell-specific major raft protein, Raftlin, is necessary for the integrity of lipid raft and BCR signal transduction. *The EMBO journal* **22:** 3015-3026.
272 Saenko Iu V, Shutov AM, Napalkova SM (2011). [X-ray irradiation stimulates the mitochondrial-dependent generation of reactive oxygen and nitrogen species in K562 leukemia cells]. *Radiatsionnaia biologiia, radioecologiia / Rossiiskaia akademiia nauk* **51:** 677-683.
273 Sakaguchi K, Herrera JE, Saito S, Miki T, Bustin M, Vassilev A *et al* (1998). DNA damage activates p53 through a phosphorylation-acetylation cascade. *Genes & development* **12:** 2831-2841.
274 Sakuragawa N (1982). Acid sphingomyelinase of human placenta: purification, properties, and 125iodine labeling. *Journal of biochemistry* **92:** 637-646.
275 Salzer U, Prohaska R (2001). Stomatin, flotillin-1, and flotillin-2 are major integral proteins of erythrocyte lipid rafts. *Blood* **97:** 1141-1143.
276 Samal B, Sun Y, Stearns G, Xie C, Suggs S, McNiece I (1994). Cloning and characterization of the cDNA encoding a novel human pre-B-cell colony-enhancing factor. *Molecular and cellular biology* **14:** 1431-1437.
277 Samapati R, Yang Y, Yin J, Stoerger C, Arenz C, Dietrich A *et al* (2012). Lung endothelial Ca2+ and permeability response to platelet-activating factor is mediated by acid sphingomyelinase and transient receptor potential classical 6. *American journal of respiratory and critical care medicine* **185:** 160-170.
278 Sampson N, Berger P, Zenzmaier C (2012). Therapeutic targeting of redox signaling in myofibroblast differentiation and age-related fibrotic disease. *Oxidative medicine and cellular longevity* **2012:** 458276.
279 Santana P, Pena LA, Haimovitz-Friedman A, Martin S, Green D, McLoughlin M *et al* (1996). Acid sphingomyelinase-deficient human lymphoblasts and mice are defective in radiation-induced apoptosis. *Cell* **86:** 189-199.
280 Sathishkumar S, Boyanovsky B, Karakashian AA, Rozenova K, Giltiay NV, Kudrimoti M *et al* (2005). Elevated sphingomyelinase activity and ceramide concentration in serum of patients undergoing high dose spatially fractionated radiation treatment: implications for endothelial apoptosis. *Cancer biology & therapy* **4:** 979-986.
281 Scarlatti F, Sala G, Ricci C, Maioli C, Milani F, Minella M *et al* (2007). Resveratrol sensitization of DU145 prostate cancer cells to ionizing radiation is associated to ceramide increase. *Cancer letters* **253:** 124-130.
282 Scheel-Toellner D, Wang K, Assi LK, Webb PR, Craddock RM, Salmon M *et al* (2004). Clustering of death receptors in lipid rafts initiates neutrophil spontaneous apoptosis. *Biochemical Society transactions* **32:** 679-681.
283 Schissel SL, Schuchman EH, Williams KJ, Tabas I (1996). Zn2+-stimulated sphingomyelinase is secreted by many cell types and is a product of the acid sphingomyelinase gene. *The Journal of biological chemistry* **271:** 18431-18436.
284 Schissel SL, Keesler GA, Schuchman EH, Williams KJ, Tabas I (1998). The cellular trafficking and zinc dependence of secretory and lysosomal sphingomyelinase, two products of the acid sphingomyelinase gene. *The Journal of biological chemistry* **273:** 18250-18259.
285 Schneider PB, Kennedy EP (1967). Sphingomyelinase in normal human spleens and in spleens from subjects with Niemann-Pick disease. *Journal of lipid research* **8:** 202-209.
286 Schnitzer JE, McIntosh DP, Dvorak AM, Liu J, Oh P (1995). Separation of caveolae from associated microdomains of GPI-anchored proteins. *Science* **269:** 1435-1439.
287 Schubert KM, Scheid MP, Duronio V (2000). Ceramide inhibits protein kinase B/Akt by promoting dephosphorylation of serine 473. *The Journal of biological chemistry* **275:** 13330-13335.

288 Schuchman EH, Levran O, Pereira LV, Desnick RJ (1992). Structural organization and complete nucleotide sequence of the gene encoding human acid sphingomyelinase (SMPD1). *Genomics* **12:** 197-205.
289 Schuchman EH, Miranda SR (1997). Niemann-Pick disease: mutation update, genotype/phenotype correlations, and prospects for genetic testing. *Genetic testing* **1:** 13-19.
290 Schütze S, Potthoff K, Machleidt T, Berkovic D, Wiegmann K, Kronke M (1992). TNF activates NF-kappa B by phosphatidylcholine-specific phospholipase C-induced "acidic" sphingomyelin breakdown. *Cell* **71:** 765-776.
291 Schütze S, Machleidt T, Kronke M (1994). The role of diacylglycerol and ceramide in tumor necrosis factor and interleukin-1 signal transduction. *Journal of leukocyte biology* **56:** 533-541.
292 Schwarzer M, Osterholt M, Lunkenbein A, Schrepper A, Amorim P, Doenst T (2014). Mitochondrial reactive oxygen species production and respiratory complex activity in rats with pressure overload-induced heart failure. *The Journal of physiology* **592:** 3767-3782.
293 Sechi AS, Wehland J (2000). The actin cytoskeleton and plasma membrane connection: PtdIns(4,5)P(2) influences cytoskeletal protein activity at the plasma membrane. *Journal of cell science* **113 Pt 21:** 3685-3695.
294 Senkal CE, Ponnusamy S, Rossi MJ, Bialewski J, Sinha D, Jiang JC *et al* (2007). Role of human longevity assurance gene 1 and C18-ceramide in chemotherapy-induced cell death in human head and neck squamous cell carcinomas. *Molecular cancer therapeutics* **6:** 712-722.
295 Severs NJ (1988). Caveolae: static inpocketings of the plasma membrane, dynamic vesicles or plain artifact? *Journal of cell science* **90 (Pt 3):** 341-348.
296 Shack S, Wang XT, Kokkonen GC, Gorospe M, Longo DL, Holbrook NJ (2003). Caveolin-induced activation of the phosphatidylinositol 3-kinase/Akt pathway increases arsenite cytotoxicity. *Molecular and cellular biology* **23:** 2407-2414.
297 Shao D, Segal AW, Dekker LV (2003). Lipid rafts determine efficiency of NADPH oxidase activation in neutrophils. *FEBS letters* **550:** 101-106.
298 Shatz M, Liscovitch M (2008). Caveolin-1: a tumor-promoting role in human cancer. *International journal of radiation biology* **84:** 177-189.
299 Shimoda-Matsubayashi S, Matsumine H, Kobayashi T, Nakagawa-Hattori Y, Shimizu Y, Mizuno Y (1996). Structural dimorphism in the mitochondrial targeting sequence in the human manganese superoxide dismutase gene. A predictive evidence for conformational change to influence mitochondrial transport and a study of allelic association in Parkinson's disease. *Biochemical and biophysical research communications* **226:** 561-565.
300 Shimohama S, Tanino H, Kawakami N, Okamura N, Kodama H, Yamaguchi T *et al* (2000). Activation of NADPH oxidase in Alzheimer's disease brains. *Biochemical and biophysical research communications* **273:** 5-9.
301 Shinghal R, Scheller RH, Bajjalieh SM (1993). Ceramide 1-phosphate phosphatase activity in brain. *Journal of neurochemistry* **61:** 2279-2285.
302 Shinohara K, Nakano H (1993). Interphase death and reproductive death in X-irradiated MOLT-4 cells. *Radiation research* **135:** 197-205.
303 Shinomiya N, Kuno Y, Yamamoto F, Fukasawa M, Okumura A, Uefuji M *et al* (2000). Different mechanisms between premitotic apoptosis and postmitotic apoptosis in X-irradiated U937 cells. *International journal of radiation oncology, biology, physics* **47:** 767-777.

304 Shinomiya N (2001). New concepts in radiation-induced apoptosis: 'premitotic apoptosis' and 'postmitotic apoptosis'. *Journal of cellular and molecular medicine* **5:** 240-253.
305 Short SC, Martindale C, Bourne S, Brand G, Woodcock M, Johnston P (2007). DNA repair after irradiation in glioma cells and normal human astrocytes. *Neuro-oncology* **9:** 404-411.
306 Simarro M, Calvo J, Vila JM, Places L, Padilla O, Alberola-Ila J *et al* (1999). Signaling through CD5 involves acidic sphingomyelinase, protein kinase C-zeta, mitogen-activated protein kinase kinase, and c-Jun NH2-terminal kinase. *Journal of immunology* **162:** 5149-5155.
307 Simons K, Ikonen E (1997). Functional rafts in cell membranes. *Nature* **387:** 569-572.
308 Simons K, Toomre D (2000). Lipid rafts and signal transduction. *Nature reviews Molecular cell biology* **1:** 31-39.
309 Simpson-Holley M, Ellis D, Fisher D, Elton D, McCauley J, Digard P (2002). A functional link between the actin cytoskeleton and lipid rafts during budding of filamentous influenza virions. *Virology* **301:** 212-225.
310 Singer SJ, Nicolson GL (1972). The fluid mosaic model of the structure of cell membranes. *Science* **175:** 720-731.
311 Singh R, Wang Y, Schattenberg JM, Xiang Y, Czaja MJ (2009). Chronic oxidative stress sensitizes hepatocytes to death from 4-hydroxynonenal by JNK/c-Jun overactivation. *American journal of physiology Gastrointestinal and liver physiology* **297:** G907-917.
312 Smart EJ, Ying YS, Mineo C, Anderson RG (1995). A detergent-free method for purifying caveolae membrane from tissue culture cells. *Proceedings of the National Academy of Sciences of the United States of America* **92:** 10104-10108.
313 Song KS, Li S, Okamoto T, Quilliam LA, Sargiacomo M, Lisanti MP (1996). Co-purification and direct interaction of Ras with caveolin, an integral membrane protein of caveolae microdomains. Detergent-free purification of caveolae microdomains. *The Journal of biological chemistry* **271:** 9690-9697.
314 Sorescu D, Weiss D, Lassegue B, Clempus RE, Szocs K, Sorescu GP *et al* (2002). Superoxide production and expression of nox family proteins in human atherosclerosis. *Circulation* **105:** 1429-1435.
315 Spence MW, Clarke JT, Cook HW (1983). Pathways of sphingomyelin metabolism in cultured fibroblasts from normal and sphingomyelin lipidosis subjects. *The Journal of biological chemistry* **258:** 8595-8600.
316 Srinivasan S, Koenigstein A, Joseph J, Sun L, Kalyanaraman B, Zaidi M *et al* (2010). Role of mitochondrial reactive oxygen species in osteoclast differentiation. *Annals of the New York Academy of Sciences* **1192:** 245-252.
317 Stadtman ER (1990). Metal ion-catalyzed oxidation of proteins: biochemical mechanism and biological consequences. *Free radical biology & medicine* **9:** 315-325.
318 Stadtman ER, Levine RL (2000). Protein oxidation. *Annals of the New York Academy of Sciences* **899:** 191-208.
319 Stiban J, Caputo L, Colombini M (2008). Ceramide synthesis in the endoplasmic reticulum can permeabilize mitochondria to proapoptotic proteins. *Journal of lipid research* **49:** 625-634.
320 Stoffel W (1999). Functional analysis of acid and neutral sphingomyelinases in vitro and in vivo. *Chemistry and physics of lipids* **102:** 107-121.
321 Storz P, Toker A (2003). Protein kinase D mediates a stress-induced NF-kappaB activation and survival pathway. *The EMBO journal* **22:** 109-120.

322 Sun Y, St Clair DK, Xu Y, Crooks PA, St Clair WH (2010). A NADPH oxidase-dependent redox signaling pathway mediates the selective radiosensitization effect of parthenolide in prostate cancer cells. *Cancer research* **70:** 2880-2890.
323 Suzuki K, Yamashita S (2014). Radiation-Induced Bystander Response: Mechanism and Clinical Implications. *Advances in wound care* **3:** 16-24.
324 Suzuoki M, Miyamoto M, Kato K, Hiraoka K, Oshikiri T, Nakakubo Y *et al* (2002). Impact of caveolin-1 expression on prognosis of pancreatic ductal adenocarcinoma. *British journal of cancer* **87:** 1140-1144.
325 Szabadkai G, Bianchi K, Varnai P, De Stefani D, Wieckowski MR, Cavagna D *et al* (2006). Chaperone-mediated coupling of endoplasmic reticulum and mitochondrial Ca2+ channels. *The Journal of cell biology* **175:** 901-911.
326 Szabó I, Gulbins E, Apfel H, Zhang X, Barth P, Busch AE *et al* (1996). Tyrosine phosphorylation-dependent suppression of a voltage-gated K+ channel in T lymphocytes upon Fas stimulation. *The Journal of biological chemistry* **271:** 20465-20469.
327 Takahashi T, Abe T, Sato T, Miura K, Takahashi I, Yano M *et al* (2002). Elevated sphingomyelinase and hypercytokinemia in hemophagocytic lymphohistiocytosis. *Journal of pediatric hematology/oncology* **24:** 401-404.
328 Tateishi Y, Sasabe E, Ueta E, Yamamoto T (2008). Ionizing irradiation induces apoptotic damage of salivary gland acinar cells via NADPH oxidase 1-dependent superoxide generation. *Biochemical and biophysical research communications* **366:** 301-307.
329 Tepper AD, Van Blitterswijk WJ (2000). Ceramide mass analysis by normal-phase high-performance liquid chromatography. *Methods in enzymology* **312:** 16-22.
330 Terman A, Kurz T, Navratil M, Arriaga EA, Brunk UT (2010). Mitochondrial turnover and aging of long-lived postmitotic cells: the mitochondrial-lysosomal axis theory of aging. *Antioxidants & redox signaling* **12:** 503-535.
331 Thallas-Bonke V, Jha JC, Gray SP, Barit D, Haller H, Schmidt HH *et al* (2014). Nox-4 deletion reduces oxidative stress and injury by PKC-alpha-associated mechanisms in diabetic nephropathy. *Physiological reports* **2**.
332 Thariat J, Hannoun-Levi JM, Sun Myint A, Vuong T, Gerard JP (2013). Past, present, and future of radiotherapy for the benefit of patients. *Nature reviews Clinical oncology* **10:** 52-60.
333 Thompson TC, Tahir SA, Li L, Watanabe M, Naruishi K, Yang G *et al* (2010). The role of caveolin-1 in prostate cancer: clinical implications. *Prostate cancer and prostatic diseases* **13:** 6-11.
334 Timme TL, Goltsov A, Tahir S, Li L, Wang J, Ren C *et al* (2000). Caveolin-1 is regulated by c-myc and suppresses c-myc-induced apoptosis. *Oncogene* **19:** 3256-3265.
335 Tomiuk S, Zumbansen M, Stoffel W (2000). Characterization and subcellular localization of murine and human magnesium-dependent neutral sphingomyelinase. *The Journal of biological chemistry* **275:** 5710-5717.
336 Touyz RM (2008). Apocynin, NADPH oxidase, and vascular cells: a complex matter. *Hypertension* **51:** 172-174.
337 Utermöhlen O, Karow U, Lohler J, Kronke M (2003). Severe impairment in early host defense against Listeria monocytogenes in mice deficient in acid sphingomyelinase. *Journal of immunology* **170:** 2621-2628.
338 Utermöhlen O, Herz J, Schramm M, Kronke M (2008). Fusogenicity of membranes: the impact of acid sphingomyelinase on innate immune responses. *Immunobiology* **213:** 307-314.
339 Van Aelst L, Joneson T, Bar-Sagi D (1996). Identification of a novel Rac1-interacting protein involved in membrane ruffling. *The EMBO journal* **15:** 3778-3786.

340 Vasquez-Vivar J, Kalyanaraman B (2000). Generation of superoxide from nitric oxide synthase. *FEBS letters* **481:** 305-306.
341 Vassilieva EV, Ivanov AI, Nusrat A (2009). Flotillin-1 stabilizes caveolin-1 in intestinal epithelial cells. *Biochemical and biophysical research communications* **379:** 460-465.
342 Venkataraman K, Riebeling C, Bodennec J, Riezman H, Allegood JC, Sullards MC *et al* (2002). Upstream of growth and differentiation factor 1 (uog1), a mammalian homolog of the yeast longevity assurance gene 1 (LAG1), regulates N-stearoyl-sphinganine (C18-(dihydro)ceramide) synthesis in a fumonisin B1-independent manner in mammalian cells. *The Journal of biological chemistry* **277:** 35642-35649.
343 Vines AM, Lyng FM, McClean B, Seymour C, Mothersill CE (2009). Bystander effect induced changes in apoptosis related proteins and terminal differentiation in in vitro murine bladder cultures. *International journal of radiation biology* **85:** 48-56.
344 Vit JP, Rosselli F (2003). Role of the ceramide-signaling pathways in ionizing radiation-induced apoptosis. *Oncogene* **22:** 8645-8652.
345 Volanti C, Matroule JY, Piette J (2002). Involvement of oxidative stress in NF-kappaB activation in endothelial cells treated by photodynamic therapy. *Photochemistry and photobiology* **75:** 36-45.
346 Volonte D, Galbiati F, Li S, Nishiyama K, Okamoto T, Lisanti MP (1999). Flotillins/cavatellins are differentially expressed in cells and tissues and form a hetero-oligomeric complex with caveolins in vivo. Characterization and epitope-mapping of a novel flotillin-1 monoclonal antibody probe. *The Journal of biological chemistry* **274:** 12702-12709.
347 Waheed AA, Freed EO (2009). *Virus research* **143:** 162-176.
348 Wang J, Wakeman TP, Lathia JD, Hjelmeland AB, Wang XF, White RR *et al* (2010). Notch promotes radioresistance of glioma stem cells. *Stem cells* **28:** 17-28.
349 Ward JF (1988). DNA damage produced by ionizing radiation in mammalian cells: identities, mechanisms of formation, and reparability. *Progress in nucleic acid research and molecular biology* **35:** 95-125.
350 Ward JF (2002). The radiation-induced lesions which trigger the bystander effect. *Mutation research* **499:** 151-154.
351 Watts JD, Aebersold R, Polverino AJ, Patterson SD, Gu M (1999). Ceramide second messengers and ceramide assays. *Trends in biochemical sciences* **24:** 228.
352 Wei YM, Li X, Xiong J, Abais JM, Xia M, Boini KM *et al* (2013). Attenuation by statins of membrane raft-redox signaling in coronary arterial endothelium. *The Journal of pharmacology and experimental therapeutics* **345:** 170-179.
353 Weichselbaum RR, Dahlberg W, Little JB (1985). Inherently radioresistant cells exist in some human tumors. *Proceedings of the National Academy of Sciences of the United States of America* **82:** 4732-4735.
354 Weyemi U, Dupuy C (2012). The emerging role of ROS-generating NADPH oxidase NOX4 in DNA-damage responses. *Mutation research* **751:** 77-81.
355 Wolden SL, Zelefsky MJ, Kraus DH, Rosenzweig KE, Chong LM, Shaha AR *et al* (2001). Accelerated concomitant boost radiotherapy and chemotherapy for advanced nasopharyngeal carcinoma. *Journal of clinical oncology : official journal of the American Society of Clinical Oncology* **19:** 1105-1110.
356 Wolff RA, Dobrowsky RT, Bielawska A, Obeid LM, Hannun YA (1994). Role of ceramide-activated protein phosphatase in ceramide-mediated signal transduction. *The Journal of biological chemistry* **269:** 19605-19609.
357 Wu BX, Rajagopalan V, Roddy PL, Clarke CJ, Hannun YA (2010). Identification and characterization of murine mitochondria-associated neutral sphingomyelinase (MA-nSMase), the mammalian sphingomyelin phosphodiesterase 5. *The Journal of biological chemistry* **285:** 17993-18002.

358 Wu J, Cheng Y, Palmberg C, Bergman T, Nilsson A, Duan RD (2005). Cloning of alkaline sphingomyelinase from rat intestinal mucosa and adjusting of the hypothetical protein XP_221184 in GenBank. *Biochimica et biophysica acta* **1687:** 94-102.
359 Wu J, Nilsson A, Jonsson BA, Stenstad H, Agace W, Cheng Y *et al* (2006). Intestinal alkaline sphingomyelinase hydrolyses and inactivates platelet-activating factor by a phospholipase C activity. *The Biochemical journal* **394:** 299-308.
360 Xing YX, Li P, Miao YX, Du W, Wang CB (2008). Involvement of ROS/ASMase/JNK signalling pathway in inhibiting UVA-induced apoptosis of HaCaT cells by polypeptide from Chlamys farreri. *Free radical research* **42:** 12-19.
361 Xu X, Bittman R, Duportail G, Heissler D, Vilcheze C, London E (2001). Effect of the structure of natural sterols and sphingolipids on the formation of ordered sphingolipid/sterol domains (rafts). Comparison of cholesterol to plant, fungal, and disease-associated sterols and comparison of sphingomyelin, cerebrosides, and ceramide. *The Journal of biological chemistry* **276:** 33540-33546.
362 Yabu T, Shiba H, Shibasaki Y, Nakanishi T, Imamura S, Touhata K *et al* (2015). Stress-induced ceramide generation and apoptosis via the phosphorylation and activation of nSMase1 by JNK signaling. *Cell death and differentiation* **22:** 258-273.
363 Yamada T, Ohyama H (1988). Radiation-induced interphase death of rat thymocytes is internally programmed (apoptosis). *International journal of radiation biology and related studies in physics, chemistry, and medicine* **53:** 65-75.
364 Yamamori T, Yasui H, Yamazumi M, Wada Y, Nakamura Y, Nakamura H *et al* (2012). Ionizing radiation induces mitochondrial reactive oxygen species production accompanied by upregulation of mitochondrial electron transport chain function and mitochondrial content under control of the cell cycle checkpoint. *Free radical biology & medicine* **53:** 260-270.
365 Yamamoto M, Toya Y, Schwencke C, Lisanti MP, Myers MG, Jr., Ishikawa Y (1998). Caveolin is an activator of insulin receptor signaling. *The Journal of biological chemistry* **273:** 26962-26968.
366 Yamanaka T, Suzuki K (1982). Acid sphingomyelinase of human brain: purification to homogeneity. *Journal of neurochemistry* **38:** 1753-1764.
367 Yamashita T, Wada R, Sasaki T, Deng C, Bierfreund U, Sandhoff K *et al* (1999). A vital role for glycosphingolipid synthesis during development and differentiation. *Proceedings of the National Academy of Sciences of the United States of America* **96:** 9142-9147.
368 Yan F, Polk DB (2001). Kinase suppressor of ras is necessary for tumor necrosis factor alpha activation of extracellular signal-regulated kinase/mitogen-activated protein kinase in intestinal epithelial cells. *Cancer research* **61:** 963-969.
369 Yang G, Truong LD, Timme TL, Ren C, Wheeler TM, Park SH *et al* (1998). Elevated expression of caveolin is associated with prostate and breast cancer. *Clinical cancer research : an official journal of the American Association for Cancer Research* **4:** 1873-1880.
370 Yano M, Kishida E, Muneyuki Y, Masuzawa Y (1998). Quantitative analysis of ceramide molecular species by high performance liquid chromatography. *Journal of lipid research* **39:** 2091-2098.
371 Yu C, Alterman M, Dobrowsky RT (2005). Ceramide displaces cholesterol from lipid rafts and decreases the association of the cholesterol binding protein caveolin-1. *Journal of lipid research* **46:** 1678-1691.
372 Yu ZF, Nikolova-Karakashian M, Zhou D, Cheng G, Schuchman EH, Mattson MP (2000). Pivotal role for acidic sphingomyelinase in cerebral ischemia-induced ceramide and cytokine production, and neuronal apoptosis. *Journal of molecular neuroscience : MN* **15:** 85-97.

373 Zeidan YH, Jenkins RW, Hannun YA (2008a). Remodeling of cellular cytoskeleton by the acid sphingomyelinase/ceramide pathway. *The Journal of cell biology* **181:** 335-350.
374 Zeidan YH, Wu BX, Jenkins RW, Obeid LM, Hannun YA (2008b). A novel role for protein kinase Cdelta-mediated phosphorylation of acid sphingomyelinase in UV light-induced mitochondrial injury. *FASEB journal : official publication of the Federation of American Societies for Experimental Biology* **22:** 183-193.
375 Zekry D, Epperson TK, Krause KH (2003). A role for NOX NADPH oxidases in Alzheimer's disease and other types of dementia? *IUBMB life* **55:** 307-313.
376 Zelefsky MJ, Fuks Z, Hunt M, Lee HJ, Lombardi D, Ling CC *et al* (2001). High dose radiation delivered by intensity modulated conformal radiotherapy improves the outcome of localized prostate cancer. *The Journal of urology* **166:** 876-881.
377 Zhai GG, Malhotra R, Delaney M, Latham D, Nestler U, Zhang M *et al* (2006). Radiation enhances the invasive potential of primary glioblastoma cells via activation of the Rho signaling pathway. *Journal of neuro-oncology* **76:** 227-237.
378 Zhang AY, Yi F, Zhang G, Gulbins E, Li PL (2006). Lipid raft clustering and redox signaling platform formation in coronary arterial endothelial cells. *Hypertension* **47:** 74-80.
379 Zhang AY, Yi F, Jin S, Xia M, Chen QZ, Gulbins E *et al* (2007). Acid sphingomyelinase and its redox amplification in formation of lipid raft redox signaling platforms in endothelial cells. *Antioxidants & redox signaling* **9:** 817-828.
380 Zhang FL, He Y, Zheng Y, Zhang WJ, Wang Q, Jia YJ *et al* (2014). Therapeutic effects of fucoidan in 6-hydroxydopamine-lesioned rat model of Parkinson's disease: Role of NADPH oxidase-1. *CNS neuroscience & therapeutics* **20:** 1036-1044.
381 Zhang Y, Yao B, Delikat S, Bayoumy S, Lin XH, Basu S *et al* (1997). Kinase suppressor of Ras is ceramide-activated protein kinase. *Cell* **89:** 63-72.
382 Zhang Y, Mattjus P, Schmid PC, Dong Z, Zhong S, Ma WY *et al* (2001). Involvement of the acid sphingomyelinase pathway in uva-induced apoptosis. *The Journal of biological chemistry* **276:** 11775-11782.
383 Zhang Y, Li X, Carpinteiro A, Gulbins E (2008). Acid sphingomyelinase amplifies redox signaling in Pseudomonas aeruginosa-induced macrophage apoptosis. *Journal of immunology* **181:** 4247-4254.
384 Zhou AY, Ryeom S (2014). Cyclosporin a promotes tumor angiogenesis in a calcineurin-independent manner by increasing mitochondrial reactive oxygen species. *Molecular cancer research : MCR* **12:** 1663-1676.
385 Zhou BB, Elledge SJ (2000). The DNA damage response: putting checkpoints in perspective. *Nature* **408:** 433-439.
386 Zhou FL, Zhang WG, Wei YC, Meng S, Bai GG, Wang BY *et al* (2010). Involvement of oxidative stress in the relapse of acute myeloid leukemia. *The Journal of biological chemistry* **285:** 15010-15015.
387 Zhou W, Jiang Z, Xu YY, Li XG (2013). Attention to normal brain volumes in glioblastoma radiotherapy: potential role in tumor invasion and vasculogenesis. *Medical hypotheses* **80:** 501-504.
388 Zou L, Kojima N, Kito M, Yagi K (1989). Purification to homogeneity of human placental acid sphingomyelinase. *Biotechnology and applied biochemistry* **11:** 217-225.
389 Zundel W, Giaccia A (1998). Inhibition of the anti-apoptotic PI(3)K/Akt/Bad pathway by stress. *Genes & development* **12:** 1941-1946.
390 Zundel W, Swiersz LM, Giaccia A (2000). Caveolin 1-mediated regulation of receptor tyrosine kinase-associated phosphatidylinositol 3-kinase activity by ceramide. *Molecular and cellular biology* **20:** 1507-1514.

APPENDIX

(Please refer to the CD for the list of proteins obtained from Mass spectrometry analysis, all the proteins mentioned in results and discussion parts are highlighted in yellow)

- List of proteins from ASM immunoprecipitation (IP) samples
- List of proteins from ceramide pull-down assay samples
- List of proteins from lipid raft samples

MS analysis was performed in the lab from Prof. Dr. Barbara Sitek by Dr. Dominik Megger from Clinical Proteomics, Medizinisches Proteom-Center, Zentrum für klinische Forschung, Ruhr-Universität Bochum, Germany.

All the data for MS are the results from two independent experiments

CURRICULUM VITAE

-removed-

ACKNOWLEDGEMENTS

-removed-

ERKLÄRUNGEN

Erklärung:

Hiermit erkläre ich, gem. § 6 Abs. (2) g) der Promotionsordnung der Fakultät für Biologie zur Erlangung der Dr. rer. nat., dass ich das Arbeitsgebiet, dem das Thema "REGULATION AND FUNCTION OF ACID SPHINGOMYELINASE (ASM)/CERAMIDE PATHWAY IN IRRADIATION-INDUCED CELL DEATH" zuzuordnen ist, in Forschung und Lehre vertrete und den Antrag von Deepa Sharma befürworte und die Betreuung auch im Falle eines Weggangs, wenn nicht wichtige Gründe dem entgegenstehen, weiterführen werde.

Essen, den _____

Prof. Dr. Erich Gulbins

Erklärung:

Hiermit erkläre ich, gem. § 7 Abs. (2) d) + f) der Promotionsordnung der Fakultät für Biologie zur Erlangung des Dr. rer. nat., dass ich die vorliegende Dissertation selbstständig verfasst und mich keiner anderen als der angegebenen Hilfsmittel bedient, bei der Abfassung der Dissertation nur die angegeben Hilfsmittel benutzt und alle wörtlich oder inhaltlich übernommenen Stellen als solche gekennzeichnet habe.

Essen, den _____

Deepa Sharma

Erklärung:

Hiermit erkläre ich, gem. § 7 Abs. (2) e) + g) der Promotionsordnung der Fakultät für Biologie zur Erlangung des Dr. rer. nat., dass ich keine anderen Promotionen bzw. Promotionsversuche in der Vergangenheit durchgeführt habe und dass diese Arbeit von keiner anderen Fakultät/Fachbereich abgelehnt worden ist.

Essen, den _____

Deepa Sharma